**An-Najah National University**

**Faculty of Graduate Studies**

# Analysis of Power Conversion Stages and Efficiency Improvement Possibilities for Grid Connected Pv System.

**By**

**Eman Omar Mahmoud Abu Hani**

**Supervisor**

**Prof. Marwan Mahmoud**

**This Thesis is Submitted in Partial Fulfillment of the Requirements for the Degree of Master of electrical power engineering, Faculty of Graduate Studies, An-Najah National University, Nablus-Palestine.**

**2018**

# ANALYSIS OF POWER CONVERSION STAGES AND EFFICIENCY IMPROVEMENT POSSIBILITIES FOR GRID CONNECTED PV SYSTEM.

**By**

**Eman Omar Mahmoud Abu Hani**

**This Thesis was defended successfully on 10/4/2018 and approved by:**

| **Defense Committee Members** | | **Signature** |
|---|---|---|
| **- Prof. Marwan M. Mahmoud** | **/ Supervisor** | **…….** |
| **- Dr. Mahmoud Salah** | **/ External examiner** | **……..……** |
| **- Dr. Moien Omar** | **/ Internal examiner** | …….. |

# Dedication

*I would like to dedicate my thesis to*

*My parents, brothers and sisters*

*My husband, daughter, and son*

*All friends and colleagues*

*……*

# Acknowledgment

I would like to express my sincere thanks to my supervisor, Prof. Dr. Marwan Mahmoud who has supported me throughout this project with his knowledge, guidance and insightful comments and observations.

Many thanks go to my Parents, my husband (Abed-Alhalim) and my family for the support they gave it to me during the entire course of my studies and to God who makes everything possible.

I would also like to thank my friends and colleagues at An -Najah National University for their assistance and encouragement.

## الإقرار

انا الموقع ادناه مقدم الرسالة التي تحمل العنوان:

**Analysis of Power Conversion Stages and Efficiency Improvement Possibilities for Grid Connected PV System**

اقر بان ما اشتملت عليه هذه الرسالة انما هي نتاج جهدي الخاص، باستثناء ما تمت الاشارة اليه حيثما ورد، وان هذه الرسالة ككل، او أي جزء منها لم يقدم من قبل لنيل أي درجة علمية او بحث علمي او بحثي لدى أي مؤسسة تعليمية او بحثية اخرى.

## Declaration

The work provided in this thesis, unless otherwise referenced, is the researcher's own work, and has not been submitted elsewhere for any other degree or qualification.

**Student's Name:** **اسم الطالب:**

**Signature:** **التوقيع:**

**Date:** **التاريخ:**

# Table of Contents

# List of Tables

# List of Figures

# List of Appendices

# List of Abbreviations

| | |
|---|---|
| AC | Alternating current. |
| AM | Air mass. |
| DC | Direct current. |
| Eff. | Efficiency. |
| $E_g$ | Energy gap. |
| FF | Fill factor. |
| MPP | Maximum power point. |
| M-S | Master –Slave. |
| NIS | New Israeli Shekel. |
| NOCT | Normal operating cell temperature. |
| PE | Percentage error. |
| PSH | Peak Sun Hours. |
| $PSH_m$ | Monthly average Peak sun hours. |
| PV | Photovoltaic. |
| SC | Single Centralized. |
| STC | Standard test condition. |

# List of Symbols

| | |
|---|---|
| $\$/W_P$ | Dollars per watt peak. |
| a | The length of the section of the PV array [m]. |
| $A_{cell}$ | The area of the cell [$m^2$]. |
| $A_{module}$ | The area of the PV module [$m^2$]. |
| $A_{PV}$ | The area of PV generator [$m^2$]. |
| $C_1$ | The linear loss coefficient. |
| $C_2$ | The square loss coefficient. |
| $d_{min.}$ | The minimum distance between two PV arrays facing south [m]. |
| $E_{in}$ | Input energy. |
| $E_{out}$ | Output energy. |
| $E_{sd}$ | The monthly average of daily solar radiation for a month [$kWh/m^2$-day]. |
| G | Solar radiation [$W/m^2$]. |
| $G_O$ | The peak solar radiation intensity [$W/m^2$]. |
| $G_{STC}$ | Solar radiation at slandered test condition [$W/m^2$]. |
| $I_{C.B}$ | The rated current of circuit breaker [A]. |
| $I_D$ | Diode current [A]. |
| $I_{fuse}$ | The rated current of fuse [A]. |
| $I_{max.array}$ | The maximum current of the PV array [A]. |
| $I_{mpp}$ | Current at maximum power point [A]. |
| $I_O$ | The leakage current of the diode [A]. |
| $I_{ph}$ | Photocurrent [A]. |
| $I_{rating}$ | The rating current of the protection device [A]. |
| $I_{SC}$ | Short circuit current [A]. |
| $\alpha_I$ | Temperature current coefficient [A/ºC]. |
| K | Boltzmann constant [1.381*10−23 J/K]. |
| K | Safety factor=1.25. |
| $K_0$-$K_2$ | Inverter model coefficients. |
| kWh | Kilo watt hour. |
| L | The latitude of the project site [degree]. |
| MWh | Miga watt hour. |
| $N_{module}$ | The number of PV modules. |
| $P_0$ | The no-load power loss [W]. |
| $P_{ac\,(t)}$ | The instantaneous ac output power [W]. |
| $P_{dc}$ | The DC power [W]. |
| $P_{dc\,(t)}$ | The instantaneous dc input power [W]. |
| $P_{dc.pu}$ | The per unit value of the DC power. |
| $P_{loss\,(t)}$ | The power loss [W]. |
| $P_{max}$ | Maximum power of the PV module [W]. |
| $P_{module}$ | The power of the PV module [$W_P$]. |

| | |
|---|---|
| $P_{mpp}$ | Power at maximum power point [W]. |
| $P_{PV}$ | The power of PV generator [$W_P$]. |
| q | Electron charge [1.602*10−19 C]. |
| $R^2$ | Coefficient of determination. |
| $R_s$ | Series resistance of the cell [Ω]. |
| $R_{sh}$ | Shunt resistance [Ω]. |
| T | Temperature [ºC]. |
| $T_{amb}$ | Ambient temperature [ºC]. |
| $T_{cell}$ | Cell temperature [ºC]. |
| $T_{STC}$ | Temperature at standard test condition [ºC]. |
| $\alpha_T$ | Temperature coefficient of maximum power [1/ ºC]. |
| V | Voltage [V]. |
| $V_{mpp}$ | Voltage at maximum power point [V]. |
| $V_{OC}$ | Open circuit voltage [V]. |
| $\alpha_V$ | Temperature voltage coefficient [V/ºC]. |
| $W_P$ | Watt peak. |
| β | The tilt angle of the PV array on a horizontal level [degree]. |
| η | Efficiency [%]. |
| $\eta_{inv.}$ | The inverter efficiency [%]. |

**Analysis of Power Conversion Stages and Efficiency Improvement Possibilities for Grid Connected PV System.**

**By**

**Eman Omar Mahmoud Abu Hani**

**Supervisor**

**Prof. Marwan Mahmoud**

## Abstract

In this thesis the improvement of large scale PV system conversion efficiency is presented. Mainly the inverter efficiency is considered to be improved by testing two different configurations of 100 kWp PV. The first configuration consists of one single centralized inverter and the second one of master-slave inverter. A Mathematical model is developed by MATLAB software to model the inverter efficiency as a function of input power then the power output is calculated by using hourly solar radiation and ambient temperature data over one year in Palestine. The simulation results show that the annual average energy production using the single centralized inverter is 181.26 MWh/year, while the annual production of master-slave inverter is 184.5MWh/year. In addition, by considering only the inverter efficiency the annual efficiency of DC/AC conversion stage for first system is 96.7% and for the second system is 98.4%.

Economic analysis shows that the additional investment in master-Slave configuration instead of using single centralized inverter can be covered within six and a half years.

# Chapter one
# Introduction

## 1.1 Introduction

The energy demand in the world is increasing by time and new types of renewable energy sources must be found in order to cover the future demands, since the conventional sources are about to be depleted. The evaluation of renewable energy in the last few years has exceeded all expectations. Solar energy is recognized as one of the most promising sources of renewable energy which use the sun's energy to produce electricity without producing any pollutants.

In this master thesis a grid connected PV system is studied. The PV system employs solar cells to utilize the solar energy as a power source to usable electric power. This power is transferred through power electronics device in order to convert the DC output power into AC output power appropriate to be injected into the electric grid.

The solar inverter is an essential part of a PV system; it is necessary and indispensable for connection with the electric power grid. Understanding how to control this device will increase the productivity of the system. The influence of the solar inverter will be studied to optimize the system efficiency.

The present research works focusing on maximizing the power output of grid-connected PV system which can be achieved by many solutions. In this master thesis master-slave configuration versus the single centralized

inverter is used for 100 kWp PV grid connected system as a case study .To a achieve this objective a MATLAB model is developed and used to describe the inverter conversion efficiency in order to calculate the produced energy using hourly solar radiation and ambient temperature data.

## 1.2 Thesis Objectives

The objectives of this thesis can be pointed as follows:

**1-** Study the performance parameters of grid connected PV system.

**2-** Study the topologies and function of power converters for grid connected PV system.

3- Survey the solar inverter types and efficiency.

4- Study the possibility of increasing the DC-AC conversion efficiency.

5- Use PVsyst software program to determine the losses in the system.

6- Use MATLAB software program to represent the proposed method for increasing the conversion efficiency.

7- discuss and evaluate the results of the simulation.

## 1.3 Problem Statement

In PV systems, inverter is an essential component that converts the direct power (DC) generated from the PV array into a usable alternating power (AC), it has a great effect on the performance of the PV system.

The efficiency of the inverter is not constant and varies from zero to nearly 98 %. Inverter maximum efficiency occurs at a loading level between 30% and 70% of the nominal power. The efficiency decreases for lower power, since all types of inverters have a minimum power self-consumption due to supply the auxiliary circuits and for the conduction and switching losses of semiconductor devices used in the inverter. So, it is very interesting to make the inverter working at its peak efficiency in order to increase the output power and reduce the payback period of PV system.

When a single inverter is used to convert the whole power generated from the PV array, the conversion efficiency is reduced drastically at low solar radiation level, such as in the morning and in the evening or during cloudy days. So it's better to substitute the single inverter into several low rating inverters connected to the PV generator in parallel.

This research presents a case study in Palestine to perform analysis and compare between two design configurations of grid connected PV systems, PV system with one central inverter and the other with multiple inverters in order to evaluate both systems based on better energy conversion.

## 1.4 Thesis Structure

This thesis is organized in eight chapters as follows:

**Chapter 1: Introduction.**

**Chapter 2: PV System Overview.**

This chapter introduces a brief review of the PV system classification and their main components :the solar cell and PV inverter; the fundamentals of photovoltaic cells, photovoltaic technologies, characteristics and performances of the solar cell, the PV inverter tasks and the classification of inverter are discussed.

**Chapter 3: PV Inverters in Large PV System.**

This chapter spots the light on the DC to AC conversion efficiency and a mathematical model of the inverter efficiency used for simulation. Also the master-slave inverter concept is discussed.

**Chapter 4: Solar Energy in Palestine**

This chapter presents the potential of solar energy and the ambient temperature in Palestine.

**Chapter 5: Sizing of PV System Components**

In this chapter, the process of selecting the main components of PV system is discussed.

**Chapter 6: Case Study Evaluation**

This chapter shows the way of improving the conversion efficiency of the PV system by using master-slave configuration instead of single centralized inverter. The flow chart of the two configurations is presented in this chapter.

**Chapter 7: Simulation Results.**

The produced energy per year, month and day is shown. The results and analysis comparison between the two configurations are discussed.

**Chapter 8: Economic Analysis.**

This chapter shows economical comparison between the two configurations. The economic analysis used in this work is based on the payback period of the two configurations.

**Chapter 9: Conclusions and Future Work.**

This chapter presents the thesis conclusions drawn from the study and the future recommendations possible within master-slave inverters.

# Chapter Two
# PV System Overview

## 2.1 Introduction

Photovoltaic (PV) system has been given a great attention worldwide among all renewable energy choices due to the fact that solar energy is environmentally friendly, clean and requires less maintenance. It generates electricity without producing emission of greenhouse gases or any other gases and its operation is virtually silent.

The capacities of PV systems range from small roof top PV systems with capacities in the range of 2-5 $kW_p$, to large PV system available with range exceeding hundreds of megawatts.

## 2.2 Classifications of Photovoltaic Systems

Photovoltaic system contains many interconnected components besides to the PV modules. It is designed to accomplish specific goals ranging from powering a small device to feeding electricity into the main distribution grid [1]. Figure 2.1 shows the main components of any PV system [2].

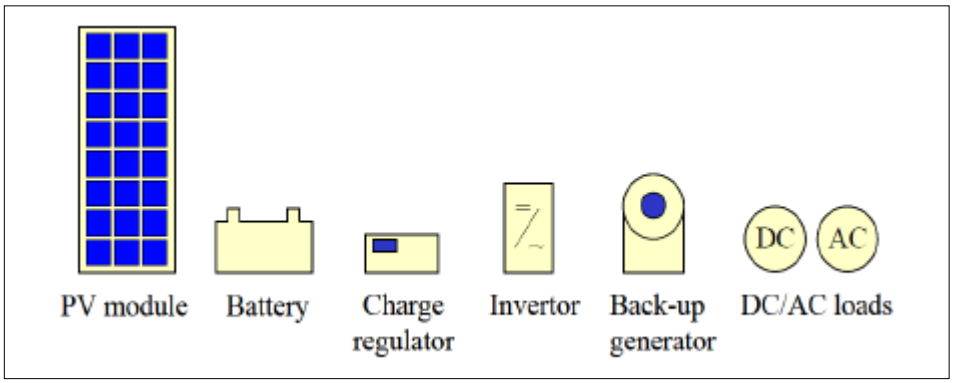


**Figure2.1:** PV system components [2].

Depending on the system configuration, PV system can be classified into two main types: stand-alone and grid-connected. The main difference between these two types is that in stand-alone systems the output energy of the system is matched with the load demand and without any connection to the main grid [2].

### 2.2.1 Stand-alone Systems

Stand-alone systems depend on solar power only. These systems may consist of the PV modules with power conditioning and control units (DC-DC converters, inverters), the load only or they can include batteries for energy storage. The capacity of the batteries must be able to store the energy produced during the day to be used at night and during periods of poor weather. Figure 2.2 shows schematically examples of stand-alone systems; (a) a simple DC PV system for powering water pump without any energy storage and (b) a complex PV system including batteries, power conditioners, and both DC and AC loads[2].

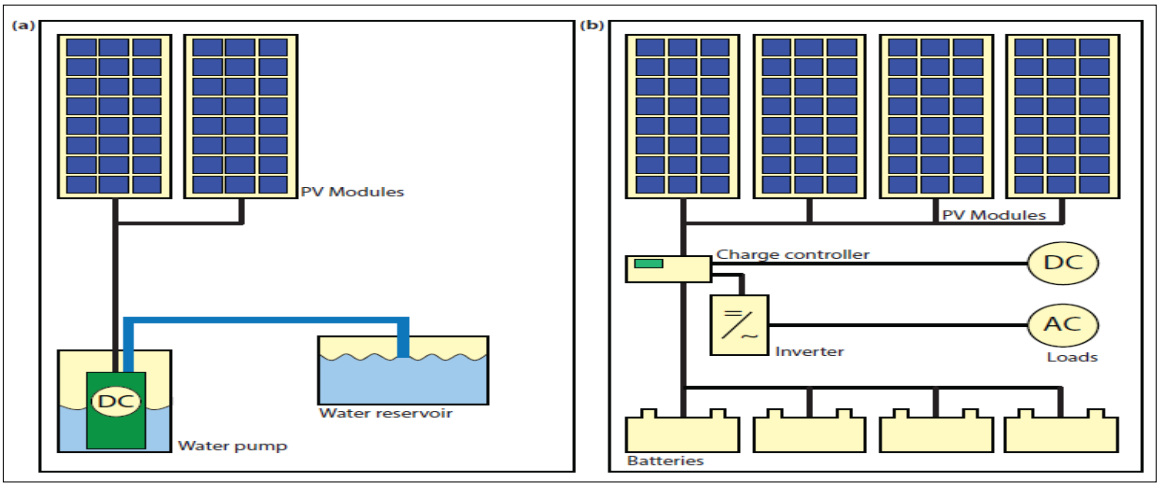


**Figure 2.2:** Stand-alone system. (a) A simple DC PV system without a battery, (b) a large PV system with both DC and AC load [2].

### 2.2.2 Grid-connected Systems

Grid-connected PV systems have increasingly become popular as building integrated applications which operate in parallel with the electric utility grid. As illustrated in Figure 2.3, they are connected to the grid via inverters, which convert the DC power into AC electricity. This type of PV system does not need batteries since the grid acquire all the generated electricity form a PV generator.

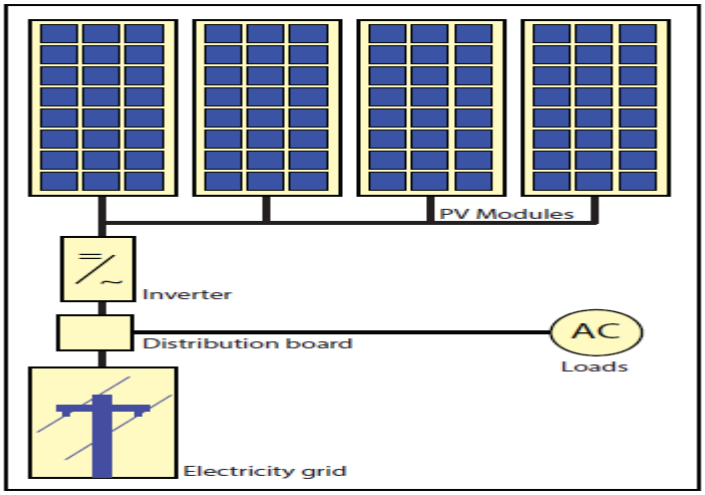


**Figure 2.3:** Schematic representation of a grid-connected PV system [2].

## 2.3 PV system components

The solar module and PV inverter are main components in grid connected PV system. This chapter will present a review of these two components in order to understand their operation.

### 2.3.1 Solar cell

Solar energy can be converted to electrical energy by photovoltaic or solar cell and this phenomena is known as photovoltaic effect, simply when light

strikes the surfaces of solar cell some of the energy is absorbed by the electrons of the semiconductor material and become free so the electrical charge carrier (holes and electrons) are generated and the current is produced.

Photovoltaic cells are made of semiconductor material usually silicon which enables the conversion of solar energy into electricity. A typical PV cell made of crystalline silicon is 12 centimeters in diameter and 0.25 millimeters thick. In full sunlight, it generates 4 amperes of direct current at 0.5 volts or 2 watts of electrical power [3].

**Figure 2.4:** Photovoltaic cell [4].

### 2.3.1.1 Solar Cell Technologies

Solar cell can be divided into two types of technologies, crystalline and amorphous (thin-film) silicon cell.

### 1- Crystalline Solar Cell:

Crystalline solar cell can be classified into two types:

- **Mono-crystalline (Single) Cells**

These are made using a single cylindrical silicon crystal. In these cells, the silicon has a single continuous crystal lattices structure with almost no defects or impurities. This type is the most efficient photovoltaic technology with 14% to 16% conversion of the solar energy into electricity. On the other hand, the manufacturing process is too complicated, resulting in slightly higher cost than other technologies [5].

The main properties of mono-crystalline PV cell are [6]:

- $V_{oc}$: 0.59 - 0.62 [V].
- $I_{SC}$=3 - 3.5 [A/100 $cm^2$].
- η: 13-16 [%].
- FF: 72-78 [%].
- Color: dark blue.

- **Poly-crystalline Cells**

They are made from the same silicon material except that instead of being grown into a single crystal, they are melted and the molten silicon is poured into a rectangular mold (cast). The cost of production is cheaper than the mono-crystalline due to simpler manufacturing process and they have become the most dominant technology. However they have a slightly lower efficiency than mono-crystalline [5].

The main properties of mono-crystalline PV cell are [6]:

- $V_{OC}$: 0.55 - 0.59 [V].
- $I_{SC}$: 2.4 - 3 [A/100cm$^2$].
- η: 10-15 [%].
- FF: 67-74 [%].
- Color: blue.

2- **Amorphous Silicon Cell**

In this type of technology, the silicon is deposited before it has crystallized into large, thin and flat substrates such as glass or plastic. Amorphous silicon absorbs lights more effectively than crystallized cell therefore, less raw material is needed which lead to a thinner cell, also known as a thin film technology. Thin film has a poor conversion efficiency varies from 6% to 10%. Light induced degradation is another disadvantage of this type; which reduced their output power over time mainly in the first year of operation then the output power tends to stabilize [5].

The main properties of amorphous silicon PV cell are [6]:

- $V_{OC}$: 0.62 - 0.8 [V].
- $I_{SC}$: 0.8 – 1.2 [A/100 cm$^2$].
- η: 6-10 [%].

- FF: 62-68 [%].

- Color: Dark green, black.

### 2.3.1.2 PV Cell Characteristics

PV cells are made from semiconductor material mainly silicon. They are designed to form an electric field positive on one side and negative on the other side forming p-n junction which is the basic structure of a solar cell. When cells facing solar energy, the electrons in the semiconductor material raise from valence band to conduction band when they absorb energy greater than energy gap ($E_g$) creating electron–hole pairs. When a voltage is applied across the cell forming an electrical circuit, then the electrons move freely resulting in a net current called photocurrent $I_{Ph}$, which is directly proportional to the intensity of the incident light falling on the cell. From previous explanation, one can notice that the solar cell acts as a diode during darkness [7].

Solar cell is usually represented by current source ($I_{Ph}$) in parallel with a diode as shown in Figure 2.5.

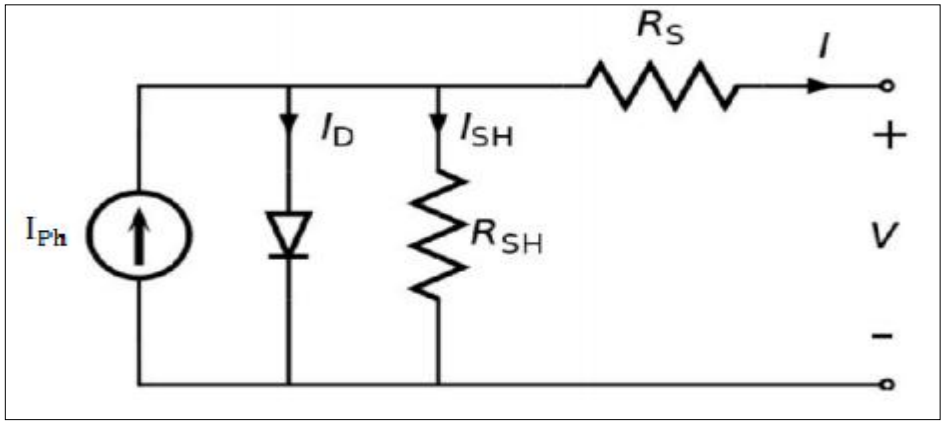


**Figure 2.5:** Equivalent circuit of a photovoltaic cell [8].

The net current is the difference between photocurrent ($I_{Ph}$) and diode current ($I_D$), which can be given by equation 2.1.

$$I = I_{Ph} - I_D - I_{sh} = I_{Ph} - I_o \left\{ \exp\left[\frac{q(V + IR_s)}{KT}\right] - 1 \right\} - \frac{V + IR_s}{R_{sh}} \quad (2.1)$$

Where,

$I_{Ph}$: Photocurrent generated by the incident light [A].

$I_D$: Diode current [A].

$I_O$: The reverse saturation or leakage current of the diode [A].

V: Voltage across the cell [V].

q: Electron charge [$1.602*10^{-19}$ C].

K: Boltzmann constant [$1.381*10^{-23}$ J/K].

T: Temperature of the cell [K].

$R_s$: Series resistance of the cell [Ω].

$R_{sh}$: Shunt resistance [Ω].

The series resistance is much smaller than the shunt resistance; therefore the photocurrent is much larger than the current absorbed by the shunt resistance and also the drop voltage across the series resistance can be neglected[6]. Then equation 2.1 becomes as:

$$I = I_{Ph} - I_D = I_{Ph} - I_o \left\{ \exp\left[\frac{q(V)}{KT}\right] - 1 \right\} \quad (2.2)$$

Figure 2.6 shows the I-V curve of a solar cell at a constant solar radiation and temperature.

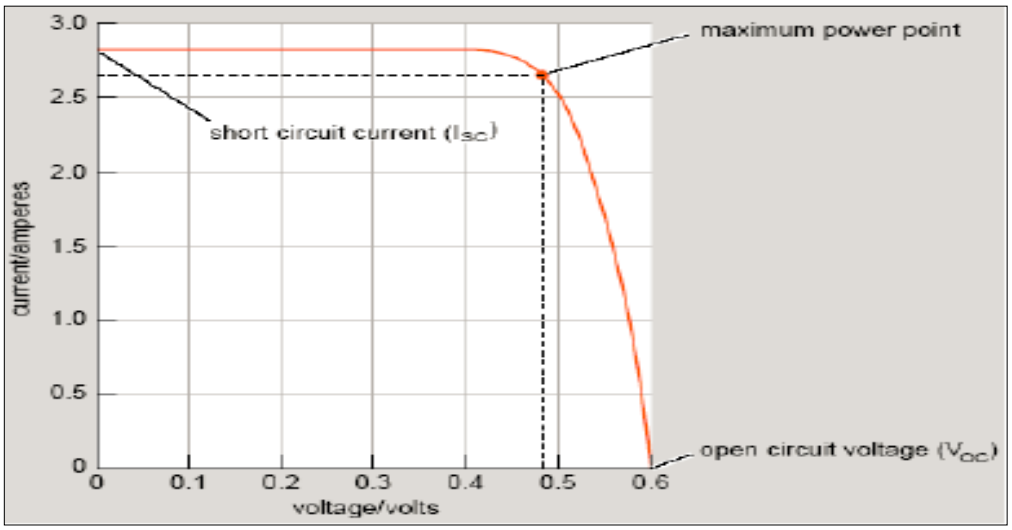


**Figure 2.6:** I-V curve of solar cell under standard cell condition [9].

Two important parameters should be understood from the I-V curve of the solar cell. The first one is the short circuit current ($I_{SC}$) and the second is the open circuit voltage ($V_{OC}$). When the terminals of the cell are shorted, then the voltage a cross the cell is zero and a maximum current follows in the junction known as ($I_{SC}$) which equals to photocurrent ($I_{SC}=I_{Ph}$). But when the terminals of the solar cell are disconnected then no current follows in the circuit and the voltage is at maximum known ($V_{OC}$) which can be expressed by equation 2.3[10].

$$V_{OC} = \frac{KT}{q} \ln\left(\frac{I_{Ph}}{I_O}\right) \tag{2.3}$$

At open circuit and short circuit cases, the output power is zero while between these two cases the power is more than zero, the maximum power point ($P_{MPP}$) occurs when the current and voltage are at maximum ($V_{MPP}$ &

$I_{MPP}$). This can be achieved by making the load resistance equals to the internal resistance of the solar cell. Figure 2.7 shows the I-V and P-V curves, the knee of the I-V curve represents the maximum power point of the solar cell [10].

$$P_{MPP} = V_{MPP} I_{MPP} \tag{2.4}$$

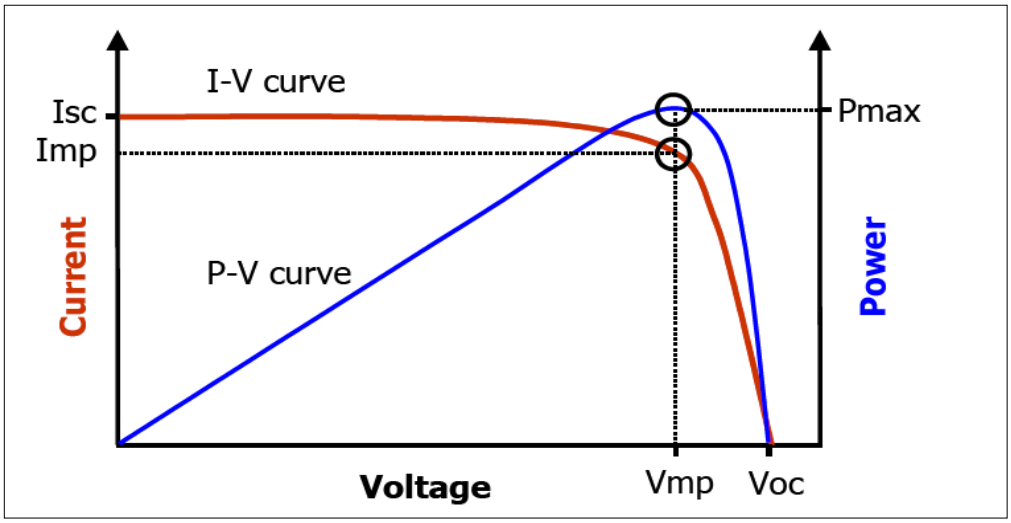


**Figure 2.7:** I-V & P-V curves for the solar cell [11].

From Figure 2.7, one can notice that the solar cell operates in two different modes depending on the connected load. The cell operates as a constant current source in the region starts form the short circuit current point ($I_{SC}$) to the maximum power point (MPP), and acts similar to constant voltage source in the region starting from maximum power point (MPP) to open circuit voltage point ($V_{OC}$).

The voltage and current at the maximum power point can be approximately calculated using the short circuit current and open circuit voltage as the following two relations 2.5 and 2.6[6].

$$V_{MPP} = 0.81V_{OC} \tag{2.5}$$

$$I_{MPP} = 0.9I_{SC} \tag{2.6}$$

Another important parameter of the PV characteristic is the fill factor FF, which is a measure of the quality of solar cell. It represents the ratio between the maximum power that can be delivered to the load and the product of the open circuit voltage $V_{OC}$ and the short circuit current $I_{SC}$. The higher the fill factor the higher output power. For high quality cell the fill factor is more than 0.7. Figure 2.8 represents the fill factor which is the ratio between the two rectangular areas seen in the Figure below and given by the following formula. The fill factor is equal to 1 (maximum value) when the two rectangular areas are equal.

$$FF = \frac{P_{MPP}}{V_{OC}\, I_{SC}} = \frac{V_{MPP} I_{MPP}}{V_{OC}\, I_{SC}} \tag{2.7}$$

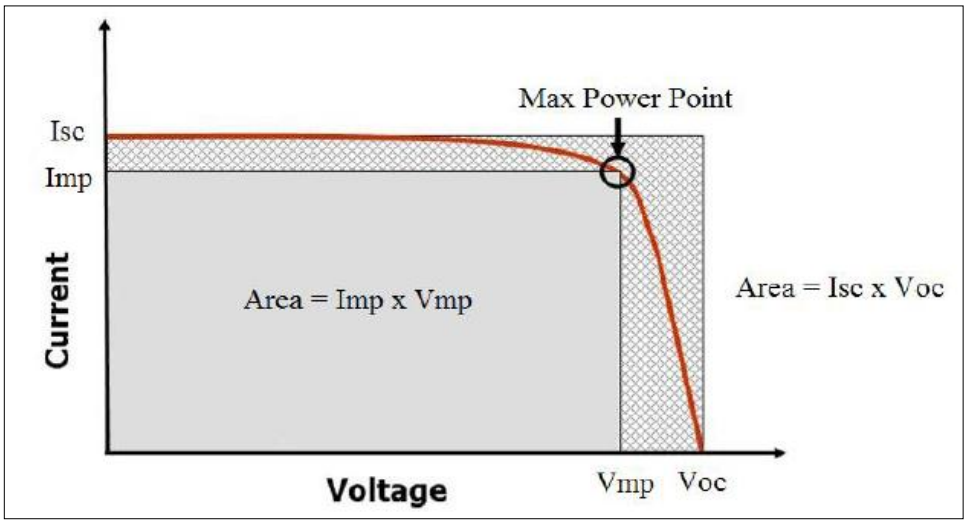


**Figure 2.8:** Fill factor [11].

PV efficiency is the most commonly used parameter to compare the performance of different solar cells. The efficiency is the ratio between the

output power produced by the solar cell to the incident or input power from solar radiation.

$$\eta = \frac{P_{out}}{P_{in}} = \frac{VI}{GA_{cell}} \tag{2.8}$$

Where,

$A_{cell}$: the area of the cell [$m^2$].

G: the solar radiation [$W/m^2$].

In order to use the efficiency parameter to compare between solar cells, the condition must be similar during measuring the efficiency. Generally, the efficiency of the PV cell is reported at standard test condition STC, and these STC relate to the IEC 60904/DIN EN standards Known as:

1- Vertical solar radiation G of 1000$W/m^2$.

2- Cell temperature T of 25 ºC with a tolerance of ±2ºC.

3- Defined light spectrum with an air mass AM of 1.5.

### 2.3.1.3 Solar Modules and Arrays

The solar cell is the basic element of PV systems. An individual solar cell produces approximately 0.6 volts under standard test condition regardless of its size and this voltage is inadequate therefore cells are connected in series in order to increase the voltage at the constant current level, and they are connected in parallel to increase the current at a constant voltage level.

photovoltaic module consists of multiple individual solar cells connected in series or in parallel to achieve the required voltage and current, and in order to protect them from the environment effect especially harsh environmental conditions they are encapsulated with tempered glass (or some other transparent material) on the front surface, and with a protective and waterproof material on the back surface [12].

Generally, the voltage of PV module is chosen to be compatible with a 12 V for battery charging and this module is known as standard modules (12 V module) [13]; for mono-crystalline solar cell 36 cells are connected in series but for poly-crystalline solar cell 40 cells are connected is series. When the output voltage and current from a single module is smaller than desired then the modules can be connected into series or parallel or mixed in order to get the required system, and this group of PV modules is called PV array. The connection method depends on which variable that needs to be increased. For a higher output voltage, the modules must be connected in series while connecting them in parallel in order to get higher currents. Figure 2.9 illustrates the construction of PV module and array [14].

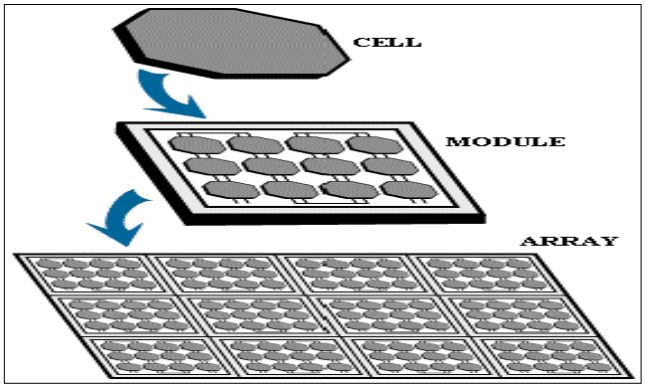


**Figure 2.9:** Relation between a solar cell, a module and an array [13].

The I-V characteristic curve for PV module or array is the same as the single solar cell taking into account the change in current and voltage according to the connection setting (series or parallel or mixed), Figure 2.10 shows the I-V curve for solar cells connected in series or parallel, so if two solar cells connected in series the current is still the same as single solar cell while the open circuit is double, but when connected in parallel the voltage doesn't change but the current becomes two times in comparison with the single solar cell [2].

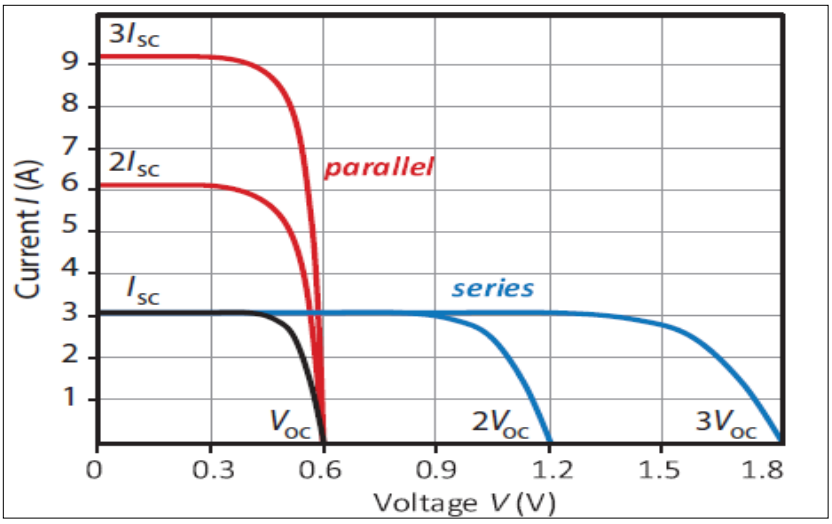


**Figure2.10:** I-V characteristic curve of solar cells connected in series or parallel [2].

### 2.3.1.4 Performance Factors of Solar Cell

The output power of photovoltaic module is affected by many factors; these factors vary by climatic conditions. The influence of these factors is discussed in this section.

### 2.3.1.4.1 Effect of Solar Radiation on PV Performance

Photovoltaic output power is affected by incident irradiation. PV cell short circuit current ($I_{SC}$) is linearly proportional to the irradiation; while open circuit voltage ($V_{OC}$) increases exponentially to the maximum value with increasing the incident irradiation and it varies slightly with the light intensity [15]. So the solar radiation has dual effect on the electrical IV characteristics of the PV cell, Figures 2.11 and 2.12 show the effect of solar radiation variation at the performance of PV module consisting of 36 cells of mono crystalline silicon [Siemens, SR50] at a constant temperature.

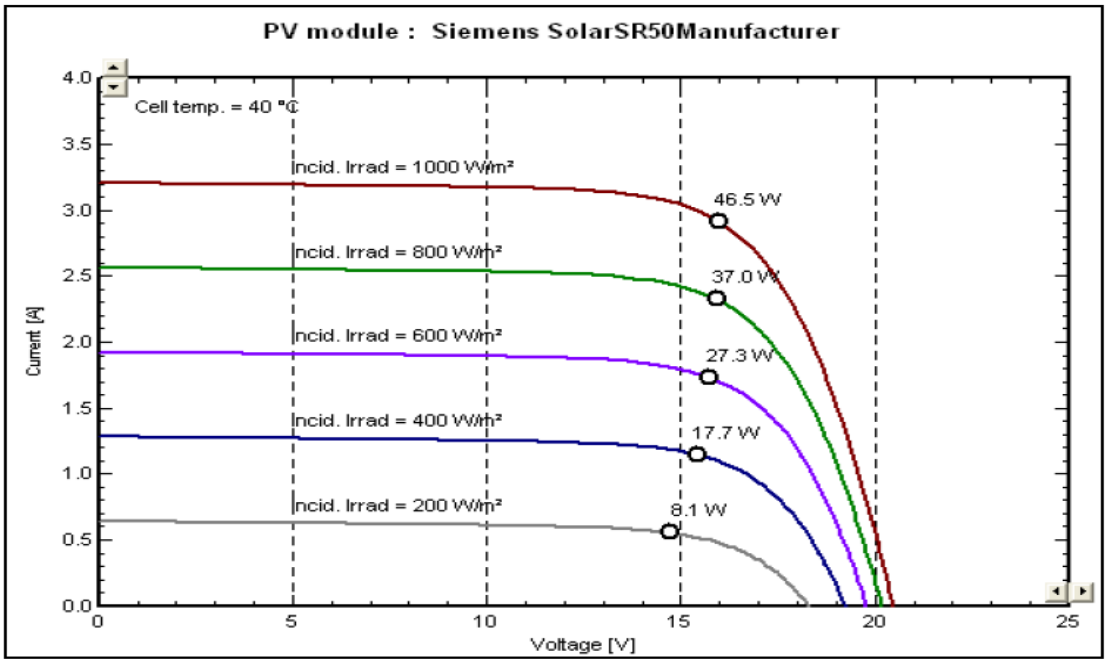


**Figure 2.11:** I-V curve of PV module at different radiation at constant temperature [16].

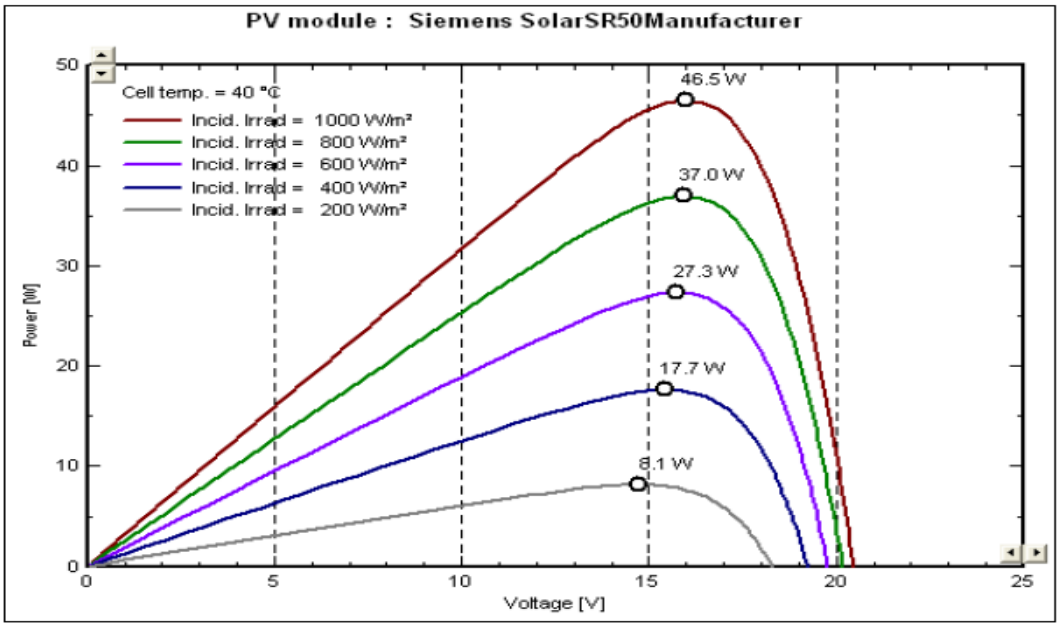


**Figure 2.12:** P-V curve of PV module at different radiation at constant temperature [16].

### 2.3.1.4.2 Effect of Temperature on PV Performance

The behavior of the PV system is affected by module temperature which is highly affected by ambient temperature so that the efficiency and the generated power produced by the system will be affected also. The short circuit current increases slightly when the PV module temperature increases above the Standard Test Condition (STC) temperature, which is 25$^{o}$C. However, open circuit voltage is enormously affected when the module temperature exceeds 25$^{o}$C. In other words, PV module voltage is reduced extremely compared to the increase in the current as the operating temperature increases. Therefore, the output power of the PV module is reduced [17]. Figures 2.13 and 2.14 explains the relation between PV module temperature with voltage, current, and power of 36 cells of mono crystalline silicon [Siemens, SR50] at constant solar radiation.

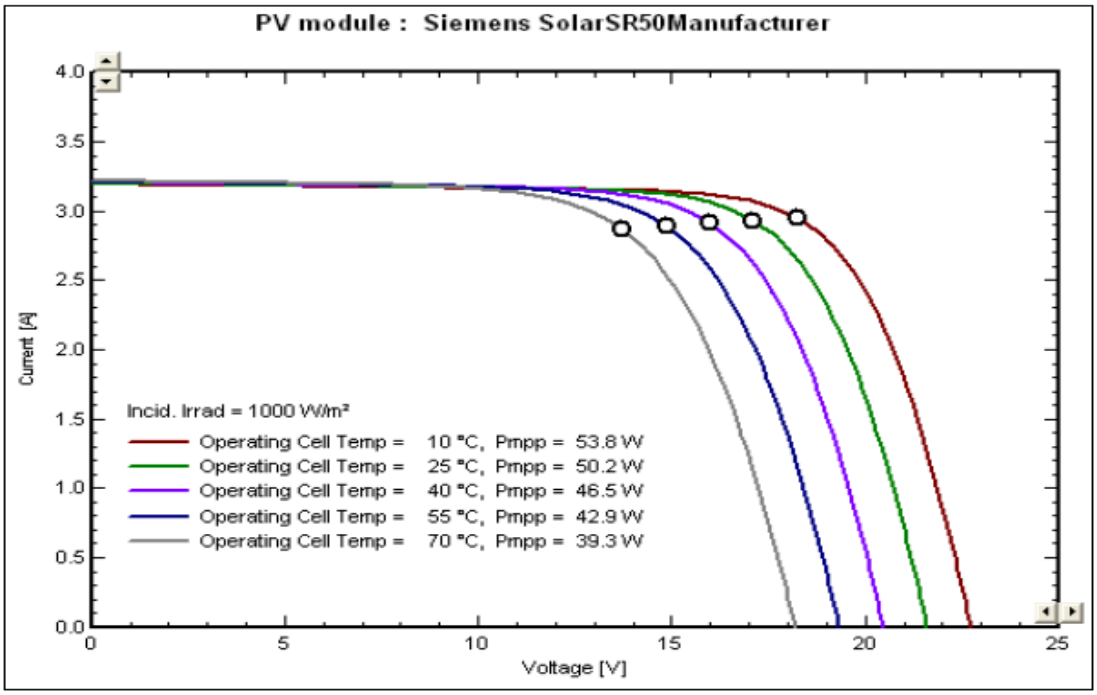


**Figure 2.13**: I-V curve with variation of temperature at constant radiation [16].

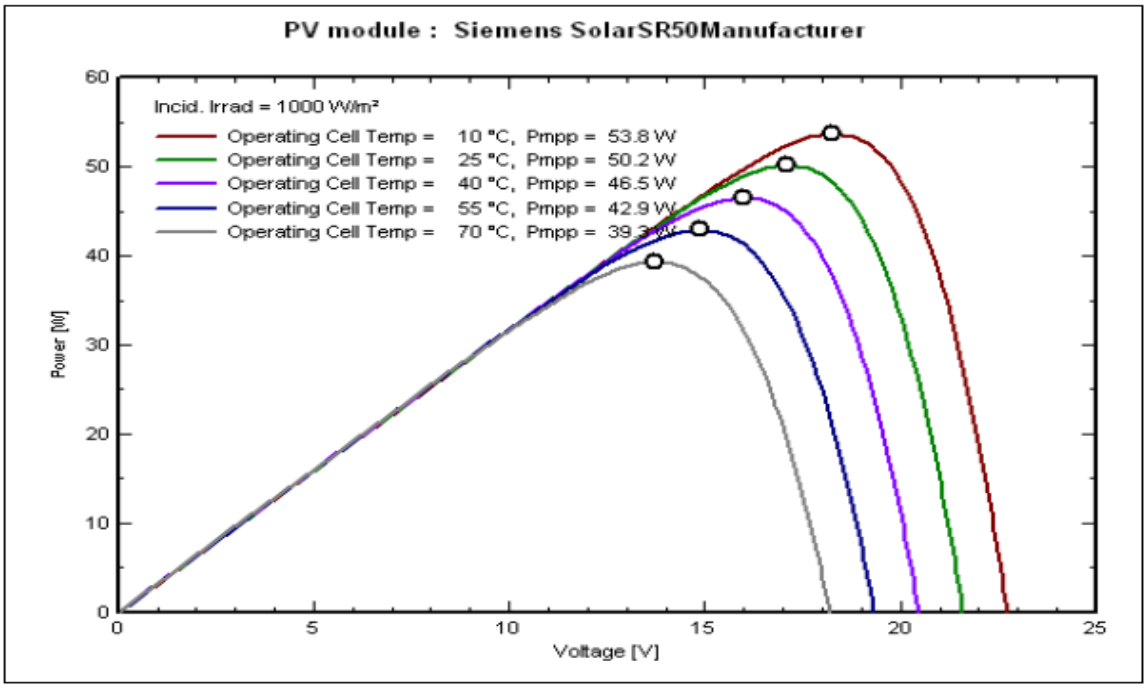


**Figure 2.14:** P-V curve with variation of temperature at constant radiation [16].

Even though both solar radiation and temperature are strongly coupled, solar radiation mostly affects the output current of PV module, while temperature basically changes the PV module output voltage.

The electrical parameters of the PV module in the datasheet are usually given at standard test condition. However, the module operates at higher temperatures and at somewhat lower solar radiation conditions in the field. For this purpose, manufactures usually include electrical parameters under Nominal Operating Cell Temperature (NOCT) which can be defined as the cell temperature that the solar cell will reach under the condition listed below [18]:

- Solar radiation on the cell surface is 800W/$m^2$.
- The ambient temperature is 20ºC.
- Wind velocity 1m/s.
- Output terminals of the cell are open.

The PV cell temperature can be calculated by using the linear approximation below for variations in ambient temperature and solar radiation [18].

$$T_{cell} = T_{amb} + \left(\frac{NOCT - 20}{800}\right) G \qquad (2.9)$$

Where,

$T_{cell}$: The cell temperature [ºC].

$T_{amb}$: The ambient temperature [ºC].

G: Solar radiation [W/$m^2$].

The mathematical equations 2.10 & 2.11 can be used to calculate the PV module output voltage and current at MPP at any solar radiation and temperature [19].

$$V_{mpp} = V_{mpp-STC} + (T_{cell} - T_{STC})\alpha_V \quad (2.10)$$

$$I_{mpp} = \frac{G}{G_{STC}} I_{mpp-STC} + (T_{cell} - T_{STC})\alpha_I \quad (2.11)$$

Where,

$V_{mpp}$, $I_{mpp}$: PV module output voltage and current at MPP at any solar radiation and temperature.

$V_{mpp-STC}, I_{mpp-STC}$: PV module output voltage and current on MPP, where these parameters are obtained from the datasheet.

$\alpha_V$, $\alpha_I$: Temperature voltage coefficient [V/ºC] and temperature current coefficient [A/ºC], these parameters are also obtained from the datasheet.

The generated power from PV module can be easily estimated using the environmental data (solar radiation and temperature) and the parameters specified in PV module datasheet. The temperature coefficient of maximum power, $\alpha_T$, is ordinarily negative, typical values for $\alpha_T$ are about -0.4% / ºC for single and poly–crystalline silicon and -0.1 to -0.2% / ºC for amorphous silicon and it can be used to calculate the PV output power using the equation below [20].

$$P_{DC} = P_{max}\left[\frac{G}{G_{STC}}\right][1 + \alpha_T(T_{cell} - T_{STC})] \quad (2.12)$$

Where,

$P_{max}$: Maximum power of the PV module [W].

$G_{STC}$: Solar radiation at standard test condition for [$W/m^2$].

$\alpha_T$: Temperature coefficient of maximum power [1/ ºC].

### 2.3.2 PV Inverter

The solar inverter is the heart of every PV system. It is used to convert the DC generated power from PV array into a usable AC power. The selection of the suitable inverter for a particular application depends on the waveform requirements for the load and on the efficiency of the inverter. The power generated from PV inverter can be fed to a commercial electrical grid (on grid) or can be used by a local power consumer (off-grid) when there is no connection with grid [21].

#### 2.3.2.1 PV Inverter Functions

The functions of the solar inverter differ from one to another depending on the application required so that one can distinguish between PV inverters depending on the basic following functions [22-23]:

1- Maximum power point tracking (MPPT)

The output power from PV module depends on environmental conditions such as the solar radiation, ambient temperature and shadowing conditions and these conditions continuously change over the day. For this reason, the Most of PV inverters have the ability to determine the optimal operating

point in order to ensure that the PV system operates at a point that gives the maximum power from the PV modules for every situation. This task is very important since it strongly affects the overall efficiency of the PV system.

2- Grid interface/Synchronization

This function is associated with grid-connected PV inverter only. Usually, voltage source inverter (VSI) is used to connect the PV modules with the AC grid and this type of inverters must have the ability to detect the grid voltage frequency and magnitude so that the inverter leaded by the grid.

3- Power decupling between AC and DC sides

Energy storage device such as an electrolytic capacitor can be used in order to adjust the fluctuation of power between DC and AC sides, due to the fluctuation nature of renewable energy sources. Therefore, the capacitor can provide uninterrupted power flow in the system and these electrolyte capacitors form the DC link and keep the voltage constant. Also, the switching frequency and the double grid frequency in single phase system can be decoupled by these capacitors.

4- Monitoring and securing (anti-islanding operation)

The PV inverter monitors the energy produced from the PV system and at the same time it monitors the power of the grid that connected with it so that when a problem occurs in the electric grid, the inverter must immediately interrupt the PV system from the grid since the PV modules always provide power during the shining of the sun. This function is so

important for the reasons of safety so the crew can repair the problem that occurs in the grid without exposure to risk.

5- low-loss conversion

Conversion efficiency is one of the most important parameters of solar inverter. This parameter determines the portion of DC input power that is converted into a usable AC power. Nowadays, with the developing of technology, inverters can operate with conversion efficiency near 98%.

### 2.3.2.2 PV Inverter Classification

Several types of PV inverters are available in the market. Generally, PV inverters can be classified into two different categories depending on basic characteristic:

1- With respect to the phase configuration of the AC side of the inverter.

2- With respect to the module wiring.

#### 2.3.2.2.1 Classification Based on Phase Configuration.

With respect to the phase configuration of the inverter AC side, PV inverter can be classified into one phase and three phases [24]:

1- Single Phase Inverter

Single phase inverter usually used in low power PV system application such as home or office roof top plant. Historically, the single-phase inverters inject current into one phase of the grid producing an imbalance

case between the phases of the grid. For stability reasons, these types of PV inverters are used up to maximum power of 5 kW in order to avoid a greater asymmetry between the phases.

2- Three Phase Inverter

For large PV systems with power rating greater than $5kW_P$, three phase inverters are used to produce a balance between the three phases of the grid. Three phase inverter is a combination of practically three single phase inverters connected to each load terminals.

**2.3.2.2.2 Classification Based on Module Wiring (Connection of the Inverter with PV Arrays and Grid).**

PV inverter can be classified into four different categories depending on the way in which the PV modules and the inverter are connected. The classification of these configurations is shown in Figure 2.15.

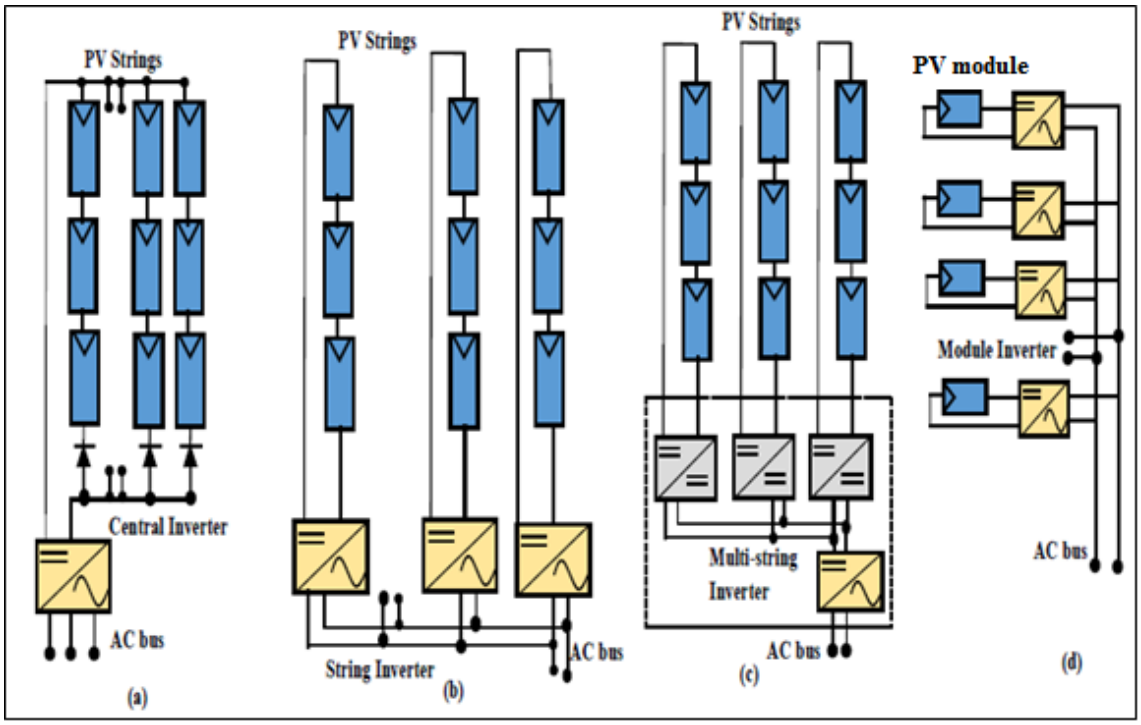


**Figure 2.15**: PV inverter configurations a. Central Inverter b. string Inverter c. Multi-string Inverter d. Module Inverter [25].

## 1- Central Inverter

In this type of configuration, the PV arrays are connected to a single central inverter as shown in Figure 2.15-a. The central inverter is available with power rating from several kW to MW and mostly used in three phase grid connected system. This topology has many advantages such as high conversion efficiency at low cost per watt, low total harmonic distortion (THD) losses in the system and required less maintenance compared to other configurations[22], [26].

However central inverter can result in mismatching power between the modules of string due to partial shading conditions resulting in decreasing the energy production of PV system. In addition to that, the reliability of the system is reduced due to the use of single central inverter. If the

inverter trips, the whole output power generation is out of the system. Also this type is quite expensive because of the long required cable between the PV arrays and the inverter resulting in high losses in these cables [22] [26].

**2- String Inverter**

The string inverters have been introduced to improve the drawbacks of the central inverters. In this topology, each of the PV string is connected to a separate inverter as shown in Figure 2.15-b. String inverters are available from 1 kW up to 10 kW power ratings and have higher price per kW as compared to central inverter and they are mostly used in low power applications such as residential applications. Besides the power rating, when this topology is compared with the central inverter, the efficiency and reliability increase of the whole system so that this topology is useful for those applications when the PV array consists of many strings and each string has its own orientation and in shadowing condition [22].

**3- Multi-String Inverter**

This type of configuration is an improvement of the string technology with a DC to DC converter for each string before it is connected to a common inverter as shown in Figure 2.15-c. Multi-string is inverter available in the market within the power range of 1kW up to 6kW. The main advantage of this topology is that each string has its own MPPT control via DC to DC converter leading to improving the efficiency of the PV system than the other configurations. However multi-string configuration has more power

loss as compared to string inverter due to two power conversion levels[22], [26].

### 4- AC Module Inverter(Micro Inverter)

Each module in this topology has its own inverter which provides independent MPPT in order to optimize the output energy from each individual module rather than an entire string. This configuration is shown in Figure 2.15-d. No DC wiring is required in the AC module inverter so that the risk of electric arcing and firing is reduced, in spite to these advantages, this inverter has low power level up to 400 W per unit leading to relatively high price and low efficiency that can't be compensated with the separate MPPT for each module. In addition, this type of inverter technology packing with the PV module as one device and the available inverter in the market does not reach the lifetime of the PV module (20 years) resulting in failure of PV module before reaching the end of its lifetime [22].

# Chapter Three
# PV Inverters in Large PV system

## 3.1 Introduction

Using one large inverter for converting the whole input power of a PV generator is a simple way but may be not the best method due to the relatively low DC to AC conversion efficiency mainly in low power range. Also this way will prevent a future expansion of the PV system. So, in order to overcome this problem a master-slave inverters is a good solution.

This chapter spots the light on the inverter conversion efficiency, master and slave inverter and their control strategy. Also, a mathematical model of DC to AC conversion efficiency for the used PV inverters is introduced.

## 3.2 DC to AC Conversion Efficiency

The DC to AC conversion efficiency is the ratio of the AC output power of inverter delivered to the grid to the DC input power of the inverter [27].

$$\eta(t) = \frac{P_{ac}(t)}{P_{dc}(t)} = \frac{P_{dc}(t) - P_{loss}(t)}{P_{dc}(t)} \quad (3.1)$$

Where:

$P_{dc}$ (t): The instantaneous dc input power.

$P_{ac}$ (t): The instantaneous ac output power.

$P_{loss}$ (t): The power loss.

Power losses of the solar inverter can be defined as [28]:

$$P_{loss} = P_0 + C_1.P_{ac} + C_2P_{ac}^2 \quad (3.2)$$

From the above equation; the power losses consist of two parts: constant and load dependent part. The constant part ($P_0$) represents the no-load power loss during the operation in order to supply the control systems and the auxiliary circuits, while the load-dependent part consists of the conduction and switching losses on the power switches which depends on the magnitude of the output current ($C_1$ represent the linear loss coefficient and $C_2$ represents the square loss coefficient). Therefore, the power loss of the solar inverter is not constant; making the efficiency depends on the load condition.

The selection of an appropriate inverter for a PV system is absolutely essential since the inverter is the heart of every PV power plant. The most important electrical characteristics are the DC to AC conversion efficiency of the PV inverter. If the power conversion efficiency of the inverter is low, then the overall efficiency of the PV system will be reduced [29].

In fact, the efficiency of the inverter is not constant. It strongly depends on the DC input power, varying from zero to nearly 99%. Therefore, it is important to make the inverter works near the optimal load conditions in order to get the peak conversion efficiency [27]. Figure 3.1 shows the efficiency curve for a commercial inverter obtained from the data provided by its manufacture, the curve shows the variation of the efficiency as a function of the ratio of output power to inverter's rated capacity ($P_{AC}/P_{inv,rated}$).

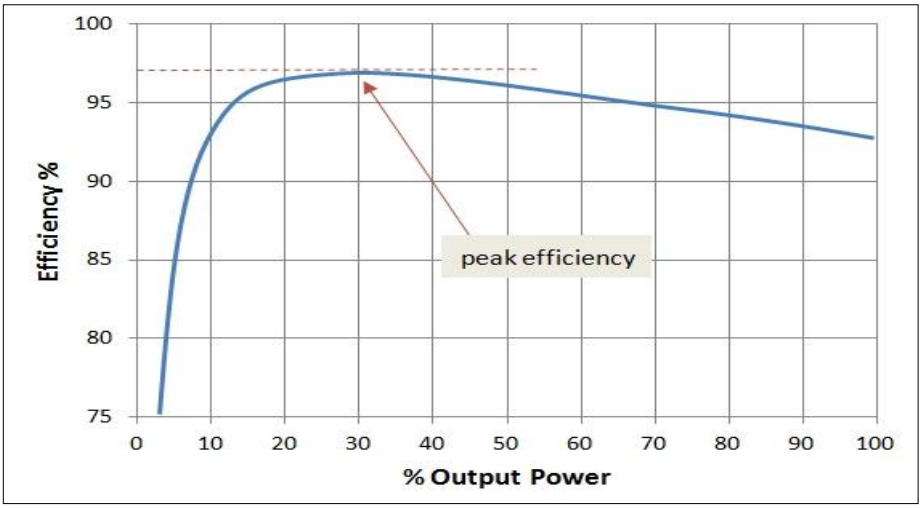


**Figure3.1:** DC to AC efficiency curve of PV inverter [30].

It can be noticed from Figure 3.1 that the inverter reaches its maximum efficiency at 30-60% of the rated power and somewhat the efficiency reduces little at full load, while it declines at a power level below 20% due to the self-consumption power required by the inverter.

Solar inverter with large rated power will operate at low efficiency during the time period when output power is less than the rated PV array power (during sunrise, sunset and cloudy days) while low rated power inverter will not be able to process part of the DC output power during the high radiation period since the output power from the PV array is more than the rated power of the inverter [27].

## 3.3 Mathematical Model of DC to AC Conversion Efficiency Curve

A simple mathematical expression found in the literature with very good accuracy can be used to describe the efficiency curve of any solar inverter; the efficiency curve can be represented by using a power function as used in [31].

$$\begin{cases} \eta_{inv} = K_0 . P_{dc.pu}^{K_1} + K_2 & P_{dc.pu} > 0 \\ \eta_{inv} = 0 & P_{dc.pu} = 0 \end{cases} \quad (3.3)$$

Where,

$\eta_{inv}$: The efficiency of the inverter [%].

$P_{dc.pu}$: The per unit value of the DC power [$P_{dc}/P_{inv.rat}$].

$K_0$-$K_2$: Mathematical coefficients that should be determined.

The model coefficients $K_0$, $K_1$and $K_2$ can be obtained by using a MATLAB fitting tool. Therefore samples of the conversion efficiency curve as shown in Figure 3.2 should be converted to data points of ($\eta$, $P_{dc.pu}$) by the help of Engauge Digitizer software then the resulting data points are usually used as input to MATLAB fitting tool. The process of extracting the data from the curve is shown in the following Figure. An image file is imported, digitized within Engauge, and Exported the curve points into a tabular text file.

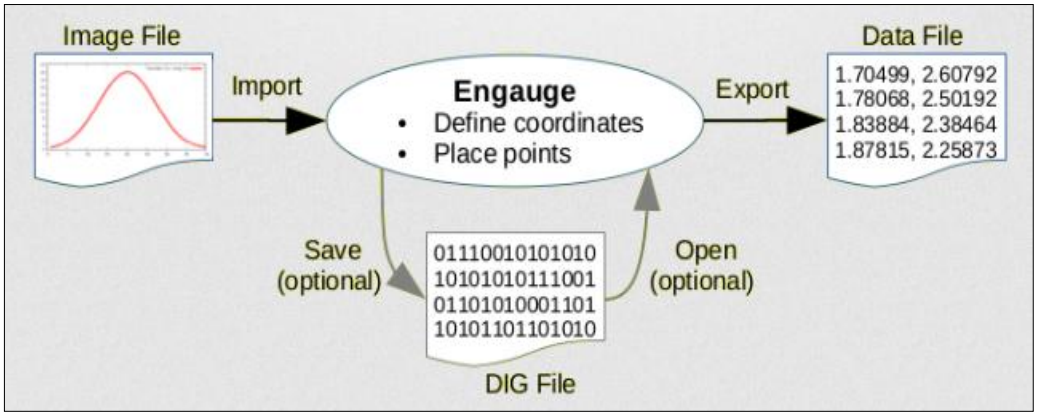


**Figure 3.2:** Manually Digitizing a Point Graph Image.

The shape of the conversion efficiency follows the expected behavior described by a power function. Figure 3.3 shows the conversion efficiency curve of the inverter SMA Tripower 25000TL-JP (points) and the fitting curve developed by MATLAB fitting tool. The fit between the conversion efficiency curve obtained from datasheet and the curve described by the mathematical model has a coefficient of determination $R^2$ greater than 0.95 for all used inverters. Where $R^2$ is a statistic that will give some information about the goodness of fit of a model. the $R^2$ is a statistical measure of how well the regression line approximates the real data points. An $R^2$ of 1 indicates that the regression line perfectly fits the data.

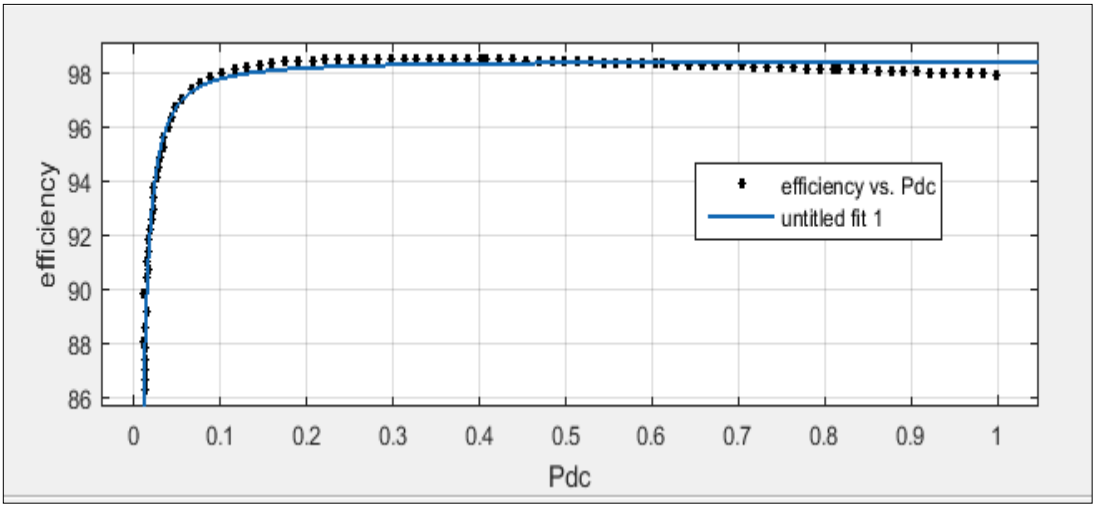


**Figure 3.3:** Fitting curve for DC to AC conversion efficiency curve of the inverter SMA Tripower 25000TL-JP.

In my work, three commercial inverters of rated powers 25 kW, 50 kW and 100 kW are used (section 5.4 explains why we selected these type of inverters). The calculated models coefficients for the chosen inverters types

are shown in Table3.1using the Engauge Digitizer software and MATLAB fitting tool.

**Table 3.1: Inverter model coefficients.**

| Rated power | $K_0$ | $K_1$ | $K_2$ |
|---|---|---|---|
| 25 kW | -0.04067 | -1.266 | 98.46 |
| 50 kW | -0.06439 | -1.483 | 98.67 |
| 100 kW | -0.005904 | -2.003 | 97.2 |

From the above Table, one can notice that for each used solar inverter, we have $K_0$ & $K_1$ are always small and less than zero while $K_2$ is large and positive. Therefore the efficiency curve for any solar inverter can be easily described by a simple mathematical model by using Engauge Digitizer software and MATLAB fitting tool. Appendix A shows the extract points ($\eta$, $P_{dc.pu}$) for each inverter and the percentage error PE in efficiency when using the developed mathematical model.

### 3.4 Master - Slave Inverter

Maximization of the productivity for the photovoltaic system is a very important goal which can be achieved by many methods, such as using high efficiency and low temperature losses solar cell technologies, sun tracking system, DC power optimizer, master-slave (M-S) configuration of DC-AC converters, etc.

My thesis focuses on the using of single centralized inverter (SC) versus the using of master-slave (M-S) inverters in which the DC output power from the photovoltaic system shared among the inverters depending on the

power rating for each used inverter. If the used inverters are equal in size then the power is divided equally among the inverters.

The SC inverter is divided into several lower power-rating inverters that connected to the same output power of PV generator where one of these inverters is operating continuously as a master inverter and the other slave inverters is switching on /off according to the DC output power of PV generator and when the output power of PV generator decreases due to the variation in atmospheric conditions the slave inverters are automatically disconnected. By this method, all inverters are operating at their optimal efficiency.

To illustrate the above fact, Figure 3.4 shows the efficiency curve for the selected single centralized inverter (100kW) managing the total power of the system (in blue) and the efficiency of the three parallel inverters which are selected to work as master-slave topologies (in red). The data used to construct these two efficiency curves have been obtained from the data sheet of each selected inverters and by using the developed mathematical model of them.

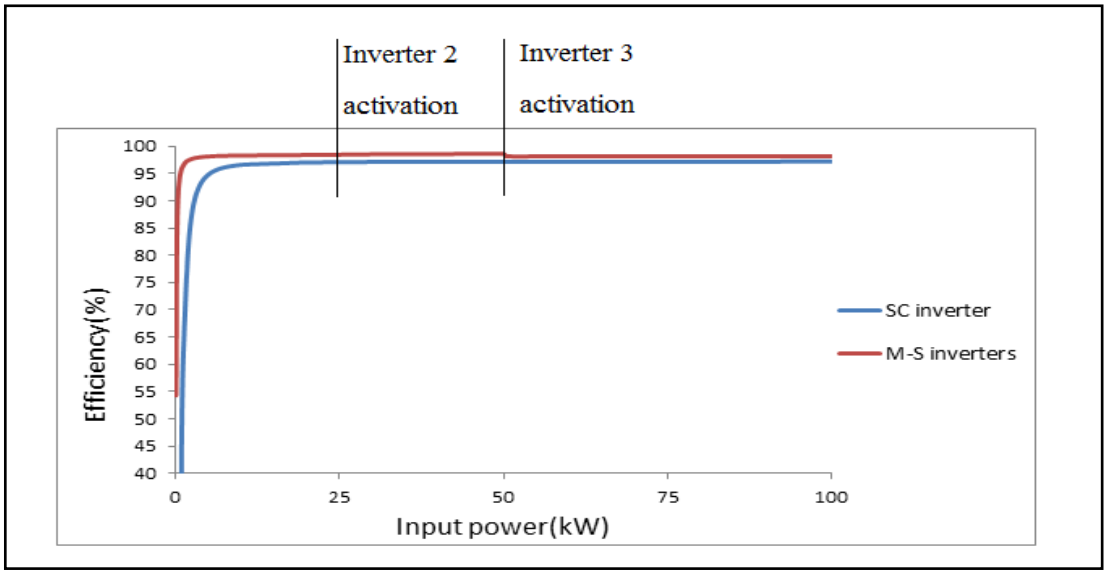


**Figure 3.4:** Efficiency curve of a single centralized inverter versus master slave inverters.

From the above Figure; the master-slave inverters are yielding better conversion efficiency at low power range.

## 3.5 Power Loss Diagram

The loss diagram provides a quick look at the quality of a PV system design, by identifying the main sources of losses. My work focuses on the inverter loss in order to compare between the two used configurations.

PVsyst software program is a good tool to calculate several loss parameters during the simulation. At the beginning the components (PV inverters and module) used in the PV system for both configurations is defined in the program by using their manufacturer's datasheets, it can be created from scratch (button "New"),then These components are stored in my own working space.

In PVSYST, the solar resource input can be the coordinates of the location. Based on location coordinates, data can be accessed from NASA website dealing with Meteorological data. the proposed site i.e. Nablus has latitude 32,22 North and longitude 35.26 ‘East.

After defining all required elements that are needed for a simulation (the system size, the type and number of PV modules and the type and number of inverters that will be used). the program provides a complete report in which the loss diagram is available for the whole year.

Figure 3.5 shows the loss diagram when using SC inverter, while Figure 3.6 provides the loss diagram when using master slave inverters.

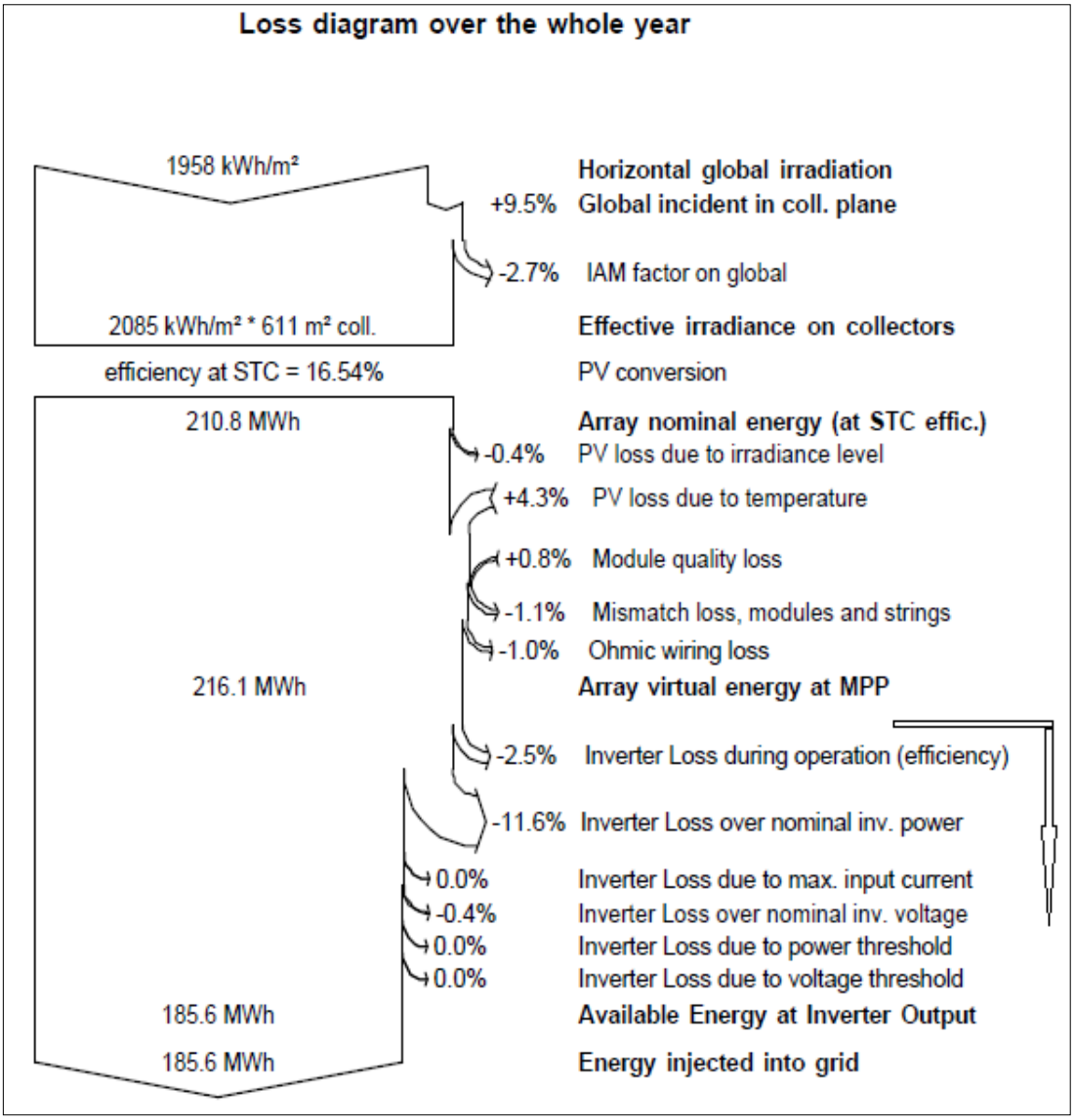


**Figure 3.5:** SC inverter loss diagram.

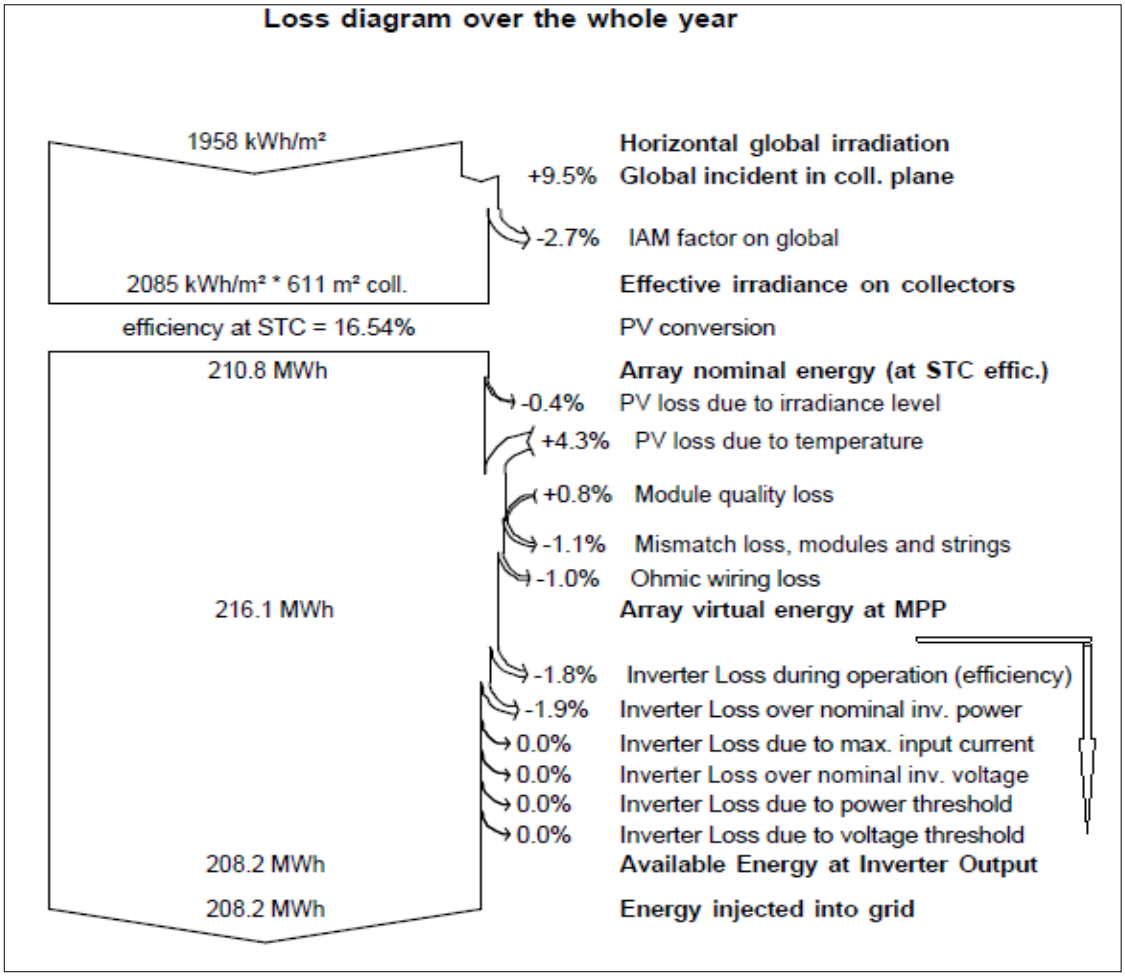


**Figure 3.6:** Master- Slave configuration loss diagram.

The power loss diagram is very useful for comparing the two configurations. From the above two diagrams, we can notice that the inverter loss is minimized when using master-slave configuration instead of SC inverter resulting in maximization of the produced energy.

# Chapter Four
# Solar Energy in Palestine

## 4.1 Introduction

In order to calculate the output power of PV system the solar radiation and ambient temperature data should be available, and these data play a significant influence in designing and sizing of the PV power system. The solar radiation and the ambient temperature depend on the geographic location, the day of the year and the time of the day.

Palestine is located between 29.3 and 33.15 north latitudes of the equator, and between 34.15 and 35.40 east longitudes of the Greenwich line. Figure 4.1 shows the map of Palestine with latitude and longitude values.

For testing the proposed model, Nablus site is considered as a case study.

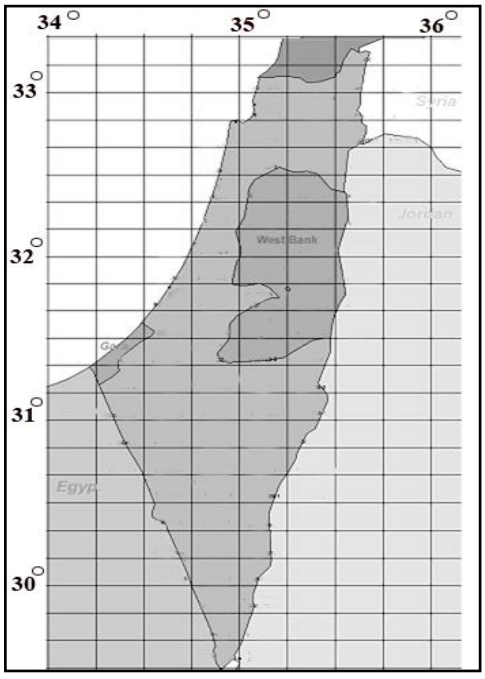


**Figure 4.1:** Palestine map with latitude and longitude values [9].

## 4.2 Solar Radiation in Palestine

Palestine has the feature of a high solar energy potential due to its location. The daily average of solar radiation intensity on horizontal surface is about 5.4 kWh/$m^2$-day and it has around 3000 sunshine hours/year, so it's suitable to use the PV system in order to produce solar electric energy in a sustainable way [32].

Solar radiation and temperature data are available over one year on hourly interval basis for Nablus site in order to use them by the simulation program. The figure below represents the monthly average of daily solar radiation in Nablus site for all months in the year. Given that the measurements were taken place on the horizontal surface and the readings are in kilo watt hour per meter square and day.

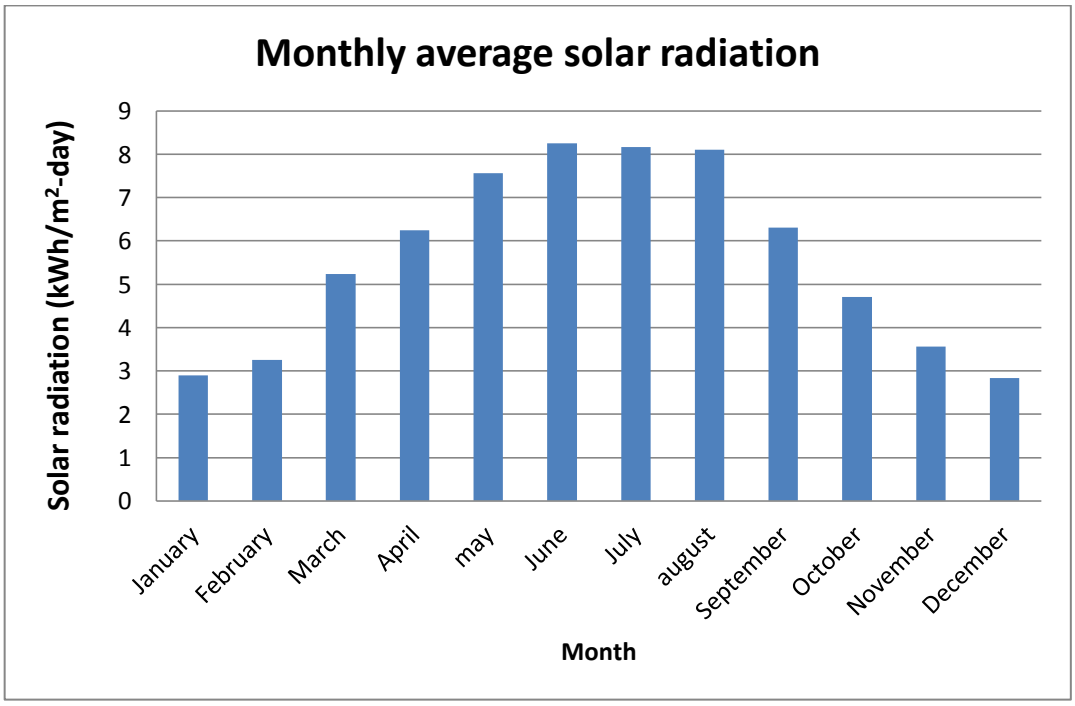


**Figure 4.2:** Monthly average of daily solar radiation for Nablus site.

From the data in Table 4.1, December has the lowest monthly average solar energy which is about 2.84 kWh /$m^2$-day while the highest one is in June which is about 8.245 kWh/$m^2$-day.

The number of hours during which solar radiation is 1,000 watts per square meter is known as Peak Sun Hours (PSH). And it is important to note that the hours of daylight are not the same as Peak Sun Hours. However, the PV panel may receive an average 7 hours of daylight per day but the average peak sun-hours may be 3 or 4 hours.

PSH can be calculated for every month from the above data using the following equation:

$$PSH_m = \frac{E_{sd}}{G_0} \quad (4.1)$$

Where:

$PSH_m$: Monthly average Peak sun hours [h]

$E_{sd}$: The monthly average of daily solar radiation for a month [kWh/$m^2$-day].

$G_0$: The peak solar radiation intensity which equals to 1000 [W/$m^2$]

So for example, $PSH_m$ in January equal to =2890/1000=2.89 hours.

Knowing the yearly average peak sun-hours for any location is a helpful tool for determining whether or not the PV system worthwhile investment for that location. The yearly average peak sun-hours for Nablus site can be calculated using equation 4.2

$$PSH = \frac{\sum PSH_m}{12} \tag{4.2}$$

$$PSH = \frac{2.89+3.25+5.23+6.25+7.56+8.25+8.17+8.1+6.3+4.7+3.56+2.84}{12}$$

$$PSH = 5.59h.$$

## 4.3 Ambient Temperatures in Palestine

As we mentioned before, the output power from PV module is affected by the ambient temperature and solar radiation changes. The change in temperature will affect the PV current slightly and linearly while the PV voltage is affected strongly and inversely. The variation of PV module efficiency with the temperature at solar radiation of 1000W/m$^2$ is shown in Figure 4.3 [34]. There is an inverse linear relation between the PV efficiency and the ambient temperature so we can control the efficiency of PV module by changing the temperature around it.

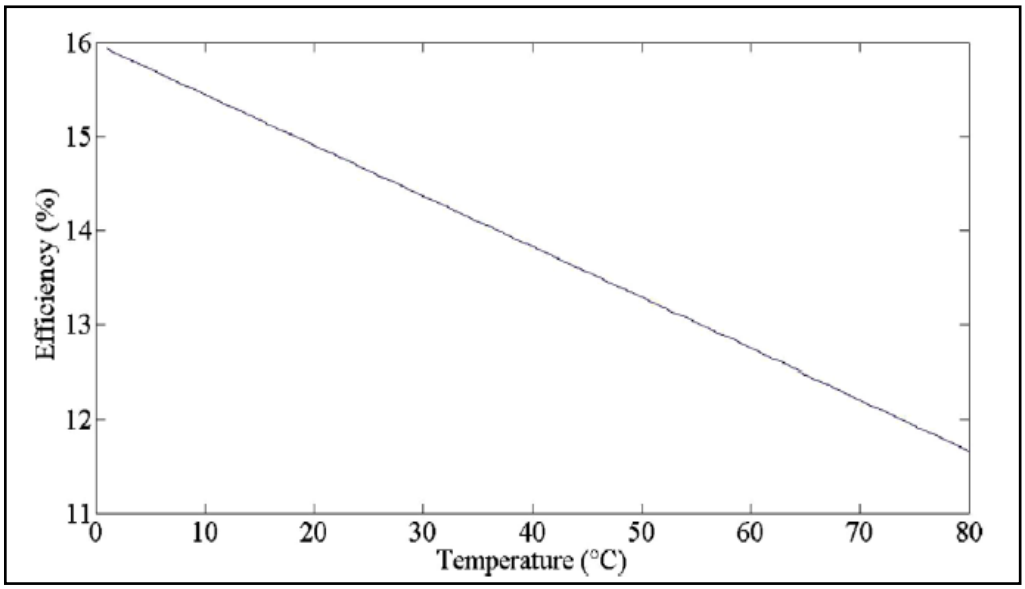


**Figure 4.3:** Photovoltaic cell efficiency versus temperature [34].

Palestine has a Mediterranean climate characterized by long, hot summers and short, cool, rainy winters, January is the coldest month with temperatures varies from 5 to 10 °C, and August is the hottest month with a temperature reaching up to 38°C [35]. Table 4.1 shows the average temperature per month for Palestine countries. The Figures stand for temperature in degrees Celsius.

**Table 4.1: Average temperature per month for Palestine countries [36].**

| Month | Average temperature | | | | | | |
|---|---|---|---|---|---|---|---|
| | Gaza | Ramallah | Nablus | Jericho | Hebron | Bethlehem | Jerusalem |
| Jan | 16 | 9 | 10 | 20 | 9 | 11 | 10 |
| Feb | 19 | 13 | 13 | 22 | 12 | 14 | 13 |
| Mar | 20 | 15 | 15 | 25 | 15 | 16 | 15 |
| Apr | 22 | 20 | 19 | 32 | 20 | 21 | 19 |
| May | 25 | 24 | 25 | 34 | 24 | 25 | 24 |
| Jun | 28 | 25 | 25 | 37 | 26 | 27 | 26 |
| July | 30 | 28 | 29 | 39 | 28 | 29 | 28 |
| Aug | 30 | 27 | 28 | 39 | 28 | 30 | 30 |
| Sep | 31 | 27 | 28 | 36 | 27 | 28 | 27 |
| Oct | 29 | 25 | 30 | 32 | 25 | 26 | 25 |
| Nov | 25 | 17 | 18 | 27 | 18 | 19 | 18 |
| Dec | 19 | 12 | 18 | 22 | 12 | 13 | 12 |

The efficiency of PV module in summer season will be decreased due to high temperatures resulting in decreasing the output power generated from the module, while in winter season the temperature is low so the PV module may produce energy near its peak power.

# Chapter Five
# Sizing of PV System Components

## 5.1 System Overview

The proposed system is a grid-connected photovoltaic system that connected to the grid without the need to a battery backup capability since the grid will also supply electricity. The proposed system is rated at 100kWp as a case study. The PV arrays and the inverters are the most important components of the system. Figure 5.1 shows a general grid-connected system without battery backup.

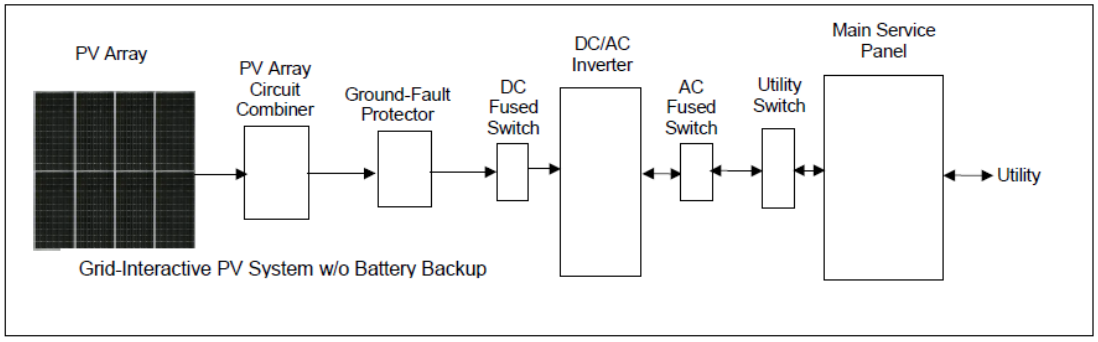


**Fig 5.1**: Grid-connected system overview [15/27].

In this thesis, two different configurations for inverter connection are studied:

First configuration: single centralized inverter.

Second configuration: master- slave inverters.

## 5.2 PV System Schematic Diagram

Figure 5.2 shows the schematic diagram for single centralized configuration with the main components of this system.

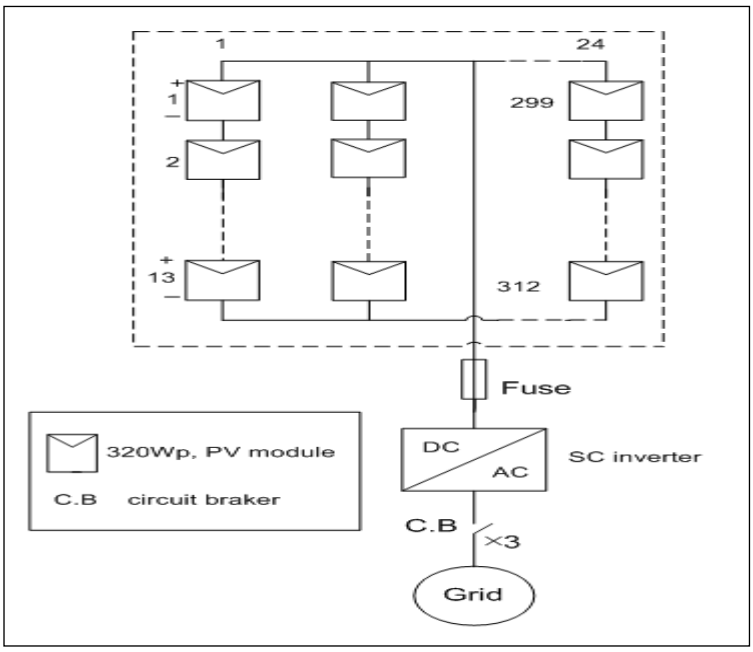


**Figure5.2:** Schematic diagram for single centralized configuration.

PV system block diagram for master-slave configuration is shown in Figure 5.3.

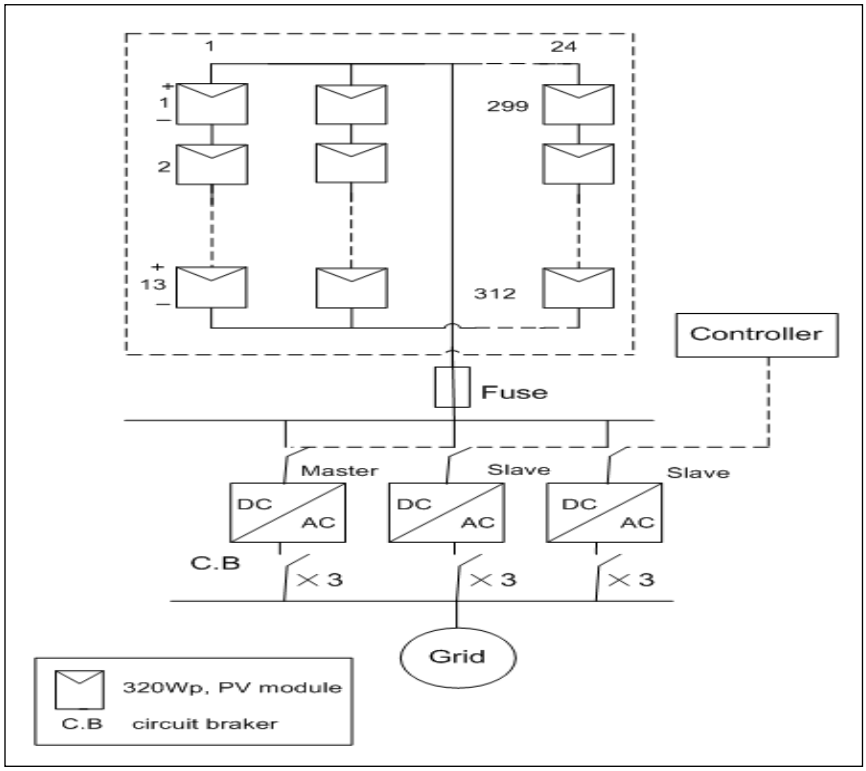


**Figure 5.3:** Schematic diagram for master-slave configuration**.**

## 5.3 Module Selection

A poly-crystalline PV module type (Amerisolar AS-6P) is used in this system with the specifications shown in Table 5.1. All the specifications are found in Appendix B-1.

**Table 5.1: Specification of Amerisolar AS-6P PV module at standard test conditions [38].**

| **Electrical characteristic at STC** | |
|---|---|
| Maximum Power($P_{max}$) | 320 W |
| Open Circuit Voltage($V_{OC}$) | 45.7 V |
| Short Circuit Current($I_{sc}$) | 9 A |
| Voltage at Nominal Power ($V_{mpp}$) | 37.1 V |
| Current at Nominal Power($I_{mpp}$) | 8.63 A |
| Number of cells | 72(6*12) |
| Area | 1.94 $m^2$ |
| Efficiency | 16.49 % |
| **Temperature Characteristic** | |
| Nominal Operating cell Temperature(NOTC) | 45ºC ±2ºC |
| Temperature coefficient of $P_{max}$ | -0.43%/ºC |
| Temperature coefficient of $V_{OC}$ | -0.33%/ºC |
| Temperature coefficient of $I_{SC}$ | 0.056%/ºC |

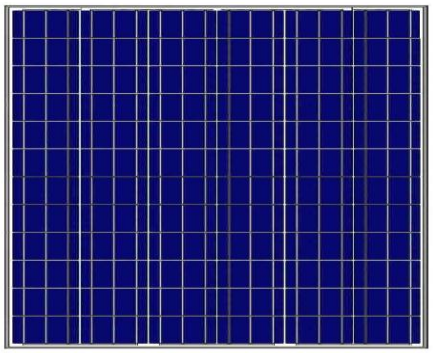

**Figure 5.4:** Amerisolar AS-6P module [38].

## 5.4 Inverter Selection

For stand-alone system, the capacity of the inverter should be more than the total amount of watts that will be used at one time; it should be 25-30%

bigger than the total watts of the appliances. In case of appliance type, motor or compressor the inverter size should be at minimum three times the capacity of those appliances to enable it capable to deliver the high starting current of those appliances. For grid tie system, the rating of inverter is equal to the rating of PV generator [39].Therefore; the selected proper inverter for the PV system rated at 100kWp should have a capacity equal to100kW. Thus, for the first configuration, the single centralized inverter type a sunny central 100 designed by SMA is selected and for master–slave configuration with N equal three inverters, two Sunny Tripower 25000TL-JP designed by SMA and one TRIO-50.0-TL-OUTD-US designed by ABB are selected. Technical data for the selected inverters is shown in Table5.2. The data sheet is found in Appendix B-2.

**Table 5.2: Technical data of the selected inverters [40-41].**

| Technical data | sunny central 100 | Tripower 25000TL-JP | TRIO-50.0-TL-OUTD-US |
|---|---|---|---|
| Max. input voltage [V] | 900 | 800 | 800 |
| Max. input current [A] | 235 | 66 | 100 |
| Rated power [kW] | 100 | 25 | 50 |
| Max. efficiency[%] | 97.6 | 98.7 | 98.6 |
| Max. output current[A] | 145 | 38 | 61 |


**Figure5.5:** The selected inverters [40-41].

## 5.5 PV Generator Sizing

In my work, I used a PV generator with a capacity of 100kW$_p$ as a case study. So in order to obtain this peak power the selected PV module is Amerisolar AS-6P which is poly-crystalline 72 cells module type rated at 320W as shown in Appendix B-1 .The number of PV modules ($N_{module}$) need for the system can be calculated as follow:

$$N_{module} = \frac{P_{PV}}{P_{module}} \tag{5.1}$$

$$N_{module} = \frac{100000}{320} = 312.5\ PV\ modules$$

### 5.5.1 Module Arrangement

After selecting the proper solar inverter and PV modules the next step is to select the optimum way to construct the PV array. National Electrical Code (NEC) Table 690.7 requires division of the maximum input voltage of the inverter by 1.13 to correct for the -10ºC input temperature [42].

Therefore, the maximum $V_{OC}$ of the PV array connected to Suny Central 100 inverter is limited to 796.5 V in order to keep the PV array output voltage below 900V.

Based on the above information, 312 modules can be arranged as 24 parallel PV strings with 13 modules connected in series for every string, giving a total nominal output voltage of 482.3 V and a total nominal output current of 207.12 A, which is in the permissible input current and voltage of the inverter.

**Table 5.3: Array Configuration.**

| Number of Modules | Number of strings | Number of modules in series |
|---|---|---|
| 312 | 24 | 13 |

### 5.5.2 PV Generator Calculation

1- The minimum area (A) needed for PV generator can be calculated as:

$$A_{PV} = A_{module} * N_{module} \quad (5.2)$$

$$A_{PV} = 1.94 * 312 = 605.28\, m^2$$

2- The PV generator open circuit voltage can be calculated as:

$$\mathrm{V_{oc\,PV}} = V_{oc\ of\ module} * N_s \quad (5.3)$$

$$\mathrm{V_{oc\,PV}} = 45.7 * 13 = 594.1\, V$$

3- The PV generator short circuit can be calculated as:

$$\mathrm{I_{sc\,PV}} = I_{sc\ of\ module} * N_P \quad (5.4)$$

$$\mathrm{I_{sc\,PV}} = 9 * 24 = 216\, A$$

4- The PV generator peak power can be calculated as:

$$P_{PV} = P_{module} * N_{module} \quad (5.5)$$

$$P_{PV} = 320 * 312 = 998.840\, kW$$

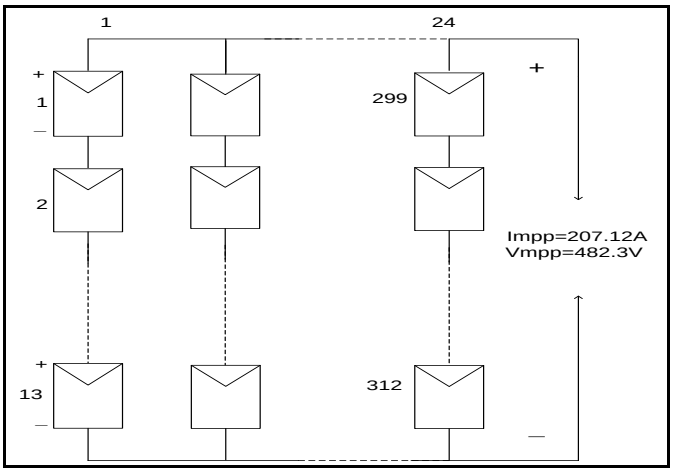


**Figure 5.6**: PV modules arrangement.

### 5.5.3 Input of PV Generator

The inputs affect the output power of PV generator:

1- Rated power of array.

2- Maximum power temperature coefficient.

3- Hourly average ambient temperature.

4- Hourly average solar radiation.

### 5.5.4 Output of PV Generator

The output of the selected PV generator is the Hourly DC output power of PV arrays ($P_{dc}$) at desired conditions hourly, which will be the input power of the used inverters.

By using equations 2.9 and 2.12 we can calculate the DC output power of the PV generator.

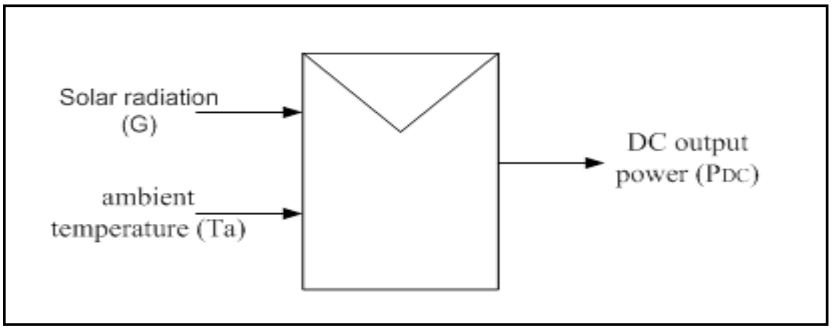


**Figure 5.7**: Input and output of PV generator.

## 5.6 The Selection of Protection Device

In order to protect all components of the PV system from damage caused by overcurrent, overcurrent protection device (circuit barker or fuse) must be included in the system.

To determine the rating current of the selected overcurrent protection device we use the following equation:

$$I_{rating} = K * I_{max.array} \quad (5.6)$$

Where,

K: Safety factor=1.25 [6].

$I_{max.array}$: The maximum current of the PV array [A].

Thus for the proposed PV, system we need one fuse at the DC side of the inverter since we have only one array in the constructed system. The rated current of the selected fuse based on the above equation:

$$I_{fuse} = 1.25 * 216 = 270\ A$$

The selected fuse rating current should be equal or a little more than 270A, considering the fuse standards in the market. Usually two fuses are needed to connect, one in the positive wire and the second in the negative wire.

To protect the AC side of the inverter, a circuit breaker is used at each phase. So for single centralized inverter we need three circuit breakers with rating current calculated according to equation 5.6:

$$I_{C.B} = 1.25 * 145 = 181.25 \text{ A}$$

For master slave inverters with three inverters nine circuit barkers should be used, the rating for them as follows:

$$I_{C.B \text{ of inverter1}} = 1.25 * 38 = 47.5 \text{ A}$$

$$I_{C.B \text{ of inverter2}} = 1.25 * 38 = 47.5 \text{ A}$$

$$I_{C.B \text{of inverter3}} = 1.2 * 61 = 76.25 \text{ A}$$

## 5.7 PV System Optimum Installation

Shadowing effect must be kept in mind during planning the PV system which consists of several PV arrays. In order to avoid shadowing during the daily peak sun hours, the minimum distance between PV arrays can be calculated according to the following equation [6]:

$$d_{min.} = a[sin\beta * \tan(23.5 + L) + cos\beta \,] \qquad (5.6)$$

Where,

$d_{min}$: The minimum distance between two PV arrays facing south [m].

a: The length of the section of the PV array [m]. As shown in Figure 5.8.

β: The tilt angle of the PV array on a horizontal level [degree].

L: The latitude of the project site [degree].

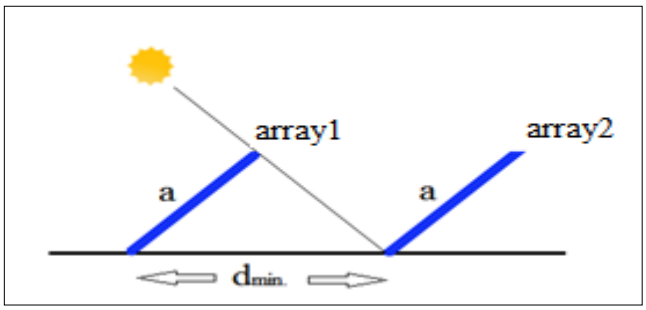


**Figure 5.8:** Minimum distance (d).

The tilt angle is the angle between the PV array surface and the horizontal surface. PV arrays are usually fixed at a certain tilt angle all the year equal to latitude value (32º in Palestine) in order to collect more solar radiation by the modules. The tilt angle is affected mainly by the latitude value of the location (L) and seasonal changes, the optimum value of tilt angle can be calculated as follow [43]:

β = L+ 20º during winter season.

β = L during spring and autumn seasons.

β = L- 10º during summer season.

For Palestine site the tilt angle will be:

β =32 +10 =42 during winter period.

β =32 during spring and autumn period.

β =32-10=22 during summer period.

If we take the tilt angle to be 28º, and two module connected in series, then the length of the constructed PV array (a) is equal to 2*width of the PV module =0.992*2=1.984 m. And after solving equation 5.6 we found that $d_{min}$= 3.1 m.

# Chapter Six
# Case Study Evaluation

## 6.1 Methodology of Analysis

The proposed PV system designed in previous chapter was simulated using MATLAB software in order to study the output power of the selected inverters using two different configurations mentioned above (single centralized and master-slave). An hourly time step is used in this simulation, by comparing the energy production of the two configurations the optimum system configuration can be found.

The work of the two configurations is as the follow:

1- Single centralized inverter: Using one and large inverter with a power rating equal to the peak power of the PV generator as mentioned in section 5.4 which is rated at 100kW. The configuration of this is shown in Figure 6.1.In this type of configuration, the SC inverter will operate continuously all the time.

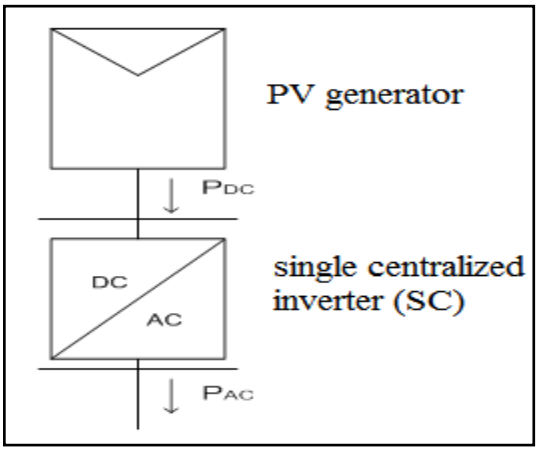


**Figure 6.1:** Single centralized (SC) configuration.

2- Master-slave configuration with N equal 3 inverters: using three inverters connected in parallel as shown in Figure 6.2. The rated power of the used inverters are as the follows: two 25kW inverters, and one 50kW as mentioned in section 5.4.

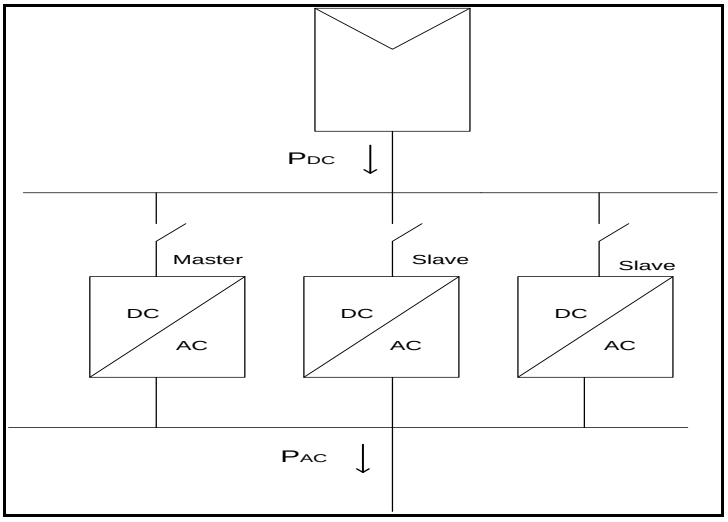


**Figure 6.2**: Master –Slave (M-S) configurations.

The mode of operation for this configuration depends on the amount of DC output power of PV generator. One of the inverters operates continuously (25kW) as a master inverter and the other two inverters are switching on/off depending on the output power of the PV generator in order to get the maximum value of the conversion efficiency. When the DC output power of the PV generator is less or equal to 25 kW only the master inverter operates. When the power exceeds 25 kW and less or equal than 50 kW two inverters operate (master and 25kW inverter) and sharing the power equally, otherwise the three inverters operate sharing the power depending on the rated power of each inverter.

The work is divided into three different scenarios for each configuration:

- First scenario: study the output energy over one year.
- Second scenario: study the output energy for each month in the year.
- Third scenario: study the output energy for a clear and a cloudy days in each month of the year.

The hourly average solar radiation and ambient temperature is available for Nablus site over one year in order to calculate the DC output power of the PV generator by using equation 2.9 and 2.12. This DC output power will be the input of the used inverters in each configuration, and then the AC output energy for each configuration is calculated using the developed inverter model by the help of MATLAB software.

## 6.2 Simulation Program Flow Chart

The following flow charts illustrate the mode of operation for the two used configurations. The flow chart in Figure 6.3 describes the operation of single centralized configuration while flow chart shown in Figure 6.4 illustrates the operation of mater-slave configuration.

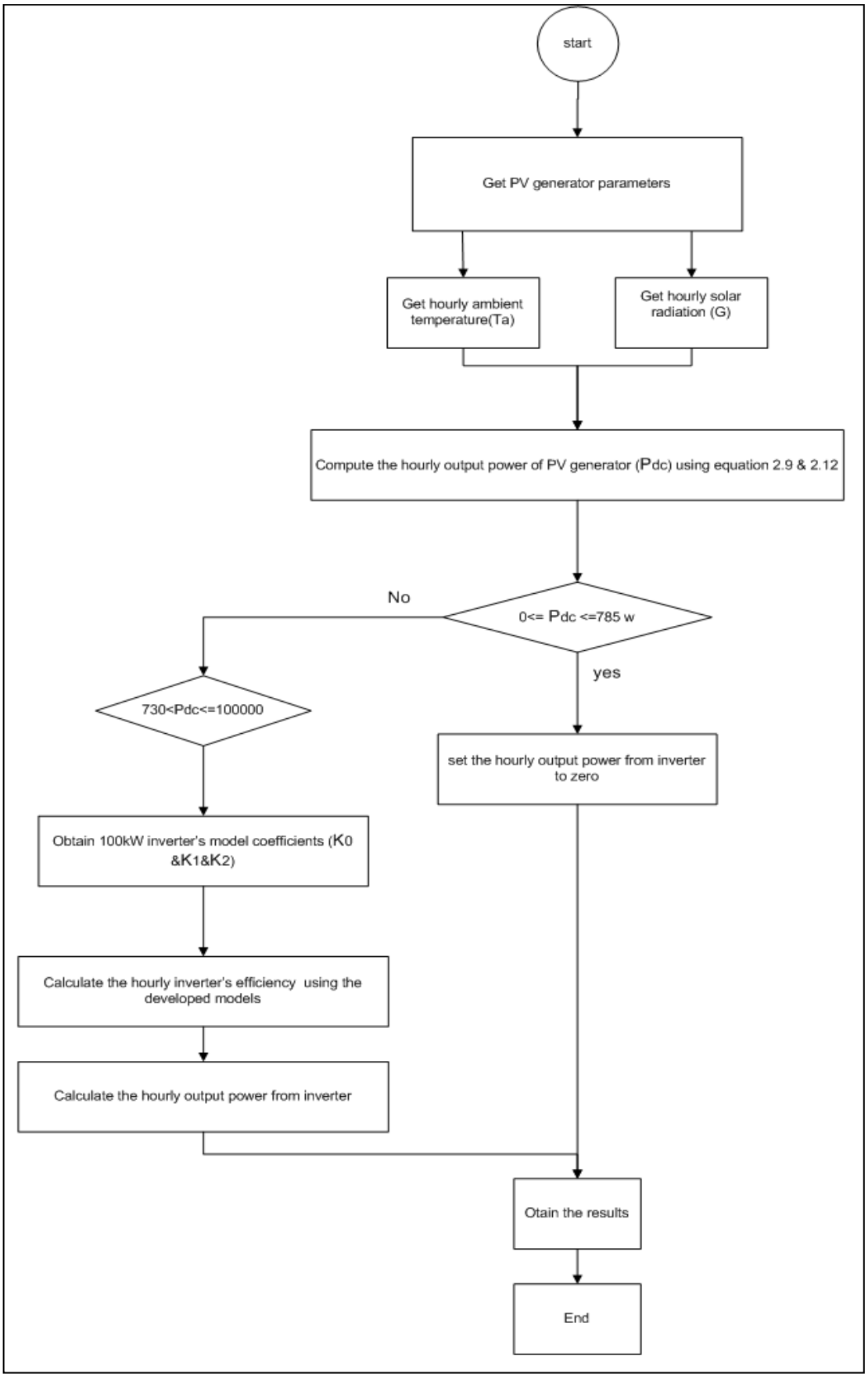


**Figure 6.3**: SC inverter Flow chart.

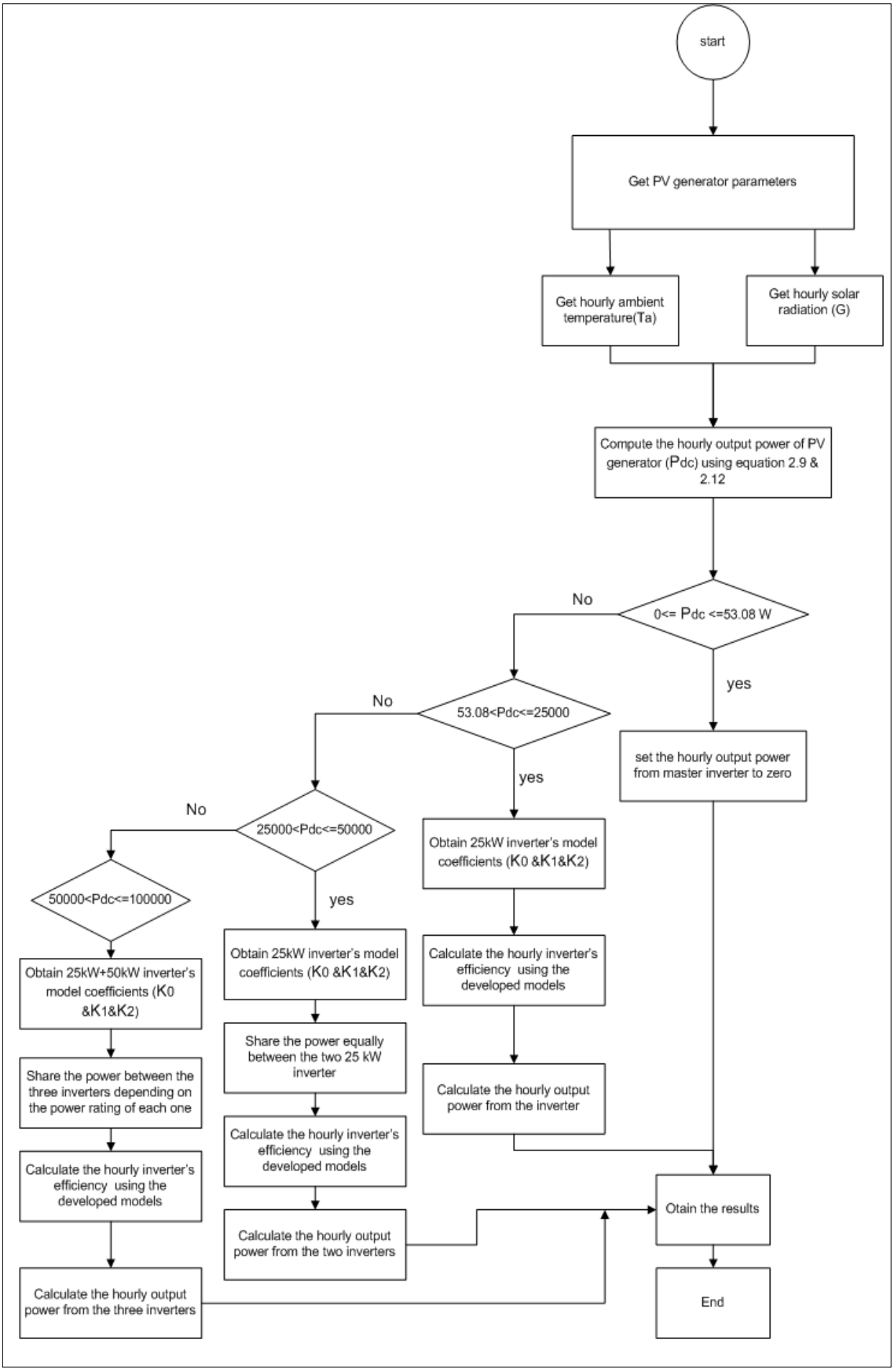


**Figure 6.4:** Master – Slave configuration Flow chart**.**

# Chapter Seven
# Simulation Results

## 7.1 First Scenario

The output energy per year is calculated for each configuration and the results are shown in Table 7.1 and Figure 7.1.

**Table 7.1: Yearly average energy production.**

| $E_{in}$ MWh/year | $E_{out}$ (MWh/year) | |
|---|---|---|
| | SC inverter | M-S inverters |
| 187.50 | 181.26 | 184.50 |
| Efficiency | 0.967 | 0.984 |

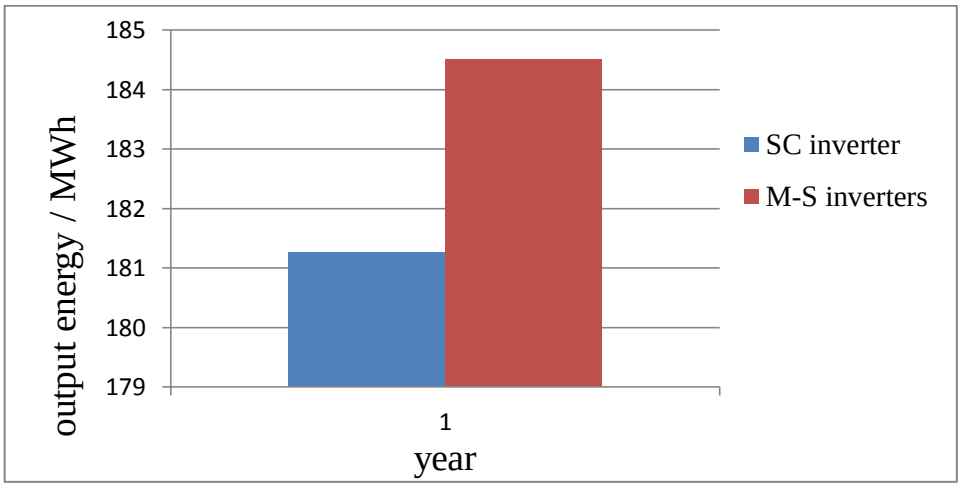


**Figure7.1:** Yearly average energy production.

From the above result, we can get maximum output energy from the inverter by using M-S configuration rather than using SC inverter. Since the power rating of SC inverter is equal to the peak power of the PV generator. Thus at low solar radiation level, such as in the morning and in the evening or during cloudy days, the solar radiation is low, resulting in

small DC output power of PV generator. So it's better to connect an inverter with small power rating to the same PV generator, hence its efficiency will be higher than the large inverter for the same operation conditions.

The conversion efficiency increases by about 2% when using M-S configuration instead of SC inverter resulting in more energy production over one year which is equal to 3.24 MWh/ year.

## 7.2 Second Scenario

In this scenario the two configurations mentioned above is used to show the output energy for each month in the year in order to show the effect of solar radiation and temperature for each month in the year.

The output energy for each month using the two configurations is shown in the following Table.

**Table 7.2: Monthly average produced energy.**

| Month | $E_{in}$ kWh/month | $E_{out}$ (kWh/month) | |
|---|---|---|---|
| | | SC inverter | M-S inverters |
| Jan | 8893.78 | 8528.70 | 8743.03 |
| Feb | 9009.91 | 8651.28 | 8859.84 |
| Mar | 15443.36 | 14915.09 | 15196.82 |
| Apr | 17420.29 | 16859.98 | 17144.07 |
| May | 21399.20 | 20719.85 | 21064.65 |
| Jun | 22072.04 | 21389.50 | 21727.20 |
| Jul | 22232.73 | 21542.13 | 21886.59 |
| Aug | 20687.35 | 20033.31 | 20360.92 |
| Sep | 17120.12 | 16576.70 | 16848.62 |
| Oct | 13652.14 | 13202.18 | 13431.75 |
| Nov | 10302.88 | 9938.04 | 10132.14 |
| Dec | 9264.79 | 8906.80 | 9108.09 |

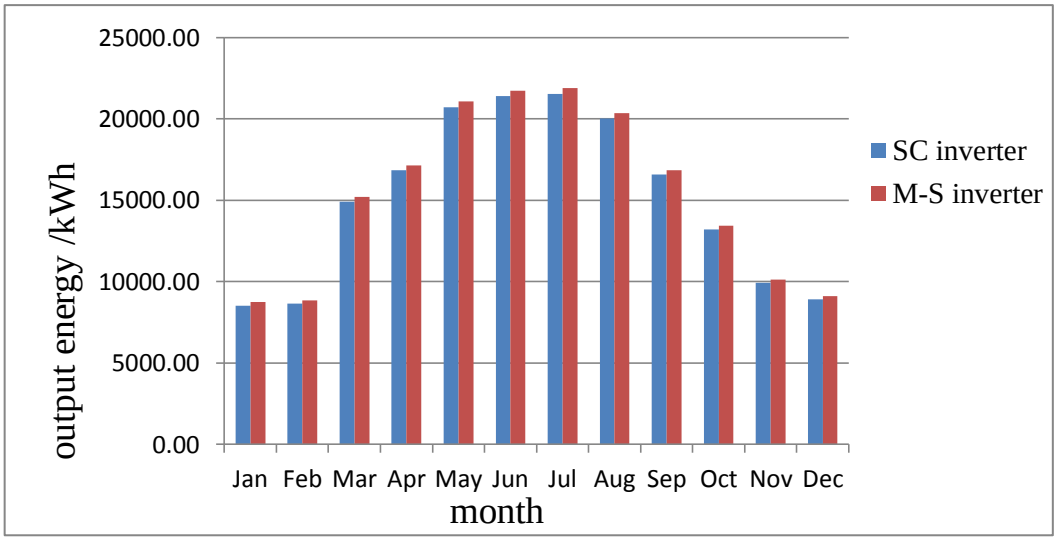


**Figure 7.2**: Monthly average produced energy.

Table 7.3 shows the efficiency of the used configurations for each month in the year.

**Table 7.3: Efficiency of inverter for each month in the year.**

| Month | Efficiency | |
|---|---|---|
| | SC inverter | M-S inverters |
| Jan | 0.959 | 0.983 |
| Feb | 0.960 | 0.983 |
| Mar | 0.966 | 0.984 |
| Apr | 0.968 | 0.984 |
| May | 0.968 | 0.984 |
| Jun | 0.969 | 0.984 |
| Jul | 0.969 | 0.984 |
| Aug | 0.968 | 0.984 |
| Sep | 0.968 | 0.984 |
| Oct | 0.967 | 0.984 |
| Nov | 0.965 | 0.983 |
| Dec | 0.961 | 0.983 |

The amount of the additional energy per month when we use the M-S configuration instead of using SC inverter is shown in Table 7.4. And from the output result, one can conclude that in winter and autumn seasons using the M-S configuration is the better choice since the number of cloudy days

is more than clear sky days in these two seasons. In addition, this configuration is also good in summer season referring to high temperature that reduce the DC output power of the PV generator as mentioned in section 2.3.1.4. Thus the master slave configuration is the better choice over all months of the year.

**Table 7.4: Additional energy production for each month.**

| Month | Additional energy production kWh/month |
|---|---|
| Jan | 214.33 |
| Feb | 208.56 |
| Mar | 281.73 |
| Apr | 284.09 |
| May | 344.80 |
| Jun | 337.71 |
| Jul | 344.45 |
| Aug | 327.61 |
| Sep | 271.93 |
| Oct | 229.57 |
| Nov | 194.10 |
| Dec | 201.29 |
| Sum | 3240.17 |

## 7. 3 Third Scenario

The two configurations mentioned above are used to show the output energy for a clear and cloudy day selected of each month in order to investigate the effect of solar radiation and temperature for clear and cloudy days.

A clear and cloudy day of each month was determined depending in the shape of the solar radiation for each day in the month. The following Figure shows the shape of the solar radiation in October as an example,

from this Figure we can select the clear day and the cloudy day for October which seen in Figure 7.4 and 7.5.

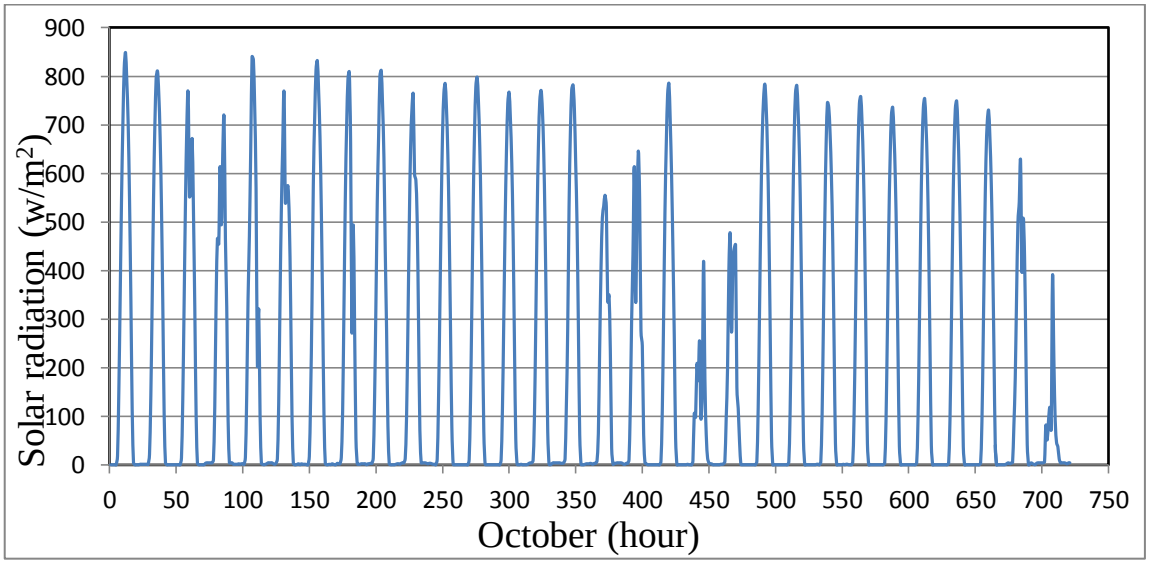


**Figure 7.3:** Solar radiation shape for October month.

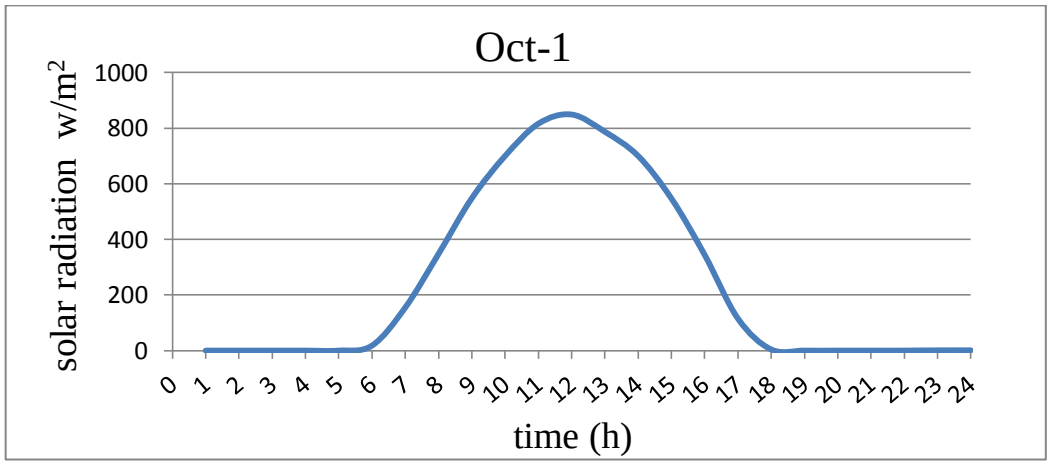


**Figure 7.4:** Clear day in October.

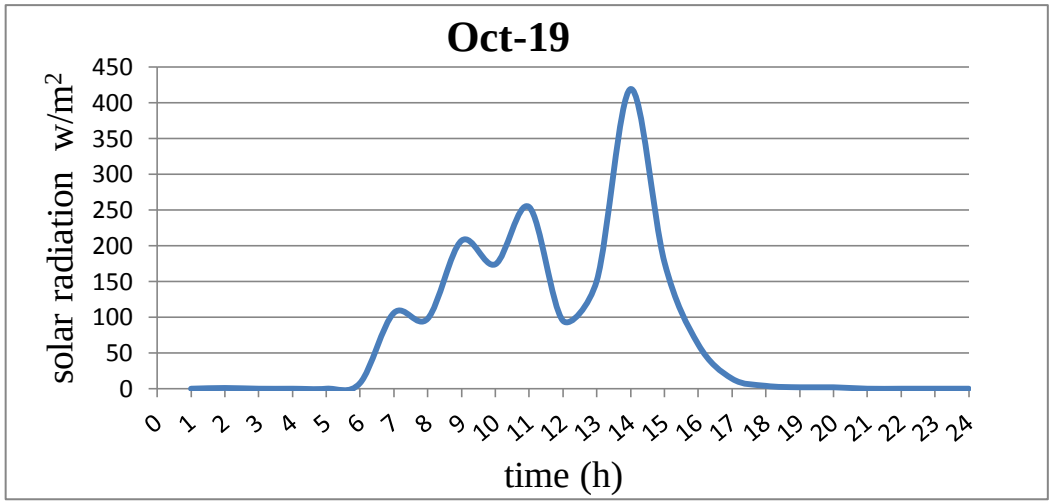


**Figure 7.5**: Cloudy day in October.

The same procedure is done for all months in order to determine the clear and cloudy days, the following Table shows the clear and cloudy days selected for each month.

**Table 7.5: Clear and cloudy day selected for each month.**

| Month | Clear day | Cloudy day |
|---|---|---|
| Jan | 28 | 2 |
| Feb | 22 | 11 |
| Mar | 26 | 9 |
| Apr | 29 | 23 |
| May | 5 | 2 |
| Jun | 11 | 4 |
| Jul | 9 | 6 |
| Aug | 2 | 8 |
| Sep | 4 | 19 |
| Oct | 1 | 19 |
| Nov | 9 | 5 |
| Dec | 3 | 18 |

### 7.3.1 Clear Day

The following two Tables show the daily output energy and the daily efficiency for a clear day in each month.

**Table 7.6: Daily output energy for clear day.**

| Clear day | $E_{in}$ kWh/day | $E_{out}$ (kWh/day) | |
|---|---|---|---|
| | | SC inverter | M-S inverters |
| 28-Jan | 446.72 | 433.55 | 439.69 |
| 22-Feb | 532.82 | 516.31 | 524.47 |
| 26-Mar | 663.10 | 643.85 | 652.94 |
| 29-Apr | 763.24 | 741.04 | 751.48 |
| 5-May | 775.76 | 752.70 | 763.85 |
| 11-Jun | 756.33 | 733.18 | 744.53 |
| 9-Jul | 740.78 | 719.03 | 729.35 |
| 2-Aug | 694.13 | 671.27 | 683.09 |
| 4-Sep | 635.94 | 616.65 | 625.91 |
| 1-Oct | 538.53 | 522.35 | 530.05 |
| 9-Nov | 450.01 | 436.80 | 442.95 |
| 3-Dec | 395.43 | 382.80 | 388.88 |

**Table 7.7: Daily efficiency for clear day.**

| Clear day | Efficiency | |
|---|---|---|
| | SC inverter | M-S inverters |
| 28-Jan | 0.971 | 0.984 |
| 22-Feb | 0.969 | 0.984 |
| 26-Mar | 0.971 | 0.985 |
| 29-Apr | 0.971 | 0.985 |
| 5-May | 0.970 | 0.985 |
| 11-Jun | 0.969 | 0.984 |
| 9-Jul | 0.971 | 0.985 |
| 2-Aug | 0.967 | 0.984 |
| 4-Sep | 0.970 | 0.984 |
| 1-Oct | 0.970 | 0.984 |
| 9-Nov | 0.971 | 0.984 |
| 3-Dec | 0.968 | 0.983 |

The energy produced in January for clear day is shown in Figure 7.6.

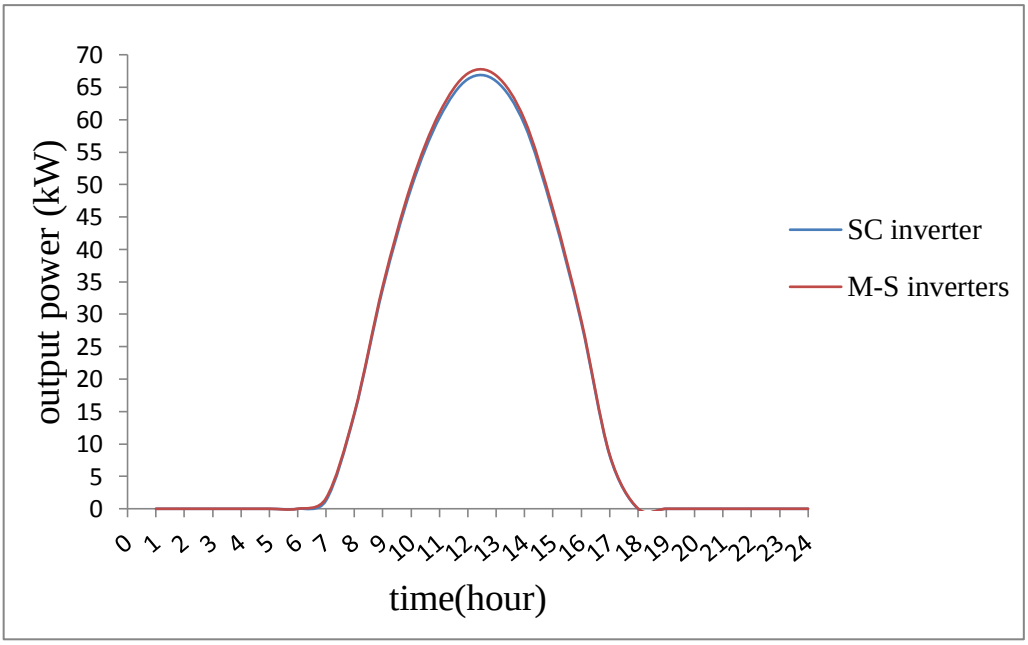


**Figure 7.6**: Power Output on 28-Jan using the two configurations.

The efficiency curve of the two configurations on 28-Jan. is shown in Figure7.7.

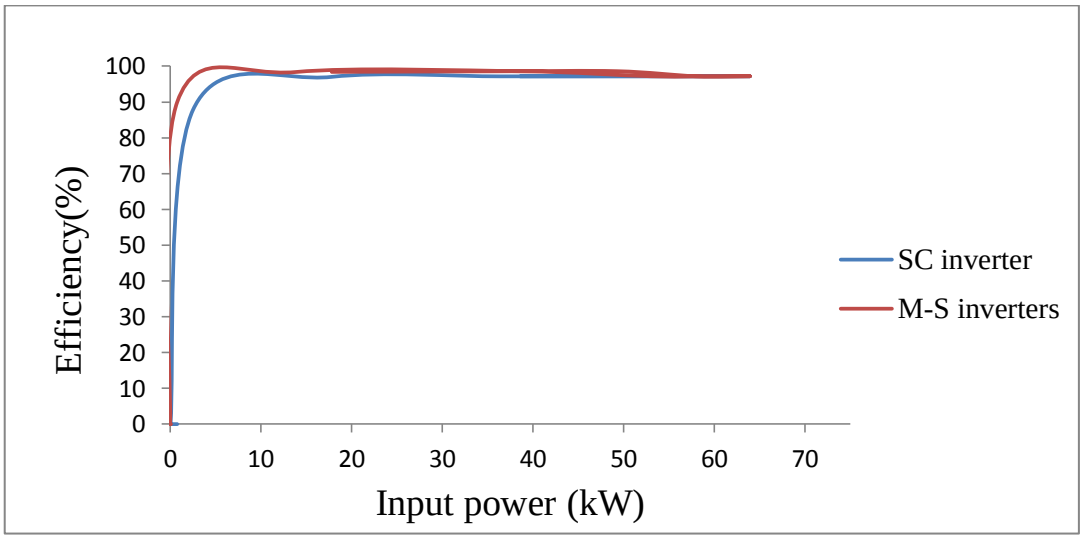


**Figure 7.7**: Efficiency curve of SC inverter and M-S inverters on 28-Jan.

### 7.3.2 Cloudy Day

The following two Tables show the output energy per day and the efficiency for a cloudy day in each month.

**Table 7.8: Daily output energy for cloudy day.**

| Cloudy day | $E_{in}$ kWh/day | $E_{out}$ (kWh/day) | |
|---|---|---|---|
| | | SC inverter | M-S inverters |
| 2-Jan | 73.00 | 64.12 | 71.31 |
| 11-Feb | 109.29 | 99.87 | 107.06 |
| 9-Mar | 176.06 | 164.61 | 172.78 |
| 23-Apr | 264.99 | 253.01 | 260.32 |
| 2-May | 507.78 | 489.43 | 499.55 |
| 4-Jun | 583.34 | 562.07 | 573.93 |
| 6-Jul | 580.75 | 560.01 | 571.35 |
| 8-Aug | 576.73 | 555.74 | 567.41 |
| 29-Sep | 576.35 | 555.38 | 567.07 |
| 19-Oct | 126.17 | 116.23 | 123.66 |
| 5-Nov | 331.35 | 317.91 | 325.78 |
| 18-Dec | 98.32 | 88.96 | 96.22 |

**Table 7.9: Daily efficiency for cloudy day.**

| Cloudy day | Efficiency | |
|---|---|---|
| | SC inverter | M-S inverters |
| 2-Jan | 0.878 | 0.977 |
| 11-Feb | 0.914 | 0.980 |
| 9-Mar | 0.935 | 0.981 |
| 23-Apr | 0.955 | 0.982 |
| 2-May | 0.964 | 0.984 |
| 4-Jun | 0.964 | 0.984 |
| 6-Jul | 0.964 | 0.984 |
| 8-Aug | 0.964 | 0.984 |
| 19-Sep | 0.964 | 0.984 |
| 30-Oct | 0.921 | 0.980 |
| 5-Nov | 0.959 | 0.983 |
| 18-Dec | 0.905 | 0.979 |

The energy produced in January for cloudy day is shown in Figure 7.8.

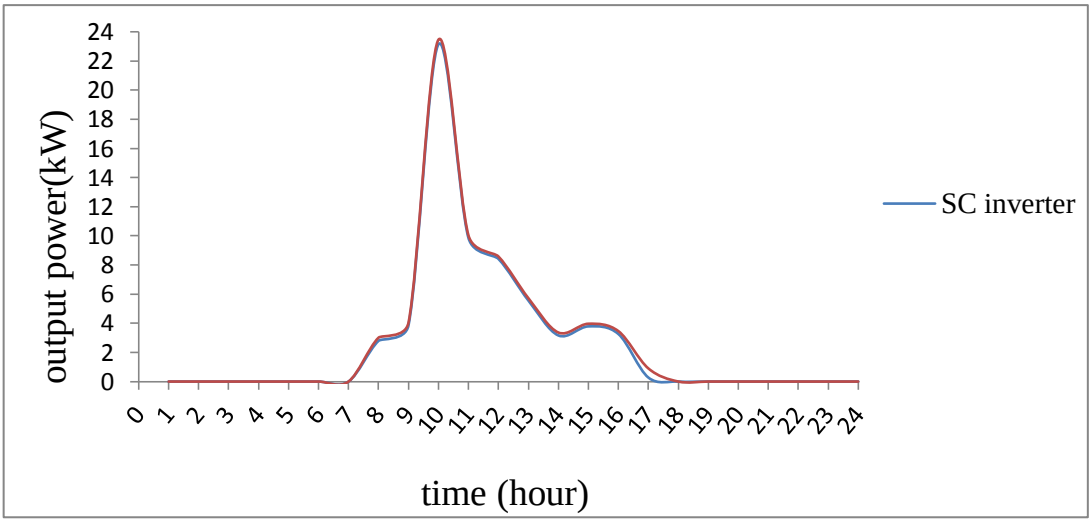


**Figure 7.8:** Power Output on 2-Jan. using the two configurations.

The Figure below shows the daily efficiency in January for cloudy day.

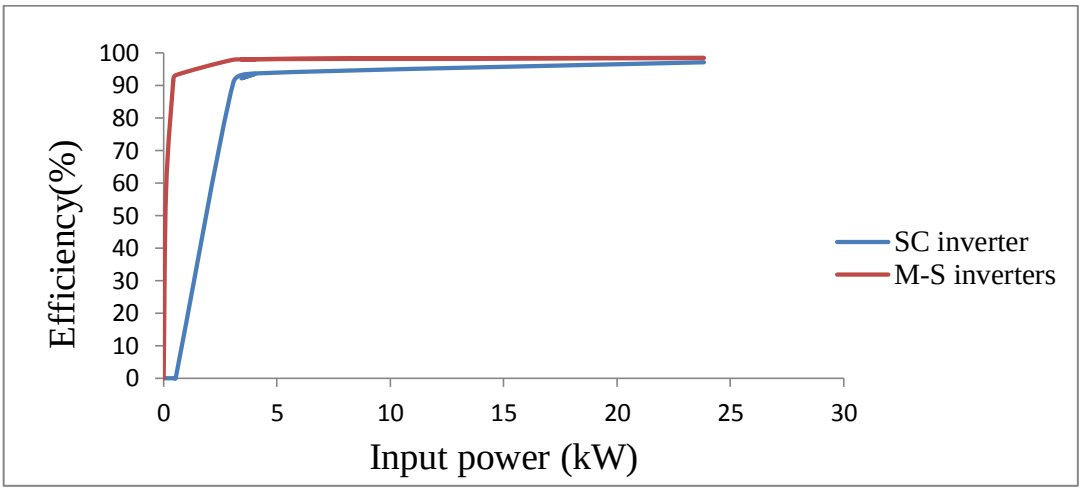


**Figure 7.9**: Efficiency curve of SC inverter and M-S inverters on 2-Jan.

From the above Tables we conclude that in the clear day using master slave inverters is profitable, also M-S inverters are more suitable in cloudy days since the solar radiation affected negatively by cloud so the DC output power of PV generator will be less, Therefore, using (M-S) configuration is more efficient than using one large inverter (SC).

The Table below shows the amount of saving energy per day when using M-S inverters instead of SC inverter for both clear and cloudy day.

**Table 7.10: Additional energy production for clear and cloudy days.**

| Clear day | Additional energy production kWh/day | Cloudy day | Additional energy production kWh/day |
|---|---|---|---|
| 28-Jan | 6.14 | 2-Jan | 7.19 |
| 22-Feb | 8.16 | 11-Feb | 7.19 |
| 26-Mar | 9.09 | 9-Mar | 8.17 |
| 29-Apr | 10.44 | 23-Apr | 7.31 |
| 5-May | 11.15 | 2-May | 10.12 |
| 11-Jun | 11.35 | 4-Jun | 11.86 |
| 9-Jul | 10.32 | 6-Jul | 11.35 |
| 2-Aug | 11.83 | 8-Aug | 11.67 |
| 4-Sep | 9.26 | 19-Sep | 11.69 |
| 1-Oct | 7.70 | 30-Oct | 7.43 |
| 9-Nov | 6.15 | 5-Nov | 7.87 |
| -03Dec | 6.09 | 18-Dec | 7.25 |

Figure 7.10 shows the power sharing between master and slave inverters for a clear day on may. It explains the reign where the master and slave inverters activated.

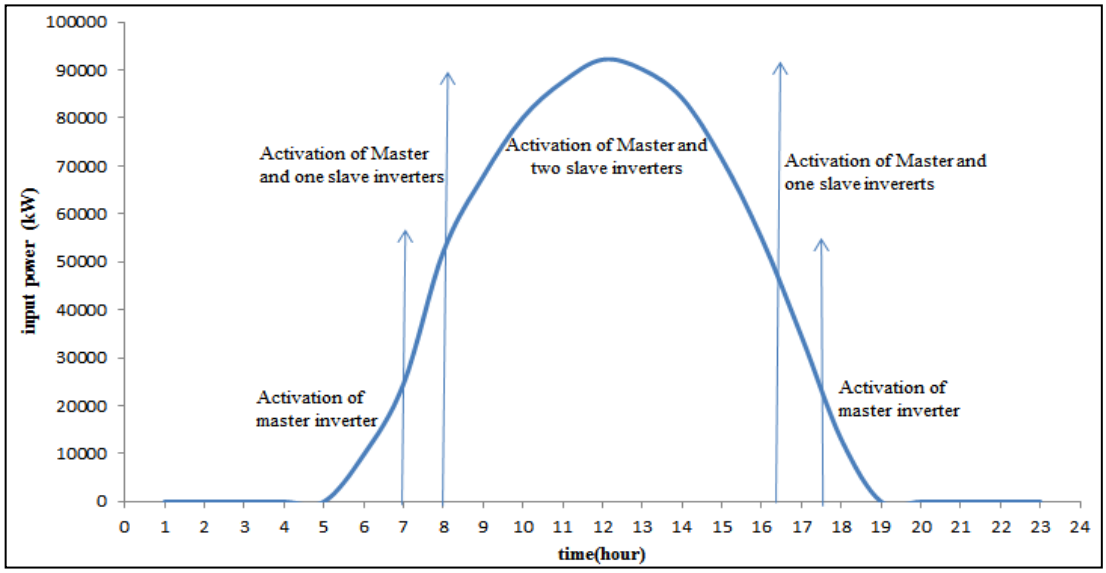


**Figure 7.10** : The power sharing between master and slave inverters.

# Chapter Eighth
# Economic Analysis

## 8.1 Introduction

This chapter shows the cost of generated energy by the two configurations in order to make economical comparison between them. The economic analysis used in this work is based on the payback period for both configurations.

## 8.2 Initial Cost of PV System

The initial cost includes the cost of the equipment need for PV system, represented in PV modules, inverters, Protection device ,wires and other components used in installation. Also, It includes labors and technicians costs for installation. These costs depend on the size and type of the component. All these costs are summed to give the overall initial cost.

Initial cost =Σ components cost + installation cost

### 1- Initial cost of photovoltaic modules.

PV-modules available in different sizes and types, any PV module characterized by its peak watt at STC. The price of peak watt is the same for mono or poly crystalline but the installation or structure cost will differ depending on the installed PV area. The ($/$W_p$) will decrease as the rated power of module increases.

**2- Initial cost of PV inverter**

Inverter available in different size and type. The Cost of PV inverter depends on its capacity, efficiency, voltage range, protection feature and technology. For this reason the designer can enter the price of these components manually in software which helps to get the exact cost.

**3- Other initial costs**

Shipping costs and accessories needed for installation and system protection, wiring and rooms should be also considered. These costs depend on the system size and vary with the kind of the project; if it for public use (may be land available free), or for private use.

## 8.3 Operation and Maintenance (O&M) Cost of PV System

The operation costs considered are incurred after installation in order to run the system for a certain number of years(system life time).

PV generator requires very little maintenance represented in cleaning the modules surface. So, the operation and maintenance cost is considered to be 3% of the capital cost.

## 8.4 Salvage Value

The salvage value is considered as the value of the project components after the system life time is finished. The salvage value is assumed to be 2 % of the capital cost.

## 8.5 Economic Analysis For Both Configurations

The price of the PV system and its installation are important factors in the Feasibility study of grid connected PV systems. These include the prices of PV modules, inverter, and all other auxiliaries parts.

For both configurations the main different in the initial cost is in the price of inverters and M-S controller. However, in SC configuration only one inverter is used rated at 100kW, while in M-S configuration three inverters are used and M-S controller that control the operation of inverters. The controller system consists of sensor for DC current, programmable logic controllers (PLC) and three contactors. The price of the used inverters and controller are shown in the table 8.1.

**Table 8.1: Cost of the used inverters and controller for both configurations.**

| M-S configuration | | | SC configuration | | |
|---|---|---|---|---|---|
| Inverter &M-S controller | Quantity | Price (NIS) | Inverter and other Component | Quantity | Price (NIS) |
| 25kW | 2 | 25,200 | 100kW | 1 | 36,000 |
| 50kW | 1 | 19,800 | **Total price** | | 36,000 |
| controller | 1 | 3,600 | | | |
| **Total price** | | 48,600 | | | |

The additional cost required for M-S configuration =48,600–36,000 =12,600 NIS

So, in order to replace the SC inverter with M-S configuration, additional investment of 12,600 NIS is needed.

### 8.5.1 Annul Saving When Using M-S Configuration Instead of SC Inverter

The simulation results show that the yearly energy production increases by 3.24 MWh/year when using M-S configuration instead of SC inverter.

So the annul saving= the additional energy production per year*cost of kWh

the annul saving=3,240*0.6=1,944 NIS.

### 8.5.2 Simple Payback Period Analysis

The payback period for M-S configuration instead of using SC inverter can be calculated using the following equation:

$$\text{Simple payback period} = \frac{\text{additional investment}}{\text{annual saving of energy}} \qquad (8.1)$$

$$\text{Simple payback period} = \frac{12{,}600}{1{,}944} = 6.48 \text{ year}$$

So we need to six and a half years in order to overcome the additional investment needed for M-S configuration, which makes this configuration economically viable.

# Chapter nine
# Conclusions and Future Work

## 9.1 Conclusions

Based on the performed analysis and the obtained results, the following conclusions are made:

1- The climate changes have great influence on the output power of PV systems unlike the traditional source of power that can be kept constant and doesn't be affected with weather conditions.

2- The PV inverters have a great effect on the overall efficiency of the PV system; it can be observed from the study, that inverter efficiency is affected strongly by the DC input power delivered by the PV generator so that the inverter efficiency is not constant and varying continuously.

4- The efficiency curve of PV inverter can be modeled by using simple mathematical expression with very good accuracy. The curve can be represented by power function. A MATLAB fitting tool is used in order to calculate the inverter model coefficients; the resulting model has a coefficient of determination greater than 0.95 for all the used inverter.

5- Engauge Digitizer software is used to convert the efficiency curve into a data points ($\eta$, $P_{dc.pu}$). These points are used as input data to MATLAB fitting tool in order to calculate the model coefficient of the efficiency curve.

6- This thesis provides in detail a way of improving the overall efficiency of grid connected PV system focusing on the efficiency of PV inverters. Master –Slave inverters are used instead of using one large (single centralized) inverter, the results over one year show that this configuration can increase the yearly energy production by 3.24 MWh/year. In addition the DC to AC conversion efficiency of the inverters increases by about 2%.

7- The additional energy production when using the master-slave inverters can be increased as the PV system becomes larger where this makes the master slave configuration more profitable.

8-The master-slave concept used in this work can be applied to any system consisted of large controlling unit such as pumping system, wind energy system, diesel system etc., in order to improve the system performance.

9- Economic analysis shows that the additional investment in master-Slave configuration instead of single centralized inverter can be covered within six and a half years.

## 9.2 Future Works

It is recommended to calculate the optimum inverter size for the proposed gird connected PV system. The sizing ratio, which is the ratio of the nominal power of PV array and inverter rated power, since the optimal size of inverter has a significant influence in increasing the system efficiency.

# References

[1] Messenger, R. A., & Ventre, G. G. "**Photovoltaic Systems Engineering"**. Second Edition. Wiley, 2003.

[2] Jäger, K. D., Isabella, O., Smets, A. H., van Swaaij, R. A., & Zeman, M. **"Solar Energy: Fundamentals, Technology and Systems"**. UIT Cambridge, 2014.

[3] Ventura, C. "**Theoretical and Experimental Development of a Photovoltaic Power System for Mobile Robot Applications"**. in Ph.D. Thesis Electrical Engineering, 2012.

[4] Green, M. A. **"Solar cells: operating principles, technology, and system applications"**. Prentice-Hall Inc, 1982, pp xii and pp 62-184.

[5] Jackson, F. **"Planning and installing photovoltaic systems"**. Earthscan, London, 2008.

[6] Mahmoud, M."**Renewable Energy Technology Lectures"**. At An-Najah National University, Nablus, Palestine, 2016.

[7] Kalogirou, S. A.**"Solar energy engineering: processes and systems"**. Academic Press, 2013.

[8] Green, M. A. **"Solar cells: operating principles, technology, and system applications"**. Prentice-Hall Inc, 1982, pp 85-100.

[9] Mo'ien, A. A.omar **"Computer–Aided Design and Performance Evaluation of PV-Diesel Hybrid System"**. M.Sc. thesis presented to the University of An-Najah National University, Nablus, Palestine, 2007.

[10] Aribisala, H. A. **"Improving the efficiency of solar photovoltaic power system"**. M.Sc. thesis presented to the University of Rhode Island, 2013.

[11] "**Guide to Interpreting I-V Curve Measurements of PV Array**". [Online] available: http://www.solmetric.com.

[12] J.V.M.D.L.T.T.G.Nofuents,Echnical handbook,**"the installation of on-ground photovoltaic plants over marginal areas, PVs in BLOOM project-Anew challenge for land valorization within a strategic eco-sustainable, approach to local development"**.

[13] Lechuga, E. C. (2010). **"Analysis of the Implementation of a Photovoltaic Plant in Catalonia "**. M.S.c A thesis presented to Lodz University of Technology, 2010.

[14] Villalva, M. G., Gazoli, J. R., & Ruppert Filho, E. **"Modeling and circuit-based simulation of photovoltaic arrays"**. In Power Electronics Conference, COBEP'09. Brazilian, 2009 September, pp. 1244-1254. IEEE.

[15] Krauter, S. T. E. F. A. N., & Hanitsch, R. "**Actual optical and thermal performance of PV-modules"**. Solar energy materials and solar cells, Vol.41, 1996, pp.557-574.

[16] Software package PVSYST V4.0 **developed by Center for the Study of Energy Problems**, university of Geneva.

[17**] "Electropaedia, Solar Power (Technology and Economics)**". [Online]. Available: http://www.mpoweruk.com/solar_power.htm.

[18]García, M. A., & Balenzategui, J. L.**"Estimation of photovoltaic module yearly temperature and performance based on nominal operation cell temperature calculations"**. Renewable energy, Vol.29,No.12, 2004, pp.1997-2010.

[19]Coelho, R. F., Concer, F., & Martins, D. C. "**A proposed photovoltaic module and array mathematical modeling destined to simulation"**. In Industrial Electronics, 2009. ISIE 2009. IEEE International Symposium, 2009 July، pp. 1624-1629.

[20] Whitaker, C. M., Townsend, T. U., Wenger, H. J., Iliceto, A., Chimento, G., & Paletta, F. **"Effects of irradiance and other factors on PV temperature coefficients"**. In Photovoltaic Specialists Conference, Conference Record of the Twenty Second IEEE ,1991October, pp. 608-613.

[21] Fraas, L. M., & Partain, L. D. **"Solar cells and their applications"** .Vol. 236, John Wiley & Sons, 2010.

[22] Schimpf, F., & Norum, L. E. "**Grid connected converters for photovoltaic, state of the art, ideas for improvement of transformerless inverters"**. In Nordic Workshop on Power and Industrial Electronics, Espoo, Finland. Helsinki University of Technology, 2008 June.

[23] "**SMA, solar technology (PV Inverters - Basic Facts for Planning PV Systems)"**. [Online]. Available:

https://www.sma.de/en/partners/knowledgebase/pv-inverters-basic-facts-for-planning-pv-systems.html.

[24] Rampinelli, G. A., Krenzinger, A., & Romero, F. C. "**Mathematical models for efficiency of inverters used in grid connected photovoltaic systems"**. Renewable and Sustainable Energy Reviews, Vol.34, 2014, pp. 578-587.

[25] Massawe, H. B. "**Grid Connected Photovoltaic Systems with Smart Grid functionality "**. M.Sc. thesis presented to Norwegian University of Science and Technology, Institutt for elkraftteknikk, 2013 June.

[26]Blaabjerg, F., Teodorescu, R., Chen, Z., & Liserre, M.**"Power converters and control of renewable energy systems"**. In Proc. 6th Int. Conf. Power Electron Vol. 1, 2004 October, pp. 1-20.

[27]Demoulias, C. (2010). **"A new simple analytical method for calculating the optimum inverter size in grid-connected PV plants"**. Electric Power Systems Research, Vol.80, No.10, pp.1197-1204.

[28] Muñoz, J., Martínez-Moreno, F., & Lorenzo, E. **"On-site characterisation and energy efficiency of grid-connected PV inverters"**.Progress in Photovoltaics: Research and Applications, Vol.19, No.2, 2011, pp.192-201.

[29] Samadi, A., Eriksson, R., Jose, D., Mahmood, F., Ghandhari, M., & Söder, L. **"Comparison of a Three-Phase Single-Stage PV System in PSCAD and PowerFactory"**. In 2nd International Workshop on Integration of Solar Power into Power Systems, 2012, pp. 237-244. Energynautics GmbH.

[30]**" Utility Solar Power and Concentration( Efficiency of Inverters**)". [Online]. Available: https://www.e-education.psu.edu/eme812/node/738**.**

[31] Khatib, T. (2013). ***"Optimization of a grid-connected renewable energy system for a case study in Nablus, Palestine"***. **International Journal of Low-Carbon Technologies**, Vol.9, No.4, 2013, pp.311-318.

[32] Mahmoud, M. M., & Ibrik, I. H. **"Techno-economic feasibility of energy supply of remote villages in Palestine by PV-systems, diesel generators and electric grid"**. Renewable and Sustainable Energy Reviews, Vol.10, No.2, 2006, pp.128-138.

[33] Energy Research center (ERC). **Metrological measurements in west bank** /Nablus, An-Najah National University, 2005.

[34] Fesharaki, V. J., Dehghani, M., Fesharaki, J. J., & Tavasoli, H.**" The effect of temperature on photovoltaic cell efficiency"**. the 1st International Conference on Emerging Trends in Energy Conservation–ETEC, Tehran, Iran ، 2011 November, pp. 20-21.

[35] Awwad, A. I. M.**"Techno-Economic Evaluation and Improvement Possibilities of Local Grid Connected House–PV Power System".** M.Sc. thesis presented to the University of An-Najah National University, Nablus, Palestine, (2015).

[36] **"Practical information (climate)"**. [Online]. Available: http://visitpalestine.ps/climate/.

[37] Dunlop, J. **"Photovoltaic systems"**. Orland Park, IL: American Technical, 2011.

[38] **"Amerisolar, Polycrystalline Solar Panels"**. [Online]. Available: http://www.weamerisolar.eu/.

[39] Buresch, M. **"Photovoltaic energy systems: Design and installation"**. New York: McGraw-Hill, 1998.

[40]**"SMA, PV inverters".** [Online]. Available: https://www.sma.de/en/products/solarinverters.html.

[41] **"ABB, Solar inverters".** [Online]. Available: http://new.abb.com/power-converters-inverters/solar.

[42] Messenger, R. A., & Abtahi, A. **"Photovoltaic systems engineering"**. CRC press, 2000.

[43] Mahmoud, M., & Nabhan, I. **"Determination of optimum tilt angle of single and multi rows of photovoltaic arrays for selected sites in Jordan"**. Solar & Wind Technology,vol.7, No.6, 1990, pp.739-745.

# Appendix

## Appendix A

**Table A.1: The extract points (η, Pdc.pu) for Tripower 25000TL-JP inverter.**

| The extract points from curve (η, $P_{dc.pu}$) | | The value of efficiency when applying the develop model (η) | PE % |
|---|---|---|---|
| η | $P_{dc.pu}$ | | |
| 88.072 | 0.012 | 87.002 | 1.214 |
| 87.036 | 0.012 | 87.325 | -0.332 |
| 86.653 | 0.012 | 87.442 | -0.911 |
| 86.269 | 0.012 | 87.558 | -1.495 |
| 88.609 | 0.013 | 88.682 | -0.083 |
| 87.803 | 0.013 | 88.884 | -1.231 |
| 87.420 | 0.013 | 88.979 | -1.784 |
| 91.025 | 0.014 | 89.554 | 1.616 |
| 90.412 | 0.014 | 89.686 | 0.802 |
| 89.146 | 0.015 | 89.954 | -0.906 |
| 91.409 | 0.016 | 90.637 | 0.844 |
| 90.757 | 0.016 | 90.755 | 0.002 |
| 91.831 | 0.017 | 91.493 | 0.368 |
| 92.214 | 0.019 | 92.194 | 0.022 |
| 92.598 | 0.020 | 92.773 | -0.189 |
| 92.982 | 0.022 | 93.260 | -0.299 |
| 93.749 | 0.023 | 93.637 | 0.119 |
| 93.365 | 0.023 | 93.673 | -0.330 |
| 94.132 | 0.026 | 94.337 | -0.217 |
| 94.516 | 0.027 | 94.607 | -0.096 |
| 94.861 | 0.030 | 95.082 | -0.233 |
| 95.245 | 0.033 | 95.457 | -0.223 |
| 95.629 | 0.035 | 95.607 | 0.022 |
| 96.012 | 0.039 | 96.013 | 0.000 |
| 96.358 | 0.044 | 96.325 | 0.035 |
| 96.742 | 0.048 | 96.569 | 0.178 |
| 97.049 | 0.056 | 96.886 | 0.168 |
| 97.356 | 0.066 | 97.195 | 0.165 |
| 97.625 | 0.077 | 97.410 | 0.220 |
| 97.817 | 0.089 | 97.587 | 0.235 |
| 98.009 | 0.102 | 97.730 | 0.285 |
| 98.125 | 0.117 | 97.847 | 0.283 |
| 98.202 | 0.131 | 97.926 | 0.281 |
| 98.280 | 0.146 | 97.995 | 0.289 |
| 98.357 | 0.160 | 98.045 | 0.317 |

| | | | |
|---|---|---|---|
| 98.396 | 0.175 | 98.089 | 0.311 |
| 98.435 | 0.190 | 98.126 | 0.313 |
| 98.435 | 0.206 | 98.160 | 0.279 |
| 98.474 | 0.221 | 98.186 | 0.293 |
| 98.475 | 0.237 | 98.208 | 0.271 |
| 98.475 | 0.252 | 98.227 | 0.252 |
| 98.514 | 0.267 | 98.243 | 0.275 |
| 98.515 | 0.282 | 98.258 | 0.261 |
| 98.515 | 0.297 | 98.271 | 0.248 |
| 98.516 | 0.312 | 98.282 | 0.237 |
| 98.517 | 0.327 | 98.293 | 0.227 |
| 98.517 | 0.343 | 98.302 | 0.218 |
| 98.479 | 0.356 | 98.310 | 0.172 |
| 98.480 | 0.371 | 98.318 | 0.165 |
| 98.480 | 0.387 | 98.325 | 0.158 |
| 98.481 | 0.402 | 98.331 | 0.152 |
| 98.481 | 0.408 | 98.333 | 0.150 |
| 98.482 | 0.423 | 98.339 | 0.145 |
| 98.482 | 0.438 | 98.344 | 0.140 |
| 98.445 | 0.453 | 98.349 | 0.097 |
| 98.445 | 0.469 | 98.354 | 0.093 |
| 98.446 | 0.484 | 98.358 | 0.089 |
| 98.446 | 0.499 | 98.362 | 0.086 |
| 98.409 | 0.514 | 98.366 | 0.044 |
| 98.409 | 0.529 | 98.369 | 0.041 |
| 98.371 | 0.543 | 98.372 | -0.001 |
| 98.372 | 0.559 | 98.375 | -0.003 |
| 98.372 | 0.574 | 98.378 | -0.006 |
| 98.335 | 0.589 | 98.381 | -0.047 |
| 98.335 | 0.604 | 98.383 | -0.049 |
| 98.335 | 0.612 | 98.384 | -0.050 |
| 98.298 | 0.627 | 98.387 | -0.091 |
| 98.298 | 0.642 | 98.389 | -0.092 |
| 98.299 | 0.658 | 98.391 | -0.094 |
| 98.261 | 0.673 | 98.393 | -0.134 |
| 98.262 | 0.688 | 98.395 | -0.135 |
| 98.262 | 0.703 | 98.397 | -0.137 |
| 98.224 | 0.717 | 98.398 | -0.177 |
| 98.225 | 0.733 | 98.400 | -0.178 |
| 98.187 | 0.748 | 98.401 | -0.218 |
| 98.188 | 0.763 | 98.403 | -0.219 |
| 98.150 | 0.779 | 98.404 | -0.259 |
| 98.150 | 0.794 | 98.406 | -0.260 |
| 98.151 | 0.809 | 98.407 | -0.261 |
| 98.151 | 0.815 | 98.407 | -0.261 |
| 98.114 | 0.831 | 98.409 | -0.301 |
| 98.114 | 0.846 | 98.410 | -0.301 |

| | | | |
|---|---|---|---|
| 98.076 | 0.862 | 98.411 | -0.341 |
| 98.077 | 0.877 | 98.412 | -0.342 |
| 98.039 | 0.891 | 98.413 | -0.381 |
| 98.040 | 0.906 | 98.414 | -0.382 |
| 98.002 | 0.922 | 98.415 | -0.422 |
| 98.002 | 0.937 | 98.416 | -0.422 |
| 97.965 | 0.952 | 98.417 | -0.462 |
| 97.965 | 0.968 | 98.418 | -0.462 |
| 97.966 | 0.983 | 98.418 | -0.462 |
| 97.928 | 0.999 | 98.419 | -0.502 |

**Table A.2: The extract points (η, Pdc.pu) for TRIO-50.0-TL-OUTD-US inverter.**

| The extract points from curve ($\eta$, $P_{dc.pu}$) | | The value of efficiency when applying the develop model ($\eta$) | PE % |
|---|---|---|---|
| $\eta$ | $P_{dc.pu}$ | | |
| 96.904 | 0.098 | 96.664 | 0.248 |
| 96.929 | 0.108 | 96.928 | 0.001 |
| 97.052 | 0.112 | 97.024 | 0.028 |
| 97.174 | 0.121 | 97.194 | -0.020 |
| 97.322 | 0.131 | 97.352 | -0.031 |
| 97.445 | 0.140 | 97.484 | -0.041 |
| 97.543 | 0.149 | 97.584 | -0.042 |
| 97.666 | 0.158 | 97.680 | -0.014 |
| 97.764 | 0.168 | 97.762 | 0.002 |
| 97.862 | 0.179 | 97.842 | 0.021 |
| 97.936 | 0.188 | 97.903 | 0.033 |
| 97.985 | 0.197 | 97.952 | 0.034 |
| 98.034 | 0.206 | 98.001 | 0.034 |
| 98.059 | 0.217 | 98.050 | 0.009 |
| 98.084 | 0.228 | 98.093 | -0.009 |
| 98.108 | 0.239 | 98.131 | -0.023 |
| 98.133 | 0.248 | 98.162 | -0.030 |
| 98.157 | 0.259 | 98.193 | -0.036 |
| 98.182 | 0.270 | 98.220 | -0.039 |
| 98.206 | 0.280 | 98.246 | -0.040 |
| 98.231 | 0.291 | 98.269 | -0.038 |
| 98.256 | 0.301 | 98.288 | -0.033 |
| 98.256 | 0.307 | 98.299 | -0.045 |
| 98.280 | 0.318 | 98.318 | -0.038 |
| 98.305 | 0.329 | 98.335 | -0.030 |
| 98.329 | 0.338 | 98.349 | -0.020 |
| 98.354 | 0.349 | 98.363 | -0.010 |
| 98.354 | 0.360 | 98.377 | -0.023 |

| | | | |
|---|---|---|---|
| 98.378 | 0.370 | 98.389 | -0.011 |
| 98.403 | 0.381 | 98.401 | 0.002 |
| 98.428 | 0.391 | 98.410 | 0.017 |
| 98.452 | 0.401 | 98.421 | 0.032 |
| 98.452 | 0.412 | 98.430 | 0.022 |
| 98.477 | 0.423 | 98.439 | 0.038 |
| 98.501 | 0.433 | 98.448 | 0.055 |
| 98.501 | 0.444 | 98.455 | 0.046 |
| 98.526 | 0.454 | 98.462 | 0.065 |
| 98.550 | 0.464 | 98.469 | 0.082 |
| 98.550 | 0.475 | 98.476 | 0.076 |
| 98.575 | 0.486 | 98.482 | 0.094 |
| 98.575 | 0.496 | 98.488 | 0.088 |
| 98.575 | 0.504 | 98.492 | 0.084 |
| 98.575 | 0.515 | 98.498 | 0.078 |
| 98.575 | 0.525 | 98.503 | 0.073 |
| 98.575 | 0.536 | 98.508 | 0.068 |
| 98.575 | 0.547 | 98.512 | 0.063 |
| 98.575 | 0.558 | 98.517 | 0.059 |
| 98.575 | 0.568 | 98.521 | 0.054 |
| 98.575 | 0.579 | 98.525 | 0.050 |
| 98.575 | 0.590 | 98.529 | 0.046 |
| 98.575 | 0.601 | 98.533 | 0.043 |
| 98.624 | 0.609 | 98.536 | 0.090 |
| 98.575 | 0.619 | 98.539 | 0.037 |
| 98.575 | 0.630 | 98.542 | 0.033 |
| 98.575 | 0.640 | 98.545 | 0.030 |
| 98.575 | 0.651 | 98.548 | 0.027 |
| 98.575 | 0.662 | 98.551 | 0.024 |
| 98.575 | 0.673 | 98.554 | 0.021 |
| 98.575 | 0.683 | 98.557 | 0.018 |
| 98.575 | 0.694 | 98.559 | 0.016 |
| 98.575 | 0.705 | 98.562 | 0.013 |
| 98.575 | 0.716 | 98.564 | 0.011 |
| 98.575 | 0.726 | 98.567 | 0.008 |
| 98.575 | 0.737 | 98.569 | 0.006 |
| 98.575 | 0.748 | 98.571 | 0.004 |
| 98.600 | 0.759 | 98.573 | 0.027 |
| 98.575 | 0.769 | 98.575 | 0.000 |
| 98.575 | 0.780 | 98.577 | -0.002 |
| 98.575 | 0.791 | 98.579 | -0.004 |
| 98.575 | 0.802 | 98.581 | -0.006 |
| 98.575 | 0.811 | 98.582 | -0.007 |
| 98.575 | 0.820 | 98.584 | -0.009 |
| 98.575 | 0.831 | 98.585 | -0.010 |
| 98.575 | 0.841 | 98.587 | -0.012 |
| 98.575 | 0.852 | 98.588 | -0.014 |

| | | | |
|---|---|---|---|
| 98.575 | 0.863 | 98.590 | -0.015 |
| 98.575 | 0.874 | 98.591 | -0.017 |
| 98.575 | 0.884 | 98.593 | -0.018 |
| 98.575 | 0.895 | 98.594 | -0.019 |
| 98.575 | 0.906 | 98.595 | -0.021 |
| 98.550 | 0.917 | 98.597 | -0.047 |
| 98.550 | 0.928 | 98.598 | -0.048 |
| 98.550 | 0.938 | 98.599 | -0.050 |
| 98.550 | 0.949 | 98.600 | -0.051 |
| 98.550 | 0.960 | 98.602 | -0.052 |
| 98.550 | 0.971 | 98.603 | -0.053 |
| 98.550 | 0.981 | 98.604 | -0.054 |
| 98.550 | 0.992 | 98.605 | -0.055 |

**Table A.3: The extract points (η, Pdc.pu) for Sunny Central 100 inverter.**

| The extract points from curve ($\eta$, $P_{dc.pu}$) | | The value of efficiency when applying the develop model ($\eta$) | PE % |
|---|---|---|---|
| $\eta$ | $P_{dc.pu}$ | | |
| 91.399 | 0.031 | 90.998 | 0.439 |
| 92.019 | 0.033 | 91.558 | 0.501 |
| 92.524 | 0.036 | 92.532 | -0.010 |
| 93.183 | 0.039 | 93.254 | -0.077 |
| 93.609 | 0.042 | 93.830 | -0.236 |
| 94.269 | 0.045 | 94.271 | -0.002 |
| 94.695 | 0.050 | 94.807 | -0.118 |
| 95.122 | 0.053 | 95.078 | 0.046 |
| 95.587 | 0.061 | 95.598 | -0.011 |
| 95.936 | 0.074 | 96.109 | -0.181 |
| 96.285 | 0.085 | 96.378 | -0.096 |
| 96.518 | 0.095 | 96.536 | -0.019 |
| 96.790 | 0.109 | 96.700 | 0.093 |
| 97.061 | 0.130 | 96.847 | 0.220 |
| 97.139 | 0.139 | 96.894 | 0.251 |
| 97.216 | 0.154 | 96.949 | 0.274 |
| 97.294 | 0.167 | 96.986 | 0.316 |
| 97.332 | 0.176 | 97.009 | 0.332 |
| 97.371 | 0.188 | 97.031 | 0.349 |
| 97.410 | 0.197 | 97.047 | 0.372 |
| 97.449 | 0.204 | 97.057 | 0.402 |
| 97.488 | 0.215 | 97.072 | 0.427 |
| 97.526 | 0.228 | 97.086 | 0.452 |
| 97.526 | 0.237 | 97.095 | 0.442 |
| 97.565 | 0.247 | 97.103 | 0.474 |

| | | | |
|---|---|---|---|
| 97.565 | 0.263 | 97.114 | 0.462 |
| 97.565 | 0.273 | 97.120 | 0.456 |
| 97.565 | 0.286 | 97.127 | 0.449 |
| 97.565 | 0.295 | 97.132 | 0.444 |
| 97.565 | 0.307 | 97.137 | 0.439 |
| 97.526 | 0.323 | 97.143 | 0.393 |
| 97.526 | 0.336 | 97.147 | 0.388 |
| 97.526 | 0.347 | 97.151 | 0.385 |
| 97.488 | 0.365 | 97.156 | 0.340 |
| 97.449 | 0.398 | 97.163 | 0.294 |
| 97.410 | 0.417 | 97.166 | 0.251 |
| 97.371 | 0.443 | 97.170 | 0.207 |
| 97.294 | 0.460 | 97.172 | 0.125 |
| 97.255 | 0.486 | 97.175 | 0.082 |
| 97.216 | 0.510 | 97.177 | 0.040 |
| 97.177 | 0.535 | 97.179 | -0.002 |
| 97.139 | 0.551 | 97.181 | -0.043 |
| 97.100 | 0.568 | 97.182 | -0.084 |
| 97.022 | 0.589 | 97.183 | -0.166 |
| 97.022 | 0.609 | 97.184 | -0.167 |
| 97.022 | 0.627 | 97.185 | -0.168 |
| 96.945 | 0.650 | 97.186 | -0.249 |
| 96.945 | 0.673 | 97.187 | -0.250 |
| 96.867 | 0.701 | 97.188 | -0.331 |
| 96.828 | 0.727 | 97.189 | -0.372 |
| 96.751 | 0.749 | 97.189 | -0.453 |
| 96.751 | 0.768 | 97.190 | -0.454 |
| 96.712 | 0.785 | 97.190 | -0.495 |
| 96.673 | 0.810 | 97.191 | -0.536 |
| 96.634 | 0.838 | 97.192 | -0.577 |
| 96.557 | 0.860 | 97.192 | -0.658 |
| 96.479 | 0.881 | 97.192 | -0.739 |
| 96.479 | 0.903 | 97.193 | -0.740 |
| 96.440 | 0.923 | 97.193 | -0.780 |
| 96.440 | 0.947 | 97.193 | -0.781 |
| 96.363 | 0.969 | 97.194 | -0.862 |
| 96.324 | 0.992 | 97.194 | -0.903 |

# Appendix B-1

Amerisolar | New Energy New World®

# AS-6P

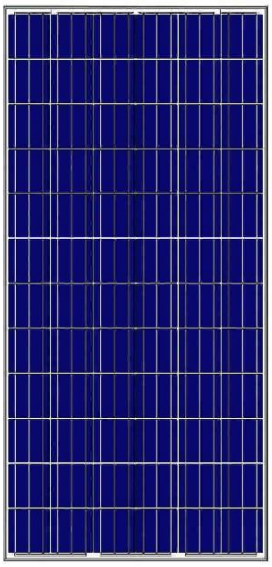

## POLYCRYSTALLINE MODULE

### ADVANCED PERFORMANCE & PROVEN ADVANTAGES

- High module conversion efficiency up to 17.01% through advanced manufacturing technology.
- Low degradation and excellent performance under high temperature and low light conditions.
- Robust aluminum frame ensures the modules to withstand wind loads up to 2400Pa and snow loads up to 5400Pa.
- Positive power tolerance of 0 ~ +3 %.
- High ammonia and salt mist resistance.
- Potential induced degradation (PID) resistance.

### CERTIFICATIONS

- IEC61215, IEC61730, IEC62716, IEC61701, UL1703, CE, ETL(USA), JET(Japan), J-PEC(Japan), MCS(UK), CEC(Australia), FSEC(FL-USA), CSI Eligible(CA-USA), Israel Electric(Israel), Kemco(South Korea), InMetro(Brazil), TSE(Turkey)
- ISO9001:2008: Quality management system
- ISO14001:2004: Environmental management system
- OHSAS18001:2007: Occupational health and safety management system

**Passionately committed to delivering innovative energy solution**

### SPECIAL WARRANTY

- 12 years limited product warranty.
- Limited linear power warranty: 12 years 91.2% of the nominal power output, 30 years 80.6% of the nominal power output.

## ELECTRICAL CHARACTERISTICS AT STC

| | | | | | | | | |
|---|---|---|---|---|---|---|---|---|
| Nominal Power ($P_{max}$) | 295W | 300W | 305W | 310W | 315W | 320W | 325W | 330W |
| Open Circuit Voltage ($V_{OC}$) | 45.2V | 45.3V | 45.4V | 45.5V | 45.6V | 45.7V | 45.8V | 45.9V |
| Short Circuit Current ($I_{SC}$) | 8.60A | 8.68A | 8.76A | 8.85A | 8.93A | 9.00A | 9.08A | 9.16A |
| Voltage at Nominal Power ($V_{mp}$) | 36.6V | 36.7V | 36.8V | 36.9V | 37.0V | 37.1V | 37.2V | 37.3V |
| Current at Nominal Power ($I_{mp}$) | 8.07A | 8.18A | 8.29A | 8.41A | 8.52A | 8.63A | 8.74A | 8.85A |
| Module Efficiency (%) | 15.20 | 15.46 | 15.72 | 15.98 | 16.23 | 16.49 | 16.75 | 17.01 |
| Operating Temperature | -40°C to +85°C | | | | | | | |
| Maximum System Voltage | 1000V DC | | | | | | | |
| Fire Resistance Rating | Type 1(UL1703)/Class C(IEC61730) | | | | | | | |
| Maximum Series Fuse Rating | 15A | | | | | | | |

STC: Irradiance 1000W/m², Cell temperature 25°C, AM1.5

## ELECTRICAL CHARACTERISTICS AT NOCT

| | | | | | | | | |
|---|---|---|---|---|---|---|---|---|
| Nominal Power ($P_{max}$) | 217W | 221W | 224W | 228W | 232W | 236W | 239W | 243W |
| Open Circuit Voltage ($V_{OC}$) | 41.6V | 41.7V | 41.8V | 41.9V | 42.0V | 42.0V | 42.1V | 42.2V |
| Short Circuit Current ($I_{SC}$) | 6.97A | 7.03A | 7.10A | 7.17A | 7.23A | 7.29A | 7.35A | 7.42A |
| Voltage at Nominal Power ($V_{mp}$) | 33.3V | 33.4V | 33.5V | 33.6V | 33.7V | 33.8V | 33.9V | 34.0V |
| Current at Nominal Power ($I_{mp}$) | 6.52A | 6.62A | 6.69A | 6.79A | 6.89A | 6.98A | 7.05A | 7.15A |

NOCT: Irradiance 800W/m², Ambient temperature 20°C, Wind Speed 1 m/s

## MECHANICAL CHARACTERISTICS

| | |
|---|---|
| Cell type | Polycrystalline 156x156mm (6x6inches) |
| Number of cells | 72 (6x12) |
| Module dimensions | 1956x992x50mm (77.01x39.06x1.97inches) |
| Weight | 27kg (59.5lbs) |
| Front cover | 4.0mm (0.16inches) low-iron tempered glass |
| Frame | Anodized aluminum alloy |
| Junction box | IP67, 3 diodes |
| Cable | 4mm² (0.006inches²), 1000mm (39.37inches) |
| Connector | MC4 or MC4 compatible |

## TEMPERATURE CHARACTERISTICS

| | |
|---|---|
| Nominal Operating Cell Temperature (NOCT) | 45°C±2°C |
| Temperature Coefficients of $P_{max}$ | -0.43%/°C |
| Temperature Coefficients of $V_{OC}$ | -0.33%/°C |
| Temperature Coefficients of $I_{SC}$ | 0.056%/°C |

## PACKAGING

| | |
|---|---|
| Standard packaging | 21pcs/pallet |
| Module quantity per 20' container | 210 pcs |
| Module quantity per 40' container | 462 pcs |

## ENGINEERING DRAWINGS

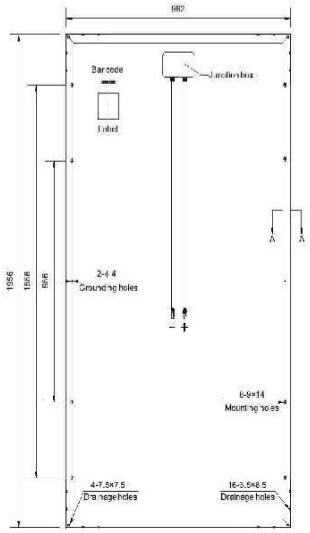


Unit: mm

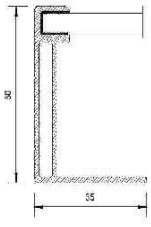


Section A-A

## IV CURVES

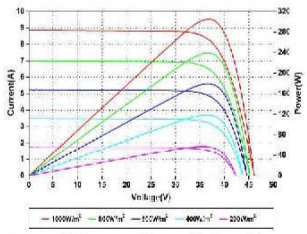


Current-Voltage and Power-Voltage Curves at Different Irradiances

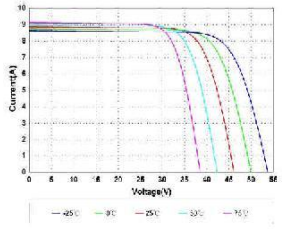


Current-Voltage Curves at Different Temperatures

Specifications in this datasheet are subject to change without prior notice.

# Appendix B-2

SUNNY TRIPOWER 25000TL-JP


**Efficient**
- Efficiency of 98.0% (as per JIS C 8961)
- Peak efficiency of 98.7%

**Flexible**
- DC input voltage of up to 1000 V
- Optimum system design thanks to multistring concept and step-up converter
- Operating temperature range from –25°C to +60°C through active OptiCool temperature management

**Convenient**
- Straightforward system visualization and monitoring thanks to Webconnect and Sunny Portal
- Integrated graphic display showing yield values and daily trends

**Innovative**
- Efficient parameterization and remote monitoring via SMA Cluster Controller and Sunny Portal for medium-sized and large-scale systems

## SUNNY TRIPOWER 25000TL-JP

The reliable specialist for decentralized systems on the medium-voltage grid

The new Sunny Tripower 25000TL-JP is the high-performance solution for use in larger, decentralized medium-voltage systems on the Japanese market. This newly developed product is based on the technologically mature Sunny Tripower platform. Users benefit from years of experience and the professional support that SMA as a market leader provides. Its peak efficiency of 98.7 percent ensures high yields, thereby guaranteeing system operators rapid amortization. The multistring concept and wide input voltage range allows for high design flexibility and compatibility with many PV modules on the market.
In addition to professional and efficient system monitoring, the optional SMA Cluster Controller also enables personalized system parameterization using Modbus.

## Efficiency Curve

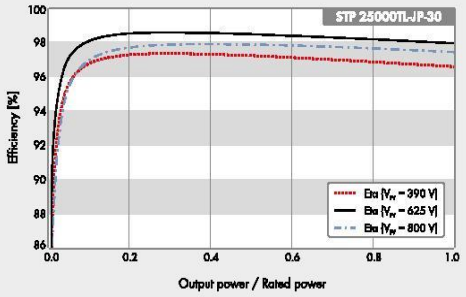


## Accessory


DC surge arrester type II, inputs A and B
DCSPD KIT3-10


Power Control Module
PWCMOD-10


Multi-function relay
MFR01-10

| | Sunny Tripower 25000TL-JP |
|---|---|
| **Input (DC)** | |
| Max. DC power (@ cos φ = 1) / DC rated power | 25,550 W / 25,550 W |
| Max. input voltage | 1,000 V |
| MPP voltage range at nominal voltage / rated input voltage | 390 V to 800 V / 625 V |
| Min. input voltage / initial input voltage | 150 V / 188 V |
| Max. input current input A / input B | 33 A / 33 A |
| Number of independent MPP inputs / strings per MPP input | 2 / A:3; B:3 |
| **Output (AC)** | |
| Rated power at nominal voltage | 25,000 W |
| Max. apparent AC power | 25,000 VA |
| Nominal AC voltage | 3 / N / PE; 420 V, 50 Hz<br>3 / N / PE; 440 V, 60 Hz |
| AC voltage range | 360 V to 480 V |
| AC power frequency / range | 50 Hz / 44 Hz to 55 Hz<br>60 Hz / 54 Hz to 65 Hz |
| Rated power frequency / rated grid voltage | 50 Hz / 420 V |
| Max. output current | 38 A |
| Power factor at rated power | 1 |
| Adjustable displacement power factor | 0.8 overexcited to 0.8 underexcited |
| THD | ≤ 3 % |
| Feed-in phases / connection phases | 3 / 3 |
| **Efficiency** | |
| Max. efficiency / efficiency as per JIS C 8961 | 98.7% / 98.0% |
| **Protective devices** | |
| DC-side disconnection point | ● |
| Ground fault monitoring / grid monitoring | ● / ● |
| DC surge arrester SPD type II | ○ |
| DC reverse polarity protection / AC short-circuit current capability / galvanically isolated | ● / ● / – |
| All-pole sensitive residual-current monitoring unit | ● |
| Protection class (as per IEC 62109-1) / overvoltage category (as per IEC 62109-1) | I / AC: III; DC: II |
| **General data** | |
| Dimensions (W / H / D) | 661 / 682 / 264 mm<br>(26.0 / 26.9 / 10.4 inch) |
| Weight | 61 kg (134.48 lb) |
| Operating temperature range | -25° C to +60° C (-13° F to +140° F) |
| Noise emission, typical | 51 dB(A) |
| Self-consumption (at night) | 1 W |
| Topology / cooling concept | Transformerless / OptiCool |
| Degree of protection (as per IEC 60529) | IP65 |
| Climatic category (according to IEC 60721-3-4) | 4K4H |
| Max. permissible value for relative humidity (non-condensing) | 100% |
| **Features** | |
| DC connection / AC connection | SUNCLIX / spring-cage terminal |
| Display | LC graphic display |
| Interface | Speedwire / Webconnect |
| Multifunction relay / Power Control Module | ○ / ○ |
| Warranty: 5 / 10 / 15 / 20 years | ● / ○ / ○ / ○ |
| OptiTrac Global Peak / FRT* / manual restart | ● / ● / ● |
| | |
| ● Standard features ○ Optional features – Not available, data at nominal conditions | |
| * according to JEAC 9701-2012 (3-4) | |
| Type designation | STP 25000TL-JP-30 |

Solar inverters

# ABB string inverters
# TRIO-50.0-TL-OUTD-US-480
# 50kW


**The most powerful ABB string inverter available today, the TRIO-50.0 has been designed to maximize the ROI in large systems. It has all the advantages of a decentralized configuration for both rooftop and ground-mounted installations.**

The new TRIO-50.0 inverter is ABB's three-phase string solution for cost efficient large decentralized photovoltaic systems for both commercial and utility applications.

## Modular design

TRIO-50.0 has a landscape modular design to guarantee maximum flexibility.

The separate and configurable AC and DC compartments increase the ease of installation and maintenance with their ability to remain separately wired from the inverter module inside the system.

The TRIO comes with the most complete wiring box configurations available including 12 or 16 DC inputs, AC and DC disconnect switches and monitored type II AC and DC surge arresters.

## Flexibility of installation

The TRIO 50's forced air cooling system over an external heatsink, designed for a simple and fast installation, enables for the maximum flexibility of installation. The option of horizontal or vertical mounting brackets enables the best use of space available beneath or behind the solar modules.

## Design flexibility

The double stage conversion topology offers the advantage of a wide input voltage range for maximum flexibility of the system design.

## Highlights:

- Modular landscape design to guarantee maximum flexibility
- Separate and configurable AC and DC compartments increase the ease of installation and maintenance
- Complete wiring box configurations; including, 12 or 16 inputs, AC and DC disconnect switches
- Forced air cooling system over external heat sink
- Mounting supports for both horizontal or vertical positions allowing 90 degrees of installation
- Wide input voltage range for maximum flexibility of the system design

## Additional highlights

- Transformerless topology
- Each inverter is set on specific grid codes which can be selected directly in the field
- Lockable wiring boxes


## Technical data and types

| Type code | TRIO-50.0-TL-OUTD-US |
|---|---|
| **Input side** | |
| Absolute maximum DC input voltage ($V_{max,abs}$) | 1000 V |
| Start-up DC input voltage ($V_{start}$) | 300...500 V (Default 360) |
| Operating DC input vwoltage range ($V_{dcmin}$...$V_{dcmax}$) | 0,7x$V_{start}$ ...950 V (min 250 V) |
| Rated DC input voltage ($V_{dcr}$) | 715 Vdc |
| Rated DC input power ($P_{dcr}$) | 51250 W |
| Number of independent MPPT | 1 |
| MPPT input DC voltage range ($V_{MPPTmin}$ ... $V_{MPPTmax}$) at $P_{acr}$ | 520-800 Vdc |
| Maximum DC input current ($I_{dcmax}$) | 100 A |
| Maximum input short circuit current | 144 A |
| Number of DC inputs string / pairs | 12 or 16 string combiner version available / standard version 2 |
| DC connection type | Input lugs (type 1), 12/16 string field wired fuse holders (type 2), 12/16 string quick connectors (type 3) |
| **Input protection** | |
| Reverse polarity protection | Yes, from limited current source; type 3: reverse polarity indicators |
| Input over voltage protection - varistor | Yes |
| Input over voltage protection - plug in modular surge arrester (optional 12 and 16 string DC combiner option) | Type 2 |
| Photovoltaic array isolation control | According to US standards |
| DC switch rating | 200 A / 1000 V |
| **Output side** | |
| AC Grid connection type | 2Ø, Y / 3W+GND or 4W+GND |
| Rated AC power ($P_{acr}$ @cosØ=1 ) | 50000 W |
| Maximum AC output power ($P_{acmax}$ @cosØ=1) | 50000 W |
| Maximum apparent power ($S_{max}$) | 50000 VA |
| Rated AC grid voltage ($V_{acr}$) | 480 V |
| AC voltage range | 422-528 |
| Maximum AC output current ($I_{acmax}$) | 61 A |
| Contributory fault current | 66 A |
| Rated output frequency ($f_r$) | 60 Hz |
| Output frequency range ($f_{min}$...$f_{max}$) | 57...63 Hz |
| Nominal power factor and adjustable range | > 0.995, 0...± 1 with max $S_{max}$ |
| AC connection type | Screw terminal block |
| **Output protection** | |
| Anti-islanding protection | According to US standards |
| Maximum external AC overcurrent protection | 90 A |
| Output overvoltage protection - varistor | Yes |
| **Operating performance** | |
| Maximum efficiency (ηmax) | 98.6% |
| Weighted efficiency (CEC) | 98.0% |
| **Safety** | |
| Isolation level | Transformerless |
| Marking | TUV |
| Safety and EMC standard | UL1741, Rule 21, HECO tester per UL 1741 SA, UL1699B, IEEE1547, IEEE1547.1, CSA C22.2 107.1-01-2001, FCC Part 15 Sub-part B Class B Limits |

## CEC efficiency = 98.0 percent

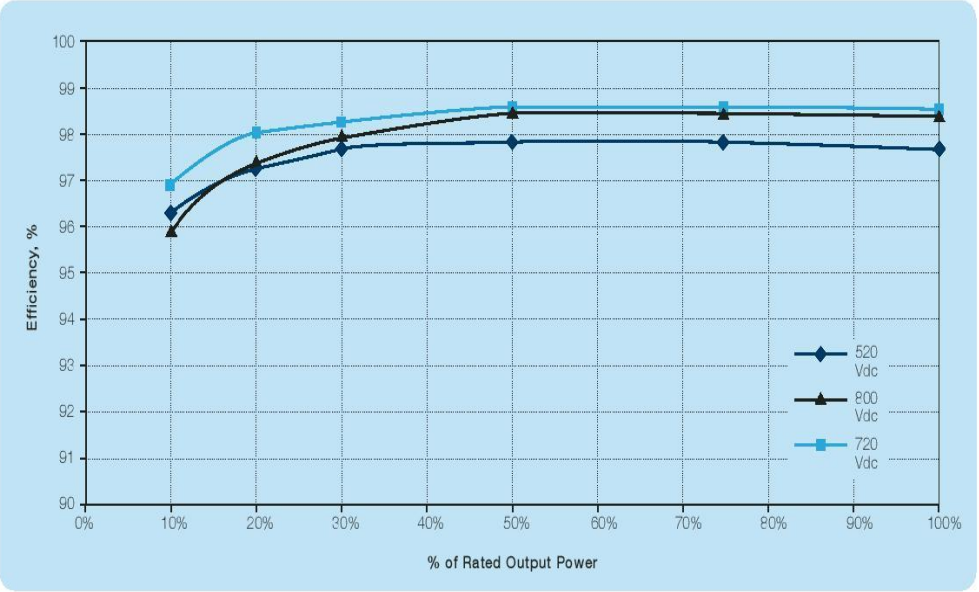


## Technical data and types (preliminary)

| Type code | TRIO-50.0-TL-OUTD-US |
|---|---|
| Communication | |
| Remote monitoring | VSN300 Wifi Logger Card (opt.), VSN700 Data Logger (opt.) |
| Wireless local monitoring | VSN300 Wifi Logger Card (opt.) |
| User interface | LEDs / No display; Aurora Manager Lite software required |
| Available port | 2 RS485 |
| Environmental | |
| Ambient temperature range | -13...+144°F (-25...+60°C) with derating > 122°F (50°C) |
| Relative humidity | 0...100 % condensing |
| Maximum operating altitude without derating | 2000 m / 6560 ft |
| Physical | |
| Environmental protection rating | NEMA 4X (NEMA 3R for fan tray) |
| Cooling | Forced air over external heatsink |
| Dimension (H x W x D) | 28.5" x 59.7" x 12.4" / 725 mm x 1491 mm x 315 mm |
| Weight | 209 lbs overall; 145 lbs power module, 33 lbs AC wiring box (Full options), 31 lbs DC wiring box (Full options) |
| Mounting system options | Wall bracket, horizontal support |

| DC Wiring Box Model Number | Description |
|---|---|
| DCWB-1-TRIO-50.0-TL-OUTD-US-480 | Input lugs for use with external combiner, DC disconnect switch, conduit entry |
| DCWB-2-TRIO-50.0-TL-OUTD-US-480/12 | Touch-safe fuse holder 12 string combiner, DC disconnect switch, AFCI, DC SPD, conduit entry |
| DCWB-2-TRIO-50.0-TL-OUTD-US-480/16 | Touch-safe fuse holder 16 string combiner, DC disconnect switch, AFCI, DC SPD, conduit entry |
| DCWB-3-TRIO-50.0-TL-OUTD-US-480/12* | Board mounted fused 12 string combiner, DC disconnect switch, AFCI, DC SPD, Amphenol connector |
| DCWB-3-TRIO-50.0-TL-OUTD-US-480/16* | Board mounted fused 16 string combiner, DC disconnect switch, AFCI, DC SPD, Amphenol connector |

*Available late 2016

| AC Wiring Box Model Number | Description |
|---|---|
| ACWB-TRIO-50.0-TL-OUTD-US-480 | AC output lugs, conduit entry |
| ACWB-A-TRIO-50.0-TL-OUTD-US-480 | AC output lugs, conduit entry and AC SPD |
| ACWB-B-TRIO-50.0-TL-OUTD-US-480 | AC output lugs, conduit entry, AC SPD and AC disconnect switch |

| Power Module Model Number | Description |
|---|---|
| TRIO-50.0-TL-OUTD-US-480-POWER MODULE | Inverter section / power module |

| Bracket Model Number | Description |
|---|---|
| TRIO-50.0-BRACKET-VERTICAL | Wall mounting bracket; 90 to 16 degrees from horizontal |
| TRIO-50.0-BRACKET-HORIZONTAL | Mounting bracket; 15 to 0 degrees horizontal |


9AKK106713A8910 EN Rev. F 02.17.2017

### Support and service

ABB supports its customers with a dedicated, global service organization in more than 60 countries, with strong regional and national technical partner networks providing a complete range of life cycle services.

For more information please contact your local ABB representative or visit:

**www.abb.com/solarinverters**

**www.abb.com**



TÜVRheinland
C US

ABB

SC 100 Outdoor / SC 100 Indoor

**Flexible**
> Extended temperature range –20 °C to +50 °C
> Compact dimensions – easier installation

**Economic**
> Innovative transformer technology resulting in improved peak efficiency up to 97.6 % and Euro Eta of 97.0 %

**Safe**
> System monitoring and analysis via integrated data logger
> Simple remote querying using remote access is possible

**Optional**
> String monitoring
> DC-input voltage range up to 1000 V
> Operation with grounded PV generators
> Also available as HE version


# SUNNY CENTRAL 100

## Powerful and Efficient

Concentrated power at an attractive price: the Sunny Central 100 outdoor is the perfect solution for PV power plants on the free field. The weatherproof enclosure and the extended temperature range make it the first choice for reliable outdoor operation - even under harsh climatic conditions. Plant operators benefit twice: the compact design of the Sunny Central 100 reduces installation work. And the innovative transformer technology improved the peak efficiency of the central inverter even further, resulting in 97.6 %. This makes it one of the most efficient inverters in its class. The indoor version is basically identical to the Sunny Central 100 Outdoor, though the special ventilation concept makes it the perfect solution for indoor applications.

# Technical Data
# SUNNY CENTRAL 100 Outdoor / 100 Indoor

| | SC 100 Outdoor / HE* | SC 100 Indoor / HE* |
|---|---|---|
| **Input data** | | |
| Max. PV power (recommended), ($P_{PV}$) | 110 kWp [1] | 110 kWp [1] |
| DC voltage range, MPPT ($U_{DC}$) | 450 V – 820 V | 450 V – 820 V |
| Max. permissible DC voltage ($U_{DC, max}$) | 900 V / optional 1000 V | 900 V / optional 1000 V |
| Max. permissible DC current Max. ($I_{DC, max}$) | 235 A | 235 A |
| Number of DC inputs (terminal without fuse) | 3 x Plus, M12 screws<br>3 x Minus, M12 screws | 3 x Plus, M12 screws<br>3 x Minus, M12 screws |
| **Output data** | | |
| Nominal AC output power ($P_{AC}$) | 100 kW | 100 kW |
| Operating grid voltage +/- 10 % ($U_{AC}$) | 400 V / 300 V* | 400 V / 300 V* |
| Nominal AC current ($I_{AC, nom}$) | 145 A / 193 A* | 145 A / 193 A* |
| Grid structure | TT, TN-S, TN-C-grid / IT-grid* | TT, TN-S, TN-C-grid / IT-grid* |
| Operating range, grid frequency ($f_{AC}$) | 50 Hz – 60 Hz | 50 Hz – 60 Hz |
| Voltage ripple, PV voltage ($U_{PP}$) | < 3 % | < 3 % |
| Harmonic distortion of grid current ($K_{IAC}$) | < 3 % at nominal power | < 3 % at nominal power |
| Power factor (cos ϕ) | ≥ 0.99 at nominal power | ≥ 0.99 at nominal power |
| **Efficiency** [2] | | |
| Max. efficiency $P_{AC, nom}$ (η) | 97.6 % / 98.5 %* | 97.6 % / 98.5 %* |
| Euroeta (η) | 97.0 % / 98.3 %* | 97.0 % / 98.3 %* |
| **Dimensions and weight** | | |
| Width / Height / Depth in mm (W / H / D) | 1280 / 1835 / 830 | 1280 / 1835 / 830 |
| Weight approx. (m) | 925 kg / 505 kg* | 925 kg / 505 kg* |
| **Power consumption** | | |
| Own consumption in operation ($P_{day}$) | < 1 % of $P_{AC, nom}$ | < 1 % of $P_{AC, nom}$ |
| Standby operating consumption ($P_{night}$) | < approx. 50 W | < approx. 50 W |
| External auxiliary voltage / grid structure | 230 V, 50 / 60 Hz TN-S-grid<br>(Optional / Yes*) | 230 V, 50 / 60 Hz TN-S-grid<br>(Optional / Yes*) |
| External back-up fuse for auxiliary supply | B 16 A, 1-pole | B 16 A, 1-pole |
| **SCC (Sunny Central Control) interfaces** | | |
| Communication (NET Piggy Back, optional) | Analog, ISDN, Ethernet, GSM | Analog, ISDN, Ethernet, GSM |
| Analog inputs | Optional 1 x PT 100, 2 x $A_{in}$ [3] | Optional 1 x PT 100, 2 x $A_{in}$ [3] |
| Overvoltage protection for analog inputs | Optional | Optional |
| Sunny String Monitor interface (COM1) | RS485 | RS485 |
| PC interface (COM3) | RS232 | RS232 |
| Electrically separated relay (ext. signal) | 1 | 1 |

**Efficiency curve**

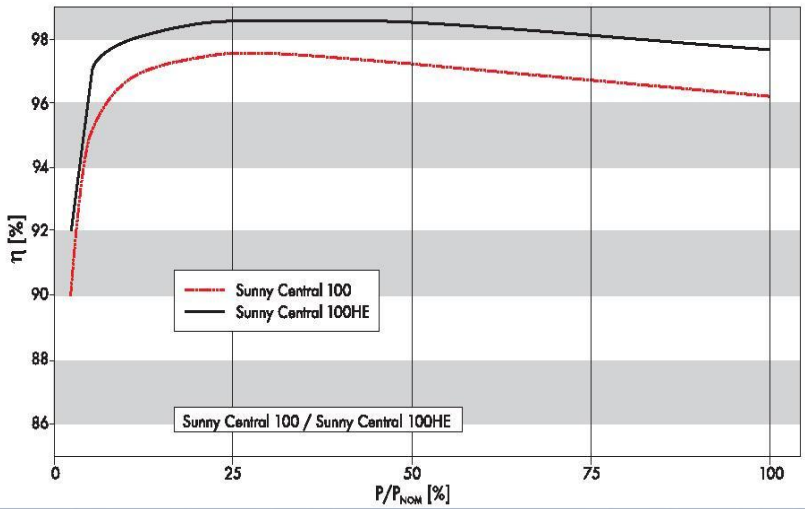

| | SC 100 Outdoor / HE* | SC 100 Indoor / HE* |
|---|---|---|
| **Features** | | |
| Display (SCC) | Yes | Yes |
| Ground fault monitoring | Yes (optionally configurable) | Yes (optionally configurable) |
| Heating | Yes | Yes |
| Emergency stop | no | Yes |
| Power switch AC side | Optional / Fuse load disconnector * | Optional / Fuse load disconnector * |
| Power switch DC side | motor-driven | motor-driven |
| Monitored overvoltage protectors AC | Optional | Optional |
| Monitored overvoltage protectors DC | Yes | Yes |
| Monitored overvoltage protectors for auxiliary supply | Optional | Optional |
| **Standards** | | |
| EMC | EN 61000-6-2, EN 61000-6-4 | EN 61000-6-2, EN 61000-6-4 |
| Grid monitoring | as per VDEW regulations | as per VDEW regulations |
| CE conformity | Yes | Yes |
| **Protection rating and ambient conditions** | | |
| Protection rating as per EN 60529 | IP44 / IP54 | IP21 |
| 1. Enclosure type according to 60721-3-4 ambient conditions: fixed location, without protection against wind and weather. 2. Enclosure type according to 60721-3-3 fixed location, with protection against wind and weather. | 1. Classification of • chemically active substances: 4C1 • mechanically active substances: 4S2 | 2. Classification of • chemically active substances: 3C1L • mechanically active substances: 3S2 |
| Permissible ambient temperature (T) | –20 °C ... +50 °C 4) | –20 °C ... +50 °C 4) |
| Relative humidity, not condensing ($U_{AIR}$) | 15 % ... 95 % | 15 % ... 95 % |
| Max. altitude (above sea level) | 1000 m | 1000 m |
| Fresh air consumption ($V_{AIR}$) | 2300 m³/h | 2300 m³/h |
| Air flow (Outdoor installation of SC 100 ourdoor) | Intake over top blown out through base | Intake and discharge over top |

* HE: High Efficiency, inverter without electric separation for the connection to a medium voltage transformer (preliminary data dated March 2008)

1) Specifications apply to irradiation values = 1,000 (kWh/(kWp x year))

2) Efficiency measured without an internal power supply at $U_{DC}$ = 500 V

3) Terminal for an analog sensor provided by the customer in two-wire and four-wire version

4) Complies with nominal values up to an ambient temperature of +40 °C, at an ambient temperature of +50 °C the nominal values are held for two hours.

**Note:** Sunny Central transport documentation, Sunny Central Installation guide and when installing the SC 100 Outdoor, a suitable foundation, sufficient ventilation and appropriate sun shading systems are necessary

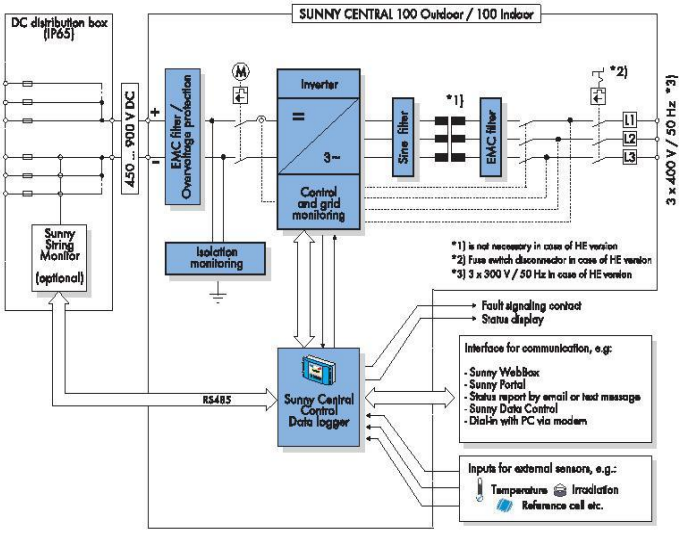

# SUNNY CENTRAL Product Overview

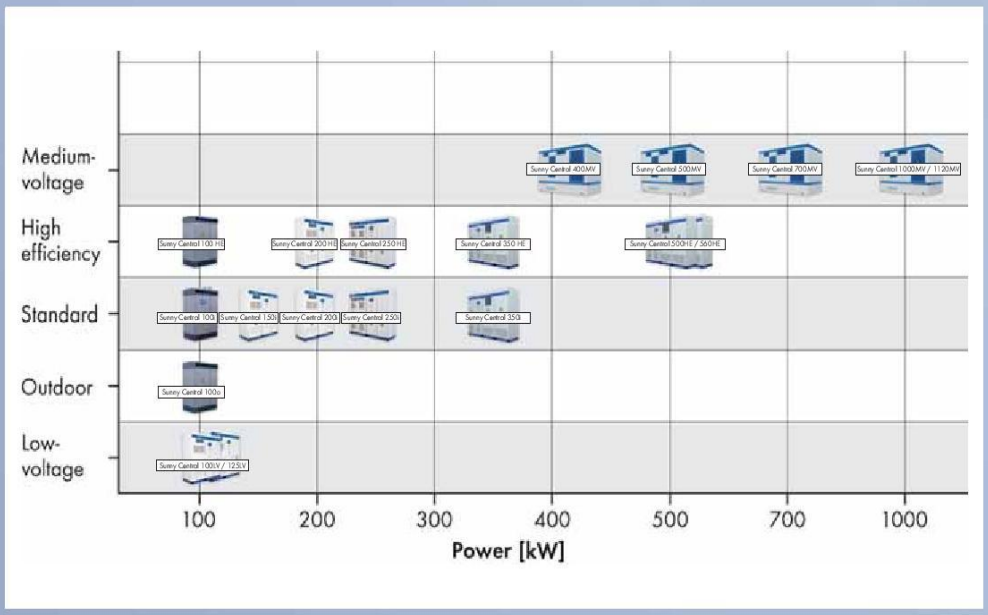


## Accessories

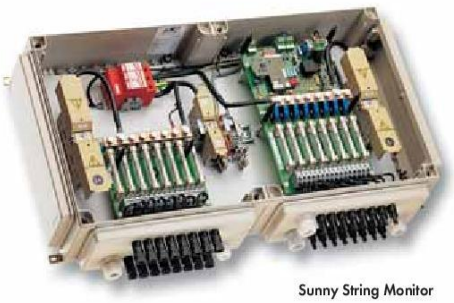

Sunny String Monitor

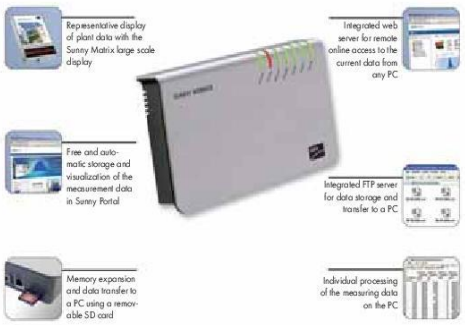

**جامعة النجاح الوطنية**

**كلية الدراسات العليا**

# تحليل مراحل تحويل الطاقة وامكانيات تحسين الكفاءة لأنظمة الخلايا الشمسية المتصلة بالشبكة الكهربائية

**إعداد**

**ايمان عمر محمود ابو هاني**

**إشراف**

**أ.د. مروان محمود**

**قدمت هذه الأطروحة استكمالاً لمتطلبات الحصول على درجة الماجستير في هندسة القوى الكهربائية، في كلية الدراسات العليا، في جامعة النجاح الوطنية، نابلس – فلسطين.**

**2018**

**تحليل مراحل تحويل الطاقة وامكانيات تحسين الكفاءة لأنظمة الخلايا الشمسية المتصلة بالشبكة الكهربائية**

**إعداد**

**ايمان عمر محمود ابو هاني**

**إشراف**

**أ.د. مروان محمود**

## الملخص

في هذه الأطروحة تم تحسين كفاءة التحويل في انظمة الخلايا الشمسية ذات القدرة العالية. حيث تم اختيار كفاءة العاكس لتحسينها من خلال اختبار نظامين مختلفين من العواكس موصلة مع نظام خلايا شمسية بقدرة 100 كيلوواط. في النظام الأول تم استخدام عاكس واحد مركزي وفي النظام الثاني تم استخدام عدة عواكس احدها اساسي والاخرى ثانوية. تم تطوير نموذج رياضي باستخدام برنامج الماتلاب لنمذجة كفاءة العاكس كدالة تتكون من الطاقة المنتجة من الخلايا الشمسية، حيث يتم حساب الطاقة المنتجة من العاكس على مدار سنة باستخدام بيانات الإشعاع الشمسي ودرجة الحرارة في فلسطين. وتبين نتائج المحاكاة أن متوسط إنتاج الطاقة السنوي باستخدام العاكس المركزي الواحد 181.26 ميجاواط ساعة، وفي حالة استخدام عدة عواكس معا كان متوسط الطاقة الناتجة خلال سنة 184.5 ميجاواط ساعة. اضافة لذلك، وبخصوص كفاءة العاكس فان كفاءة التحويل السنوية للنظام الأول 96.7٪ وللنظام الثاني 98.4٪.

ويبين التحليل الاقتصادي أنه يمكن تغطية الاستثمار الإضافي في النظام الثاني المكون من عدة عواكس بدلا من استخدام العاكس المركزي الوحيد خلال ستة أعوام ونصف.